Development of Experimental Techniques: Sharp Views into the Nano Cosmos

Christian G. Schroer

DESY & Universität Hamburg

HELMHOLTZ
RESEARCH FOR GRAND CHALLENGES

Universität Hamburg
DER FORSCHUNG | DER LEHRE | DER BILDUNG

DESY.

Complexity in Nature: Characteristic Length Scales

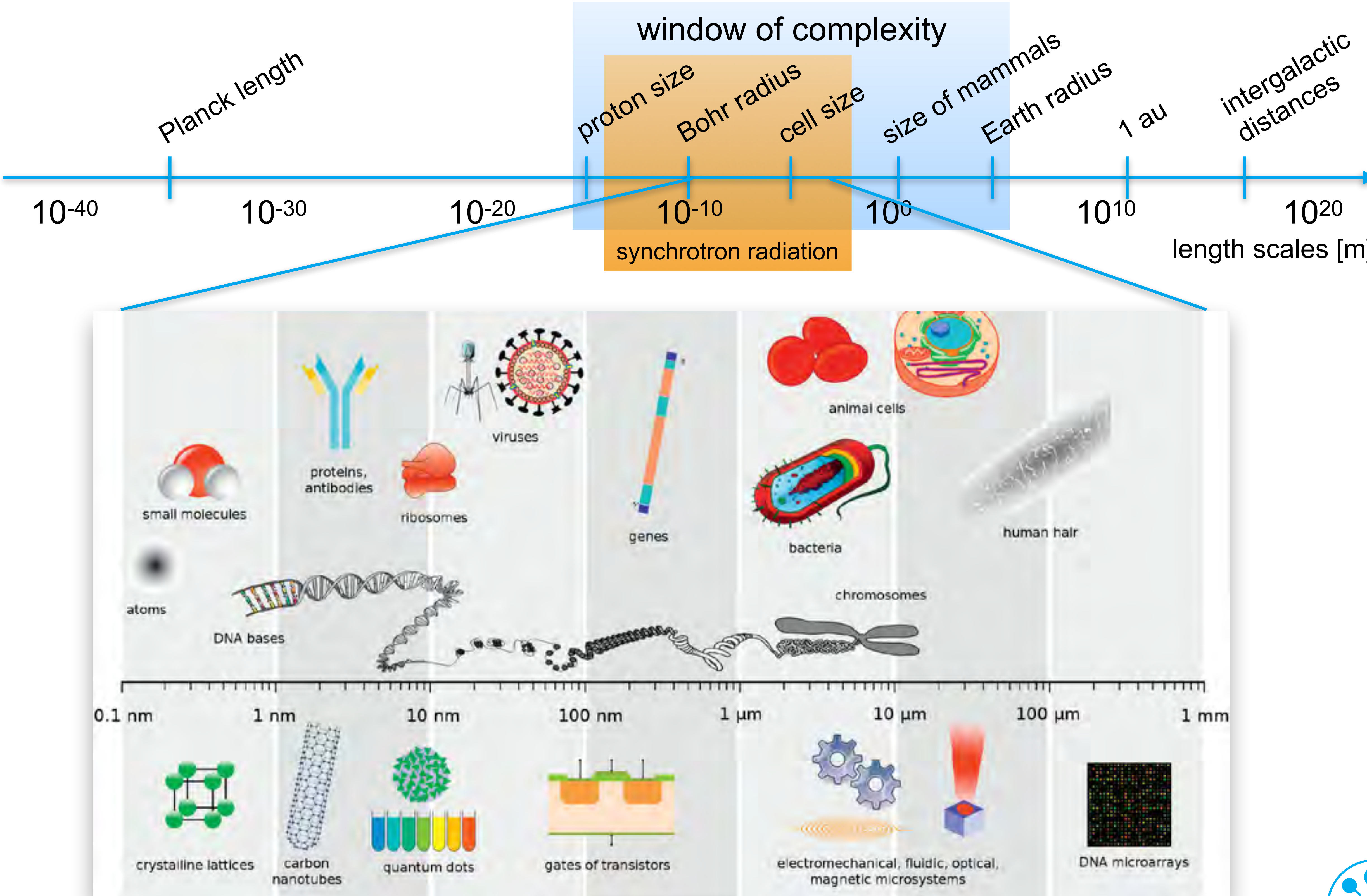

What we need to do:

Quantitive in-situ measurement of physical properties of matter

- on all relevant length scales
- on all relevant time scales

→ (in principle) from Å to millimeters

Key technology: bright, coherent x-rays with time structure

Requirements:

- high coherent flux
  - → x-ray free-electron lasers
  - → diffraction-limited storage rings (PETRA IV)
- efficient nanofocusing
  - → optics
- stability on nanometer scale

Fusion of real and reciprocal space!

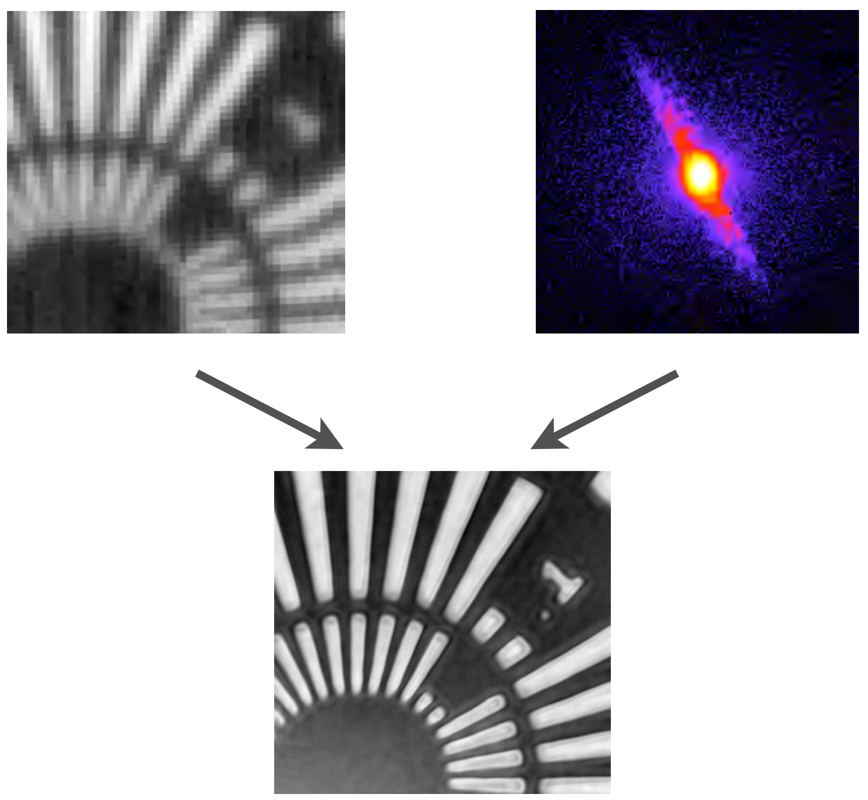

DESY: Accelerator-Based Light Sources

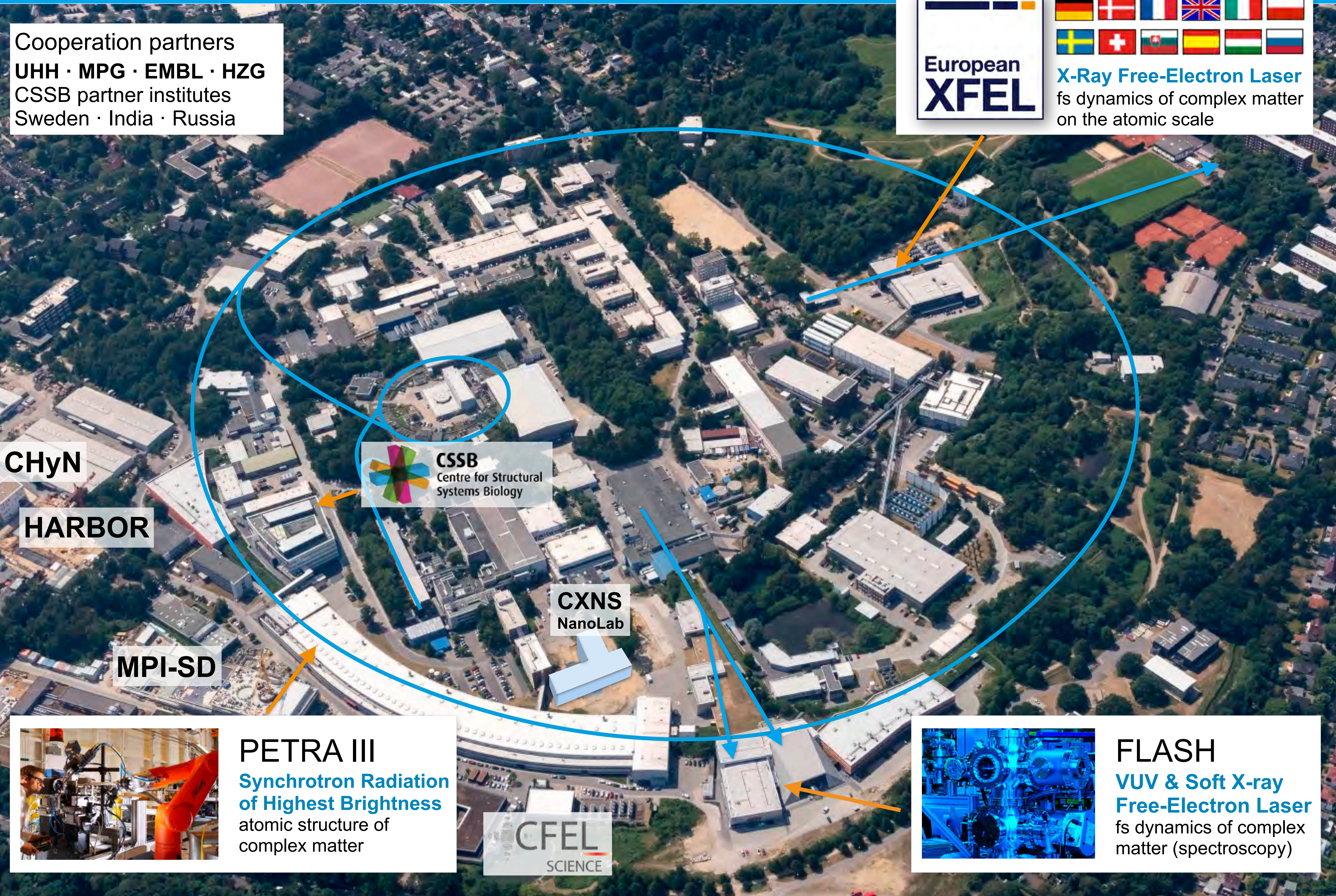

PETRA III

DESY's bright synchrotron radiation source

History of PETRA:

- 1978 built for high-energy physics, first direct observation of the gluon, since 1988 pre-accelerator for HERA
- starting July 2007: rebuilding PETRA as a synchrotron radiation source (PETRA III)
- Sept. 2010: start of user operation with the first three beamlines
- End of 2013: all 15 beamlines fully operational in Max v. Laue Hall
- Mar. 2014 - Apr. 2015: Shutdown for extension project after the DORIS III shutdown
- 2016: First beamlines in the extension operational

electron energy:	6 GeV
stored current:	100 mA (top-up)
emittance:	**1.2 nm rad**
circumference:	**2304 m**
photon energy range:	250 eV — 150 keV
beamlines in operation:	21
beamlines under construction:	3
beamlines in planning:	2
user operation (hours/year):	5000 h (4000 h)

PETRA III Beamlines

Max v. Laue Hall

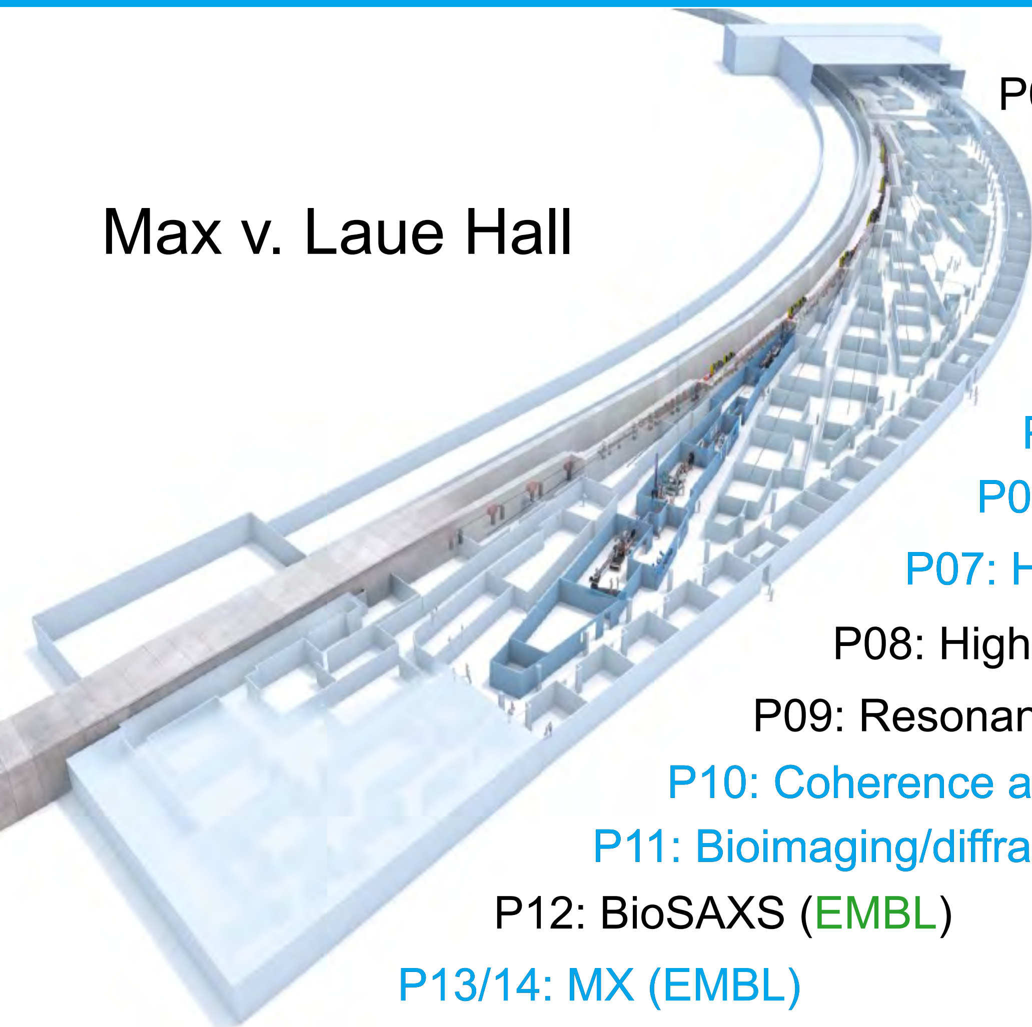

P01: Dynamics beamline, IXS, NRS
P02.1: Powder diffraction & total scattering
P02.2: Extreme conditions
P03: Micro-, nano-SAXS, WAXS
P04: Variable polarisation XUV
P05: Micro-, nano-tomography (HZG)
P06: Hard X-ray micro-, nanoprobe
P07: High-energy materials sci. (HZG, DESY)
P08: High-resolution diffraction
P09: Resonant scattering/diffraction
P10: Coherence applications
P11: Bioimaging/diffraction
P12: BioSAXS (EMBL)
P13/14: MX (EMBL)

Imaging

Verbundforschung

Federal Ministry of Education and Research

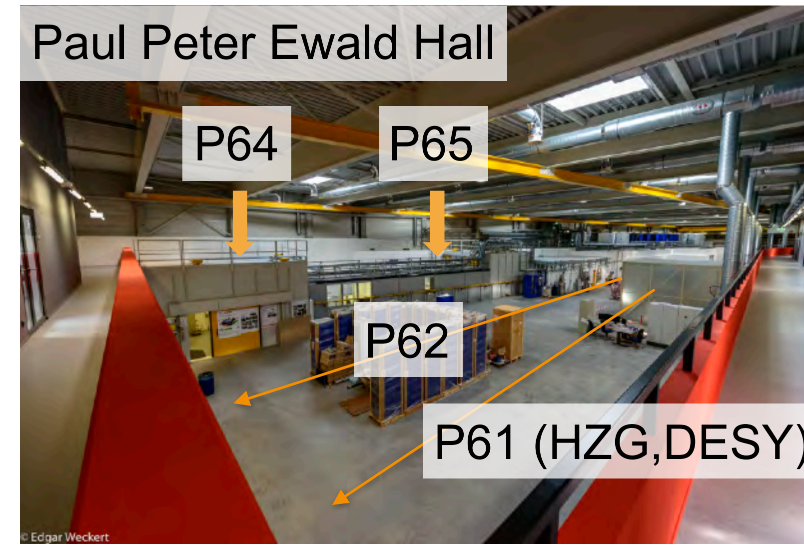

P61: High-energy wiggler beamline (HZG, DESY operational 2019)
P62: Small-angle X-ray scattering (under construction)
P63: MPG catalysis (in planning)
P64: Advanced XAFS
P65: Applied XAFS
P66: Time-resolved luminescence spectroscopy (operational 2021)

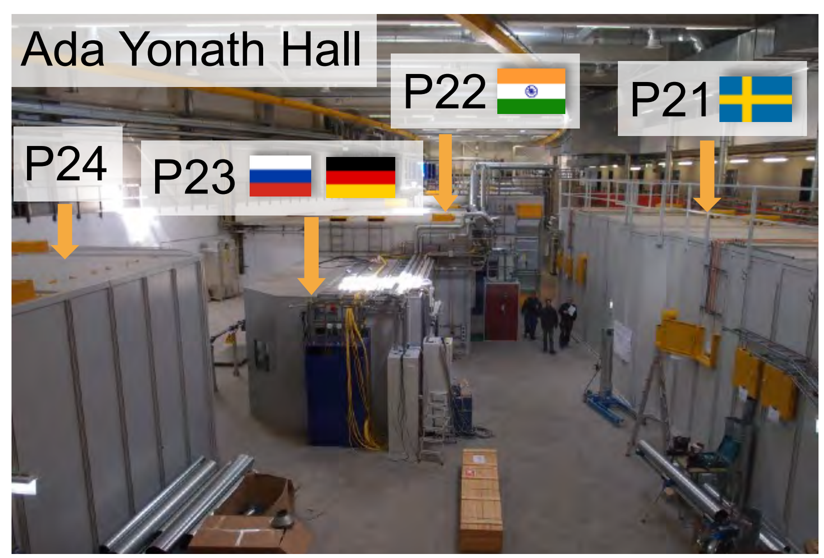

P21: Swedish materials science beamline
P22: Hard X-ray photoelectron spectroscopy
P23: In-situ and nano diffraction beamline
P24: Chemical crystallography
P25: HIMAX, NRS (in planning)

X-ray Scanning Microscopy

Broad field of applications:

> Main advantage: large penetration depth

→ *in-situ* and *operando* studies

→ 3D bulk analysis without destructive sample preparation

> X-ray analytical contrasts: XRD, XAS, XRF, ...

→ elemental, chemical, and structural information

Today: „mesoscopic gap"

real-space resolution: down to about 10 nm

XRD and XAS: atomic scale

Many interesting physics and chemistry (e. g. catalysis) at the 1 - 10 nm scale!

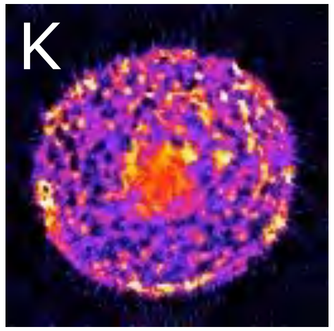

C. G. Schroer, APL **79**, 1912 (2001).

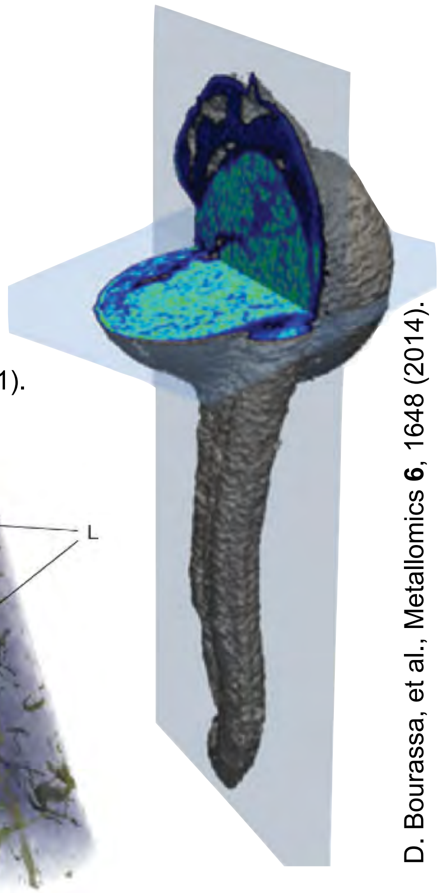

D. Bourassa, et al., Metallomics **6**, 1648 (2014).

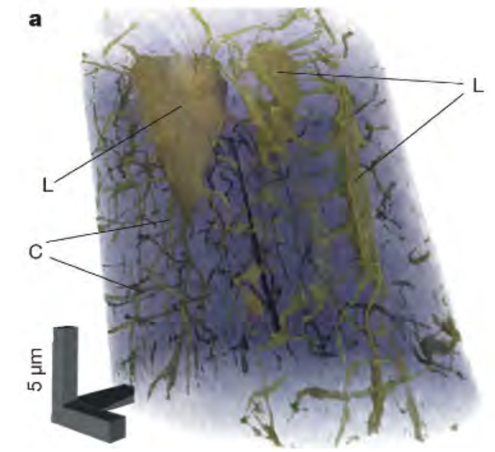

M. Dierolf, et al., Nature **467**, 436 (2010).

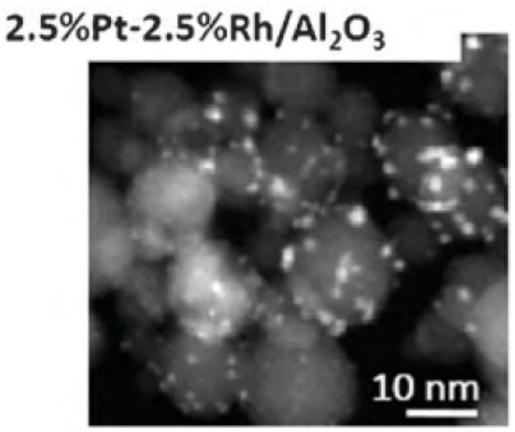

catalysts

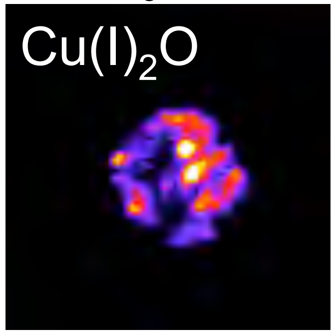

C. G. Schroer, et al., APL **82**, 3360 (2003).

X-ray Microscopy

Many interesting physics and chemistry questions:

investigate local states:

- individual defects (0D): changes in electron density, charge ordering
- (structural) domain boundaries (2D), e. g., in multiferroics
- mesoscopic dynamics at (solid-state) phase transitions
- catalytic nanoparticles (under reaction conditions)
- ...

Mesoscale also very important for nanotechnology (e. g., defects in devices)!

ferroelectric phase transition

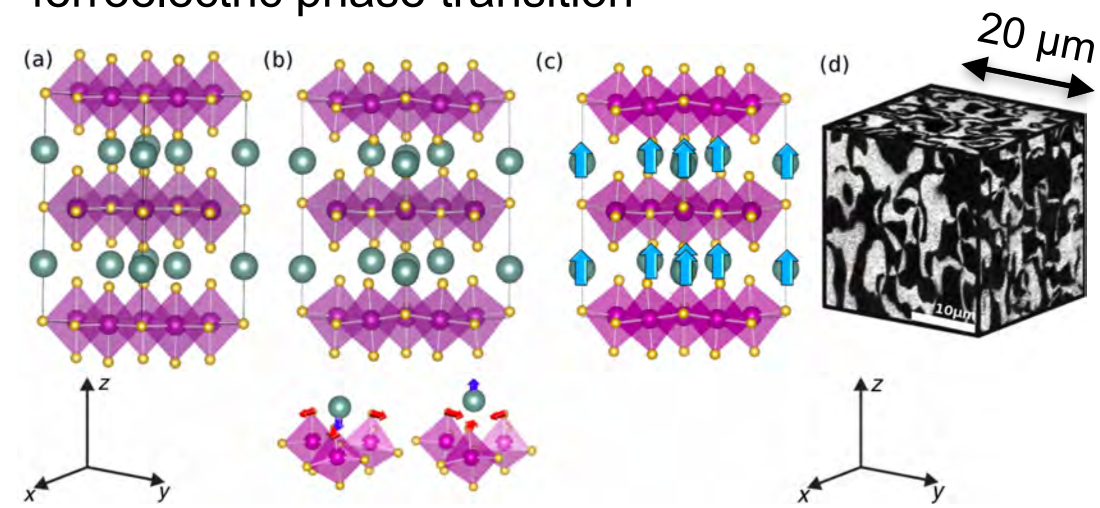

Griffin, et al., PRX **2**, 041022 (2012).

variation of supercond. gap

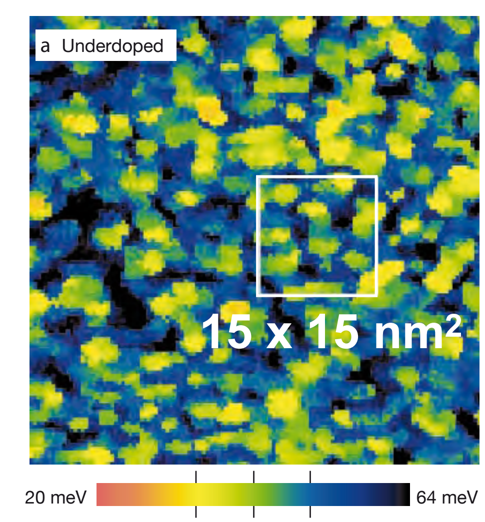

Lang, et al., Nature **415**, 412 (2002).

nanoelectromechanical switch

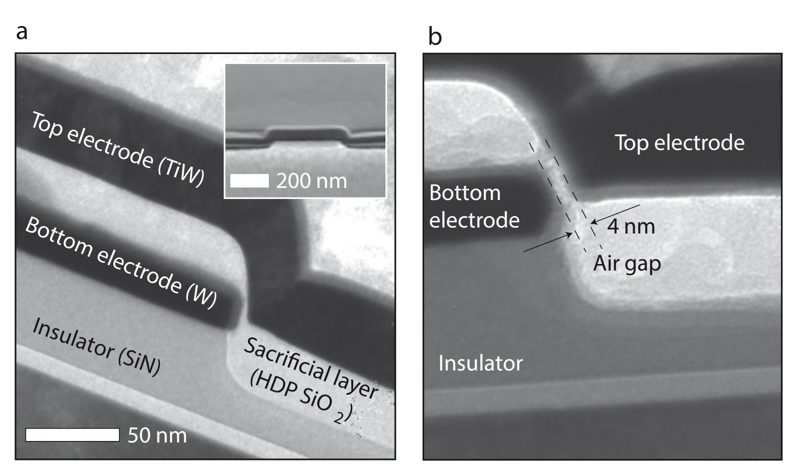

Lee, et al., Nature Nanotech. **8**, 36 (2012).

Current State of X-Ray Microscopy

Conventional x-ray microscopy

→ optics limit spatial resolution: diffraction limit

$$d = \frac{\lambda}{2n \sin\alpha}$$

(typically: a few tens of nanometers)

optics are technology limited!
Theoretical extrapolation of x-ray optical performance to the atomic level.

[PRB **74**, 033405 (2006); H. Yan, et al., PRB **76**, 115438 (2007)]

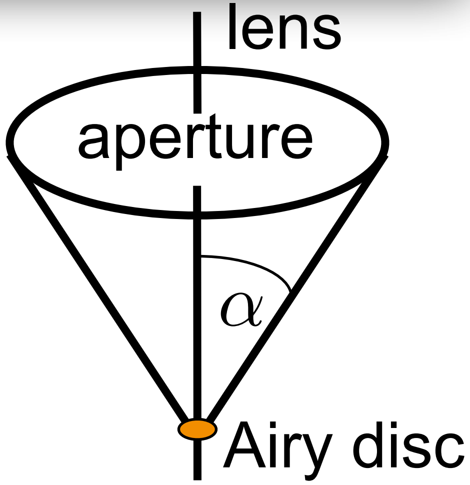

Coherent x-ray imaging techniques (CXDI, ptychography)

→ no imaging optics needed!

→ limited by statistics of far-field diffraction patterns ...

highest resolution: a few nanometers, focusing coherent beam
[PRL **101**, 090801 (2008); Y. Takahashi, et al., PRB **80**, 054103 (2009);
A. Schropp, et al., APL 100, 253112 (2012)]

Spectral Brightness

10000x more "light" per decade (since 1965)!!

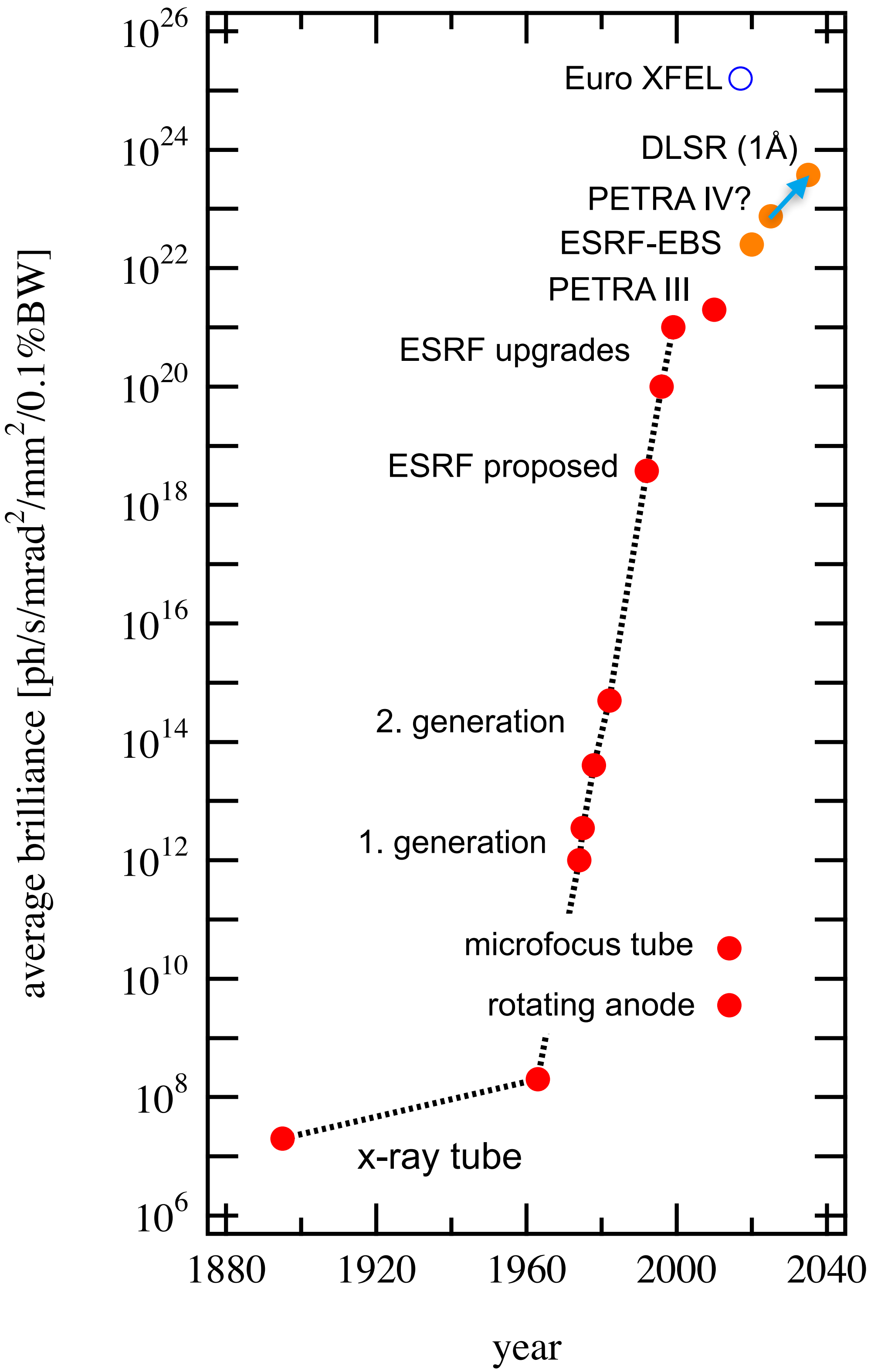

Spectral brightness:

$$B_{sp} = \frac{F}{\Omega \cdot A \cdot \Delta E / E}$$

Flux per phase-space volume

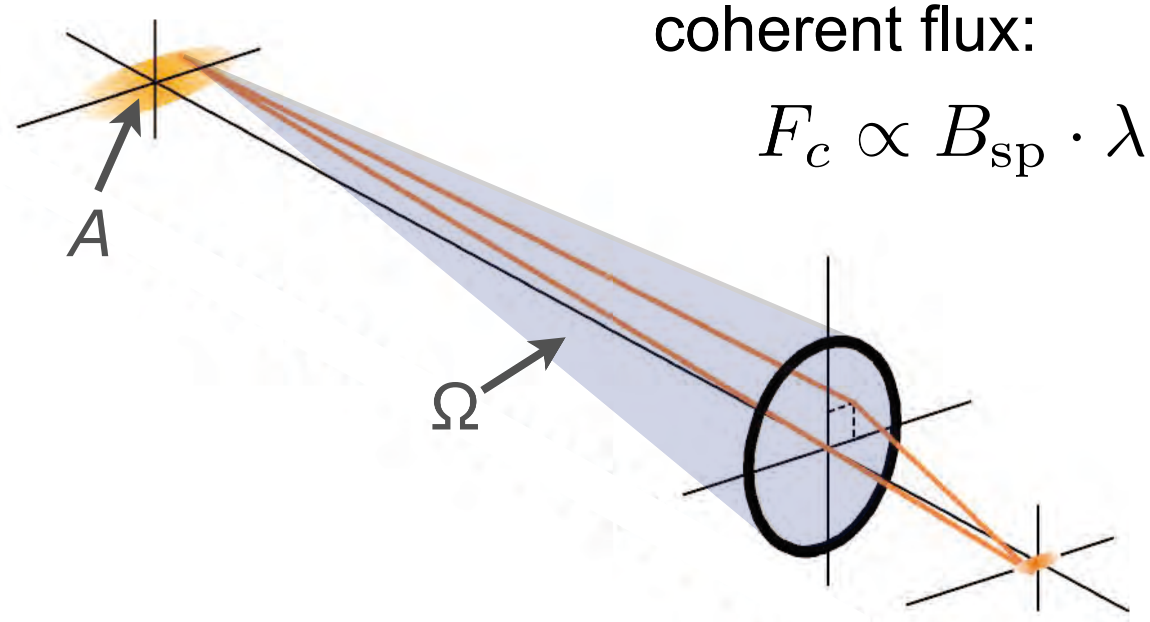

coherent flux:

$$F_c \propto B_{sp} \cdot \lambda^2 \cdot \frac{\Delta E}{E}$$

Improvements in brightness:

- faster measurements (time resolution)
- nano-imaging (spatial resolution)
- spectroscopy (energy resolution)

Spectral Brightness

10000x more “light” per decade (since 1965)!!

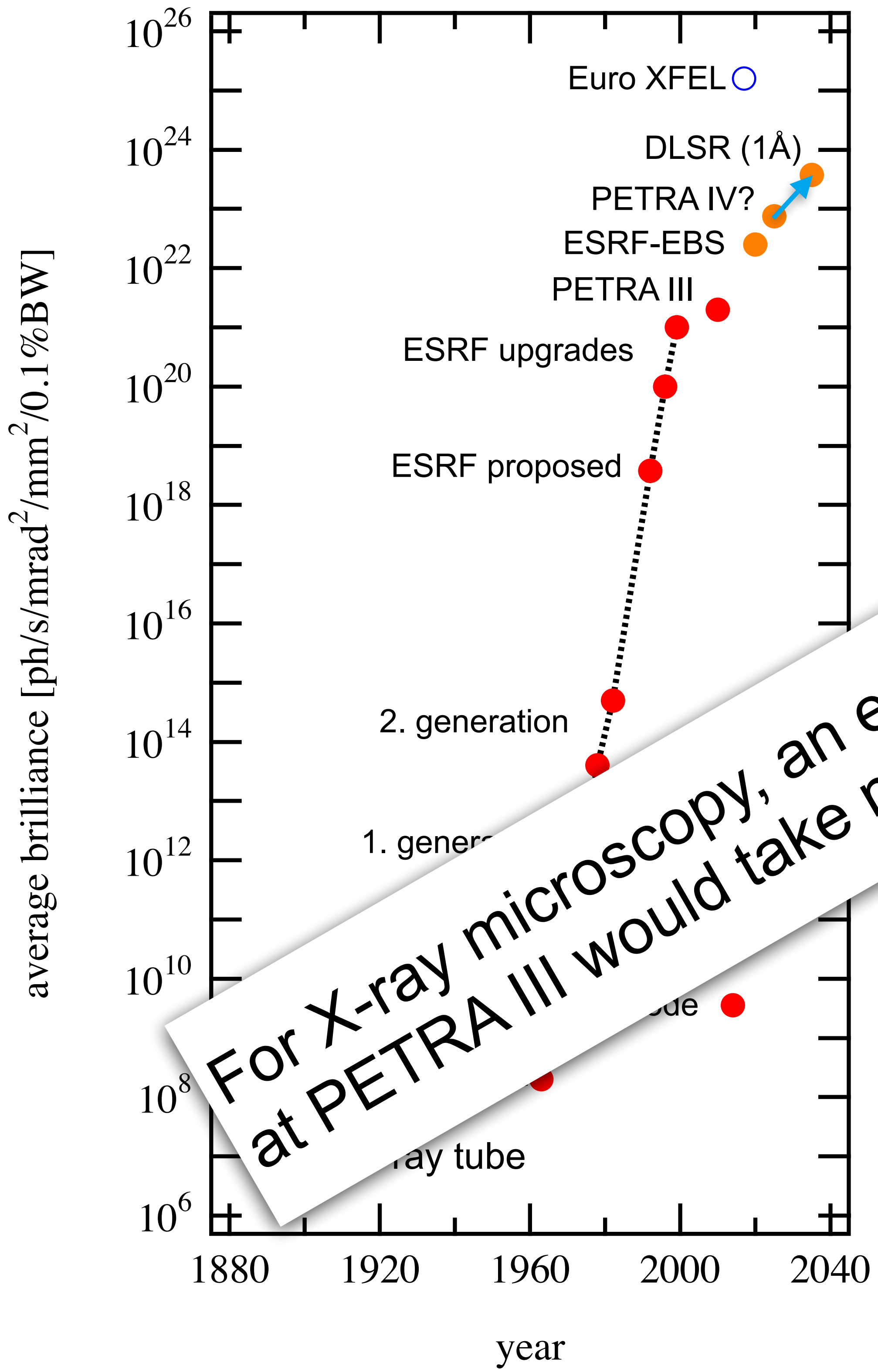

Spectral brightness:

$$B_{\mathrm{sp}} = \frac{F}{\Omega \cdot}$$

Flux per phase

For X-ray microscopy, an experiment that requires 1 s of exposure time at PETRA III would take more than 30000 years at x-ray tube!!!

herent flux:

$$F_c \propto B_{\mathrm{sp}} \cdot \lambda^2 \cdot \frac{\Delta E}{E}$$

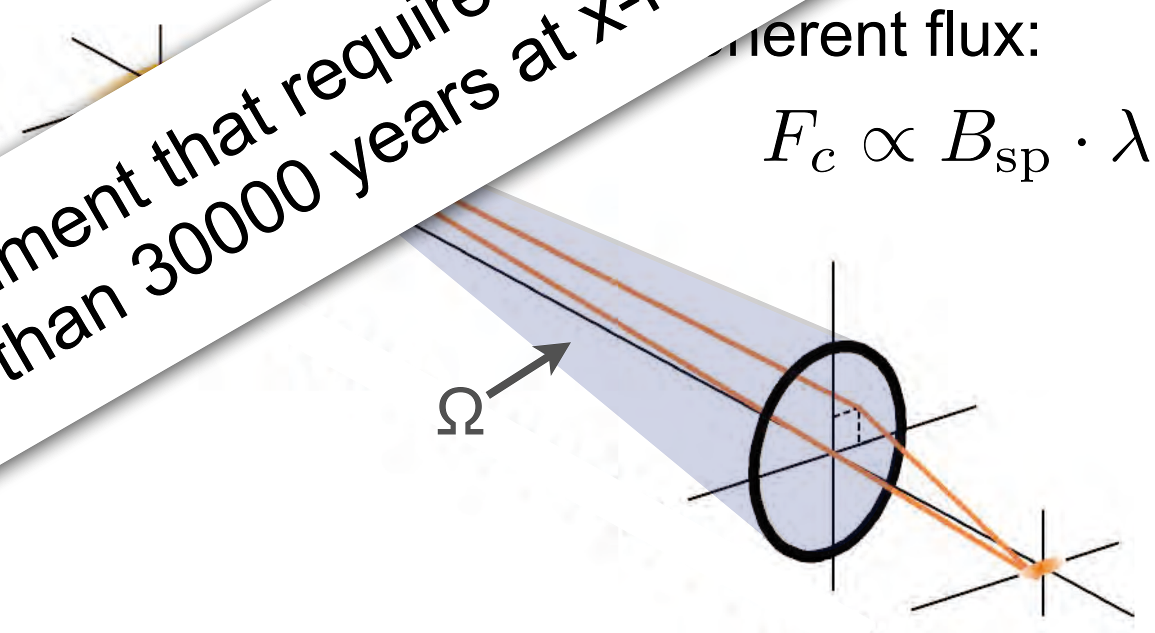

Improvements in brightness:

- faster measurements (time resolution)
- nano-imaging (spatial resolution)
- spectroscopy (energy resolution)

Nanofocusing Optics

reflection:

- mirrors (25 nm)
  H. Mimura, et al., APL **90**, 051903 (2007)
- capillaries
- wave guides (~10 nm)
  S. P. Krüger, et al., J. Synchrotron Rad. **19**, 227 (2012)

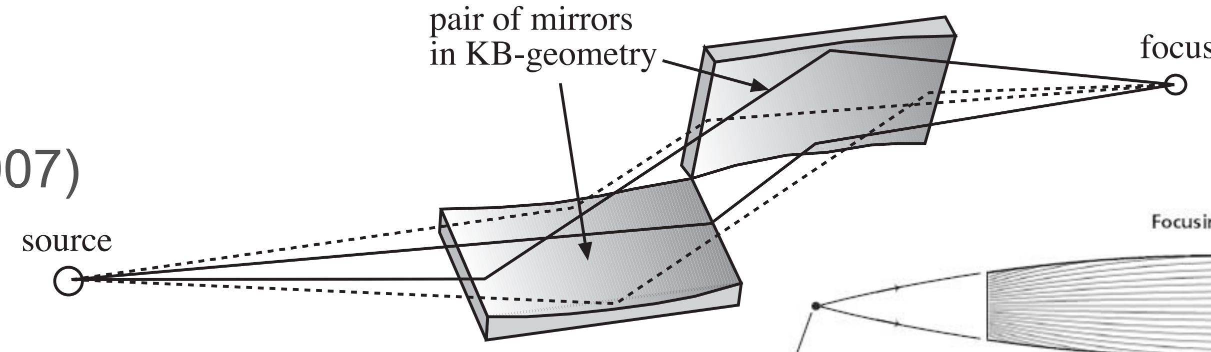

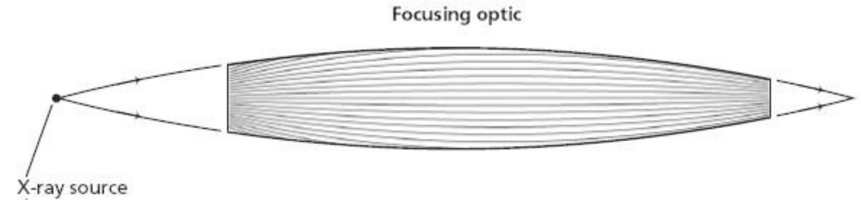

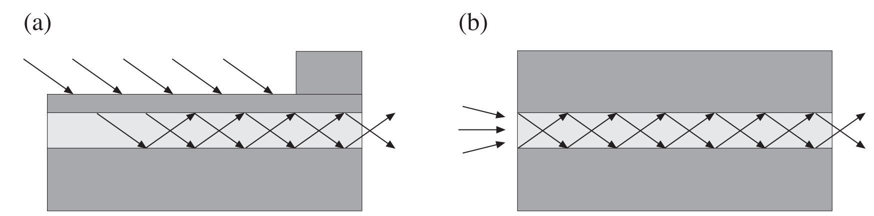

diffraction:

- Fresnel zone plates (< 10 nm)
  J. Vila-Comamala, et al., Ultramic. **109**, 1360 (2009)
- multilayer mirrors (7 nm)
  H. Mimura, et al., Nat. Phys. **6**, 122 (2010)
- multilayer Laue lenses (8 nm)
  A. Morgan, et al., Sci. Rep. **5**, 09892 (2015)
- bent crystals

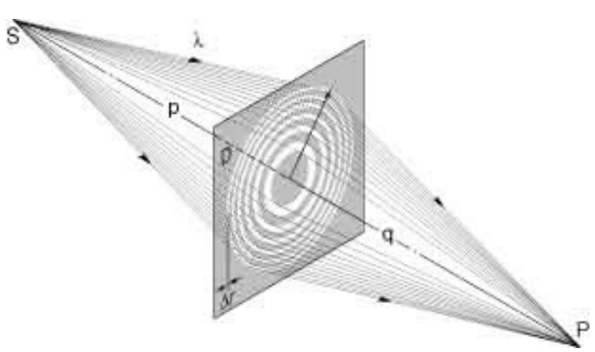

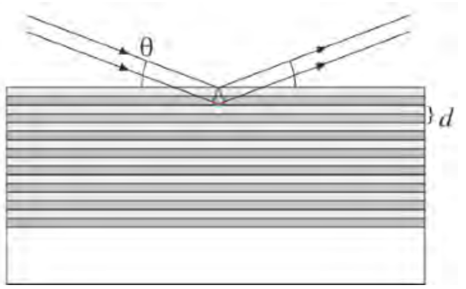

refraction:

- lenses (43 nm, 18 nm)
  C. G. Schroer, et al., AIP Conf. Ser. **1365**, 227 (2011)
  J. Patommel, et al., APL **110**, 101103 (2017)

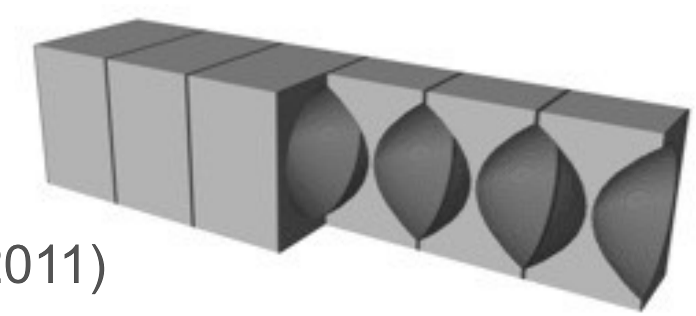

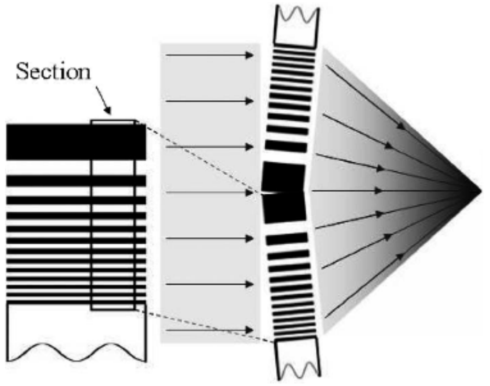

X-Ray Microscopy Techniques: Full-Field Imaging

Projection imaging:

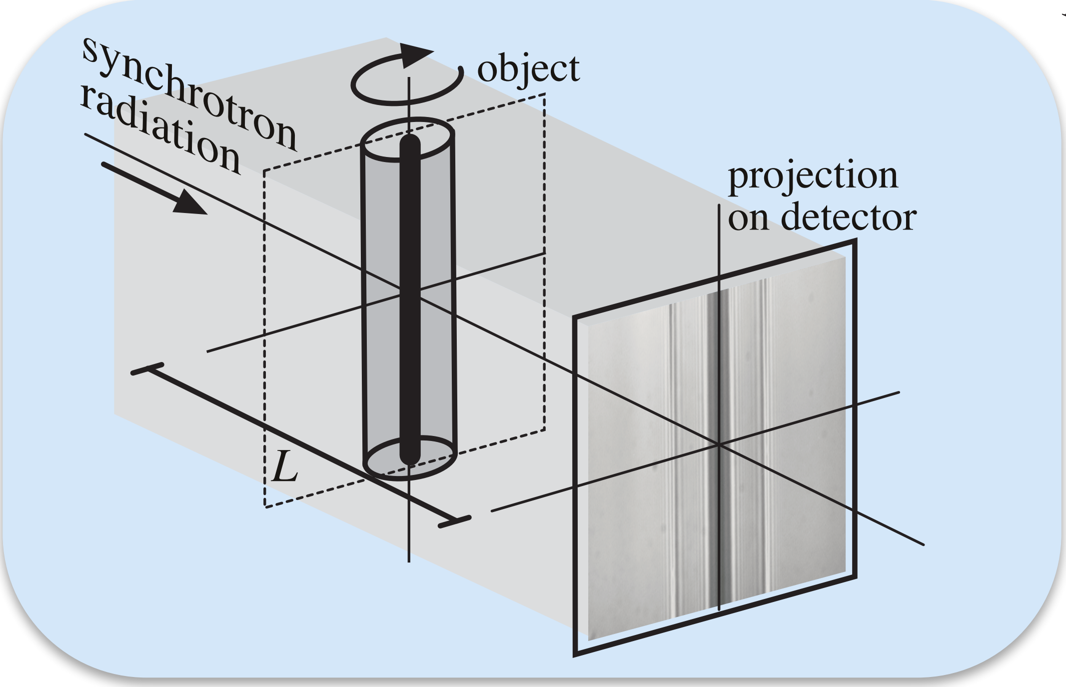

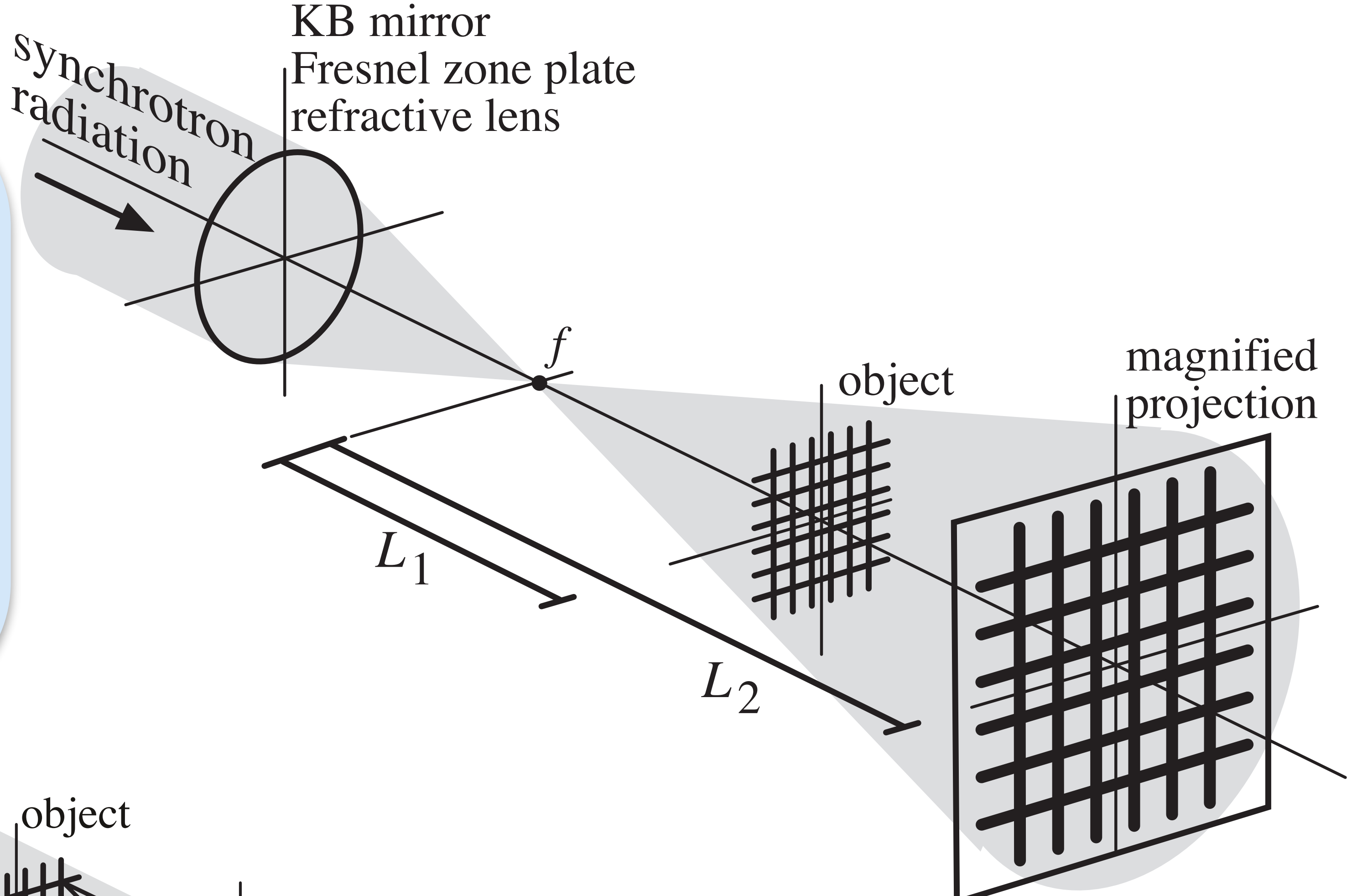

Imaging through objective lens:

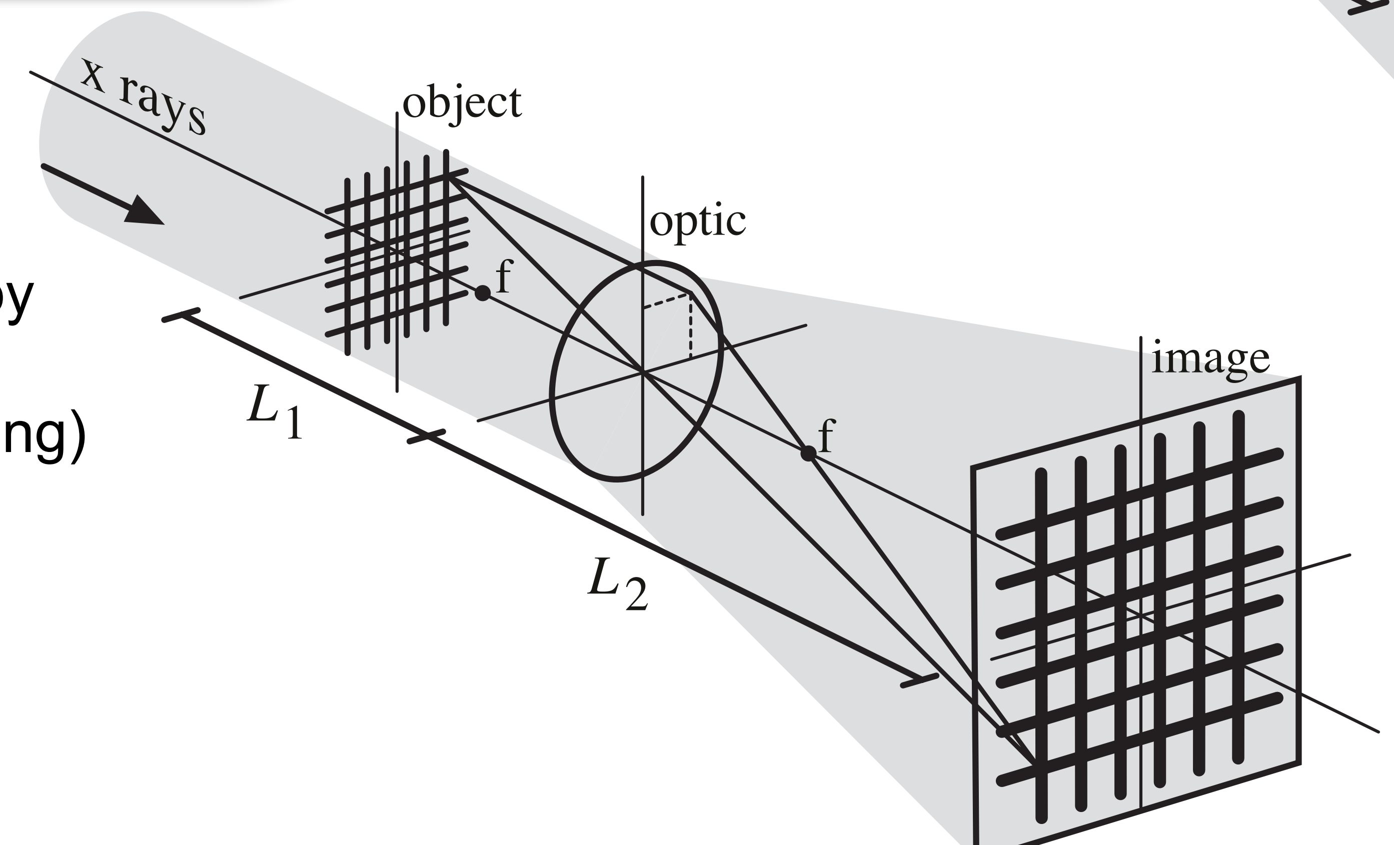

x-rays focused by condensor (aperture matching)

Example: Projection Imaging (Phase Contrast)

Example: plant physiology

0.5 mm

root of mahogany tree
(W. H. Schröder, FZ Jülich)

Reveal inner structures of object:

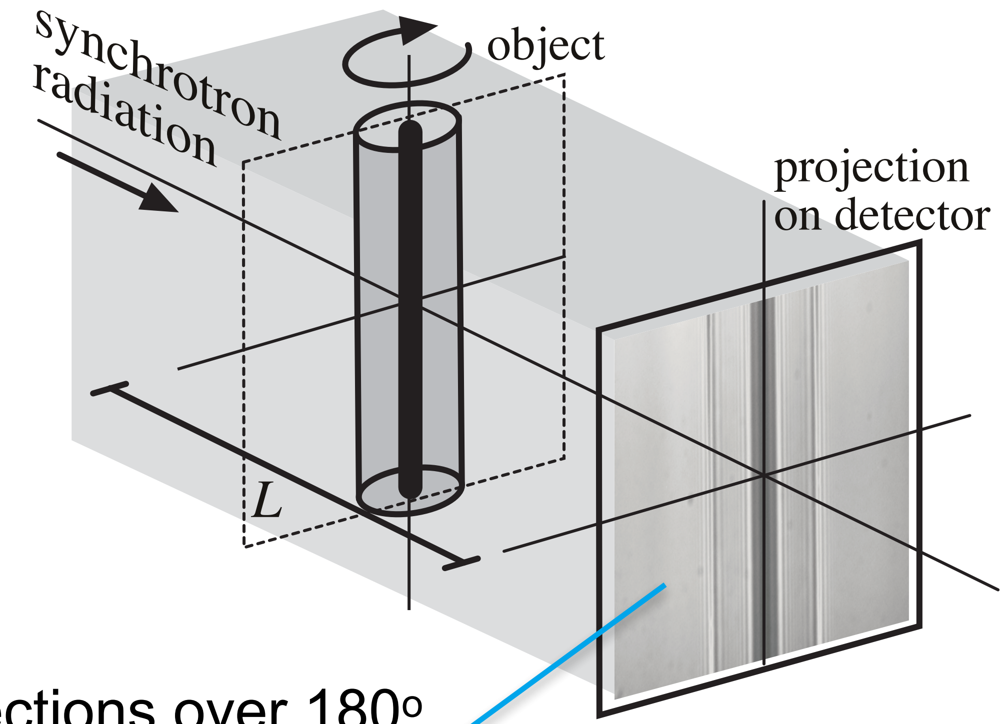

1250 projections over 180°

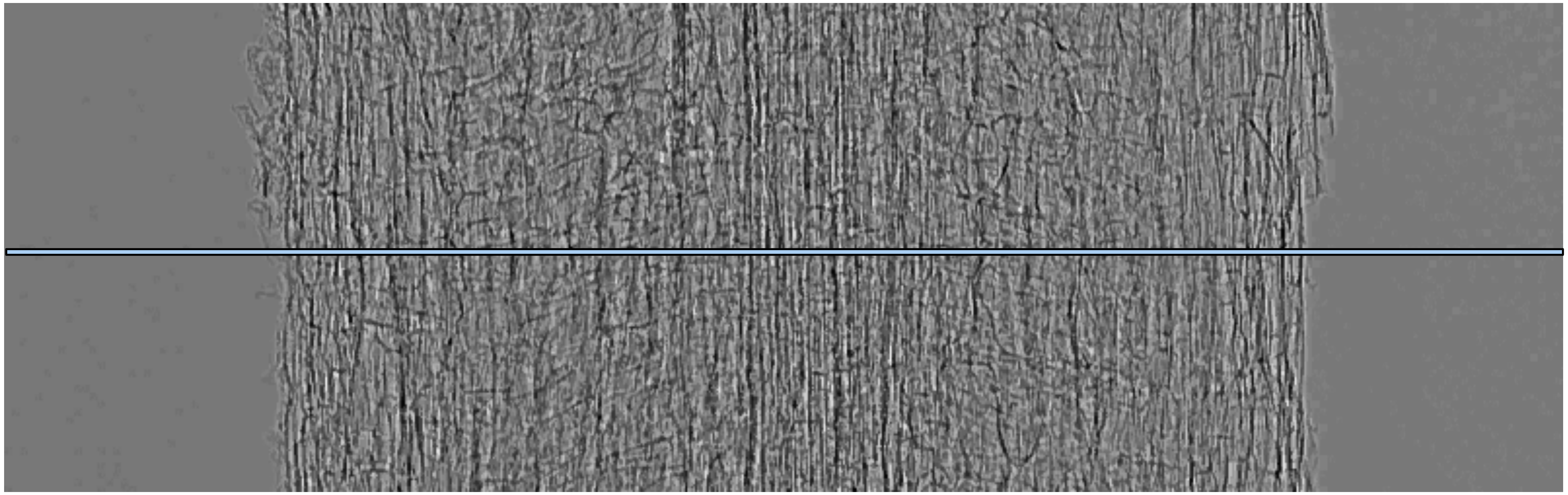

energy: 20 keV
L = 50 mm
pixel size: 1.4 µm

3D Reconstruction

Many slices:

3D structure

root of mahogany tree
(W. H. Schröder, FZ Jülich)

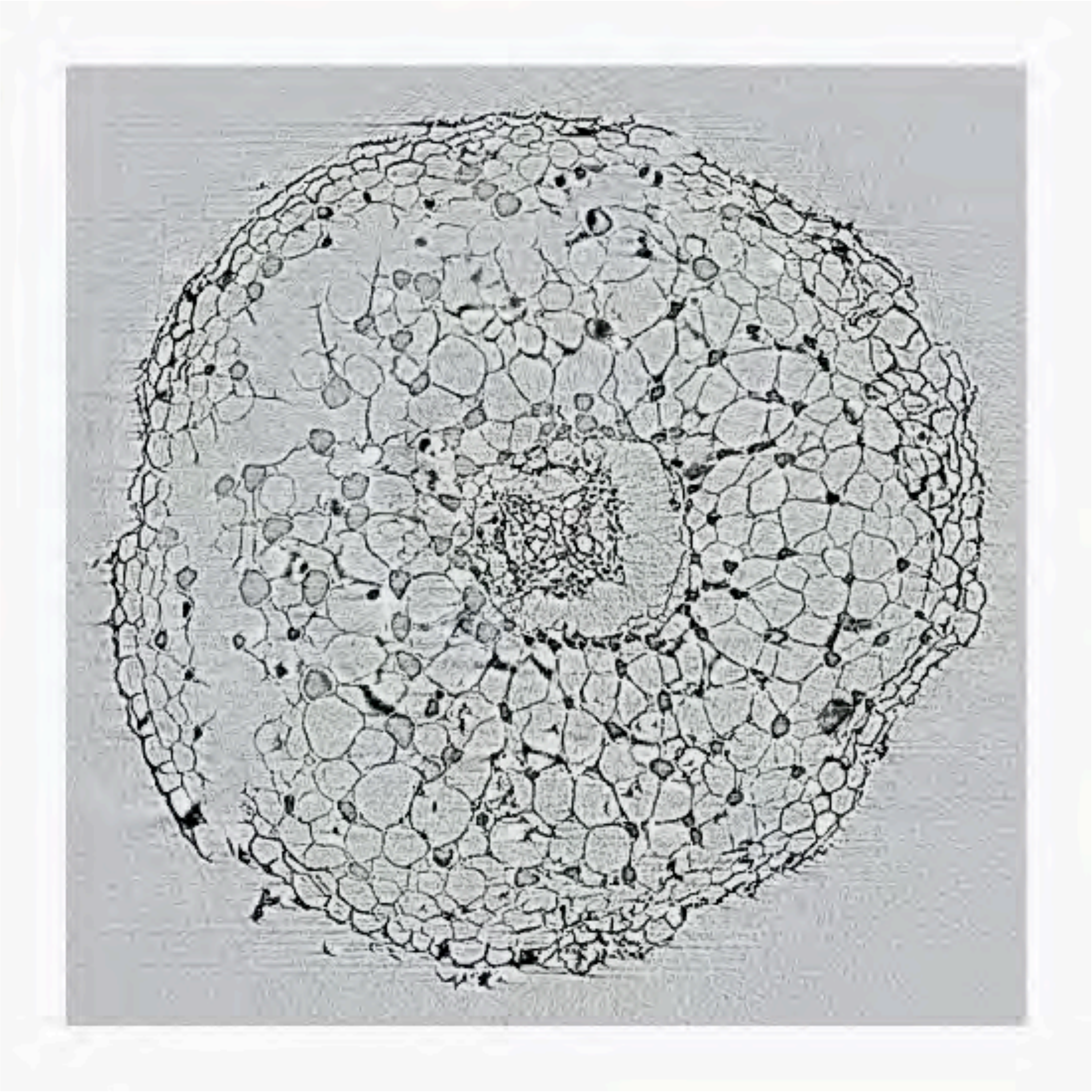

resolution: ~ 3 µm

Visualize Catalysts in Action

Methane often wasted during oil production:

First step to convert methane into liquid fuels (syngas production):

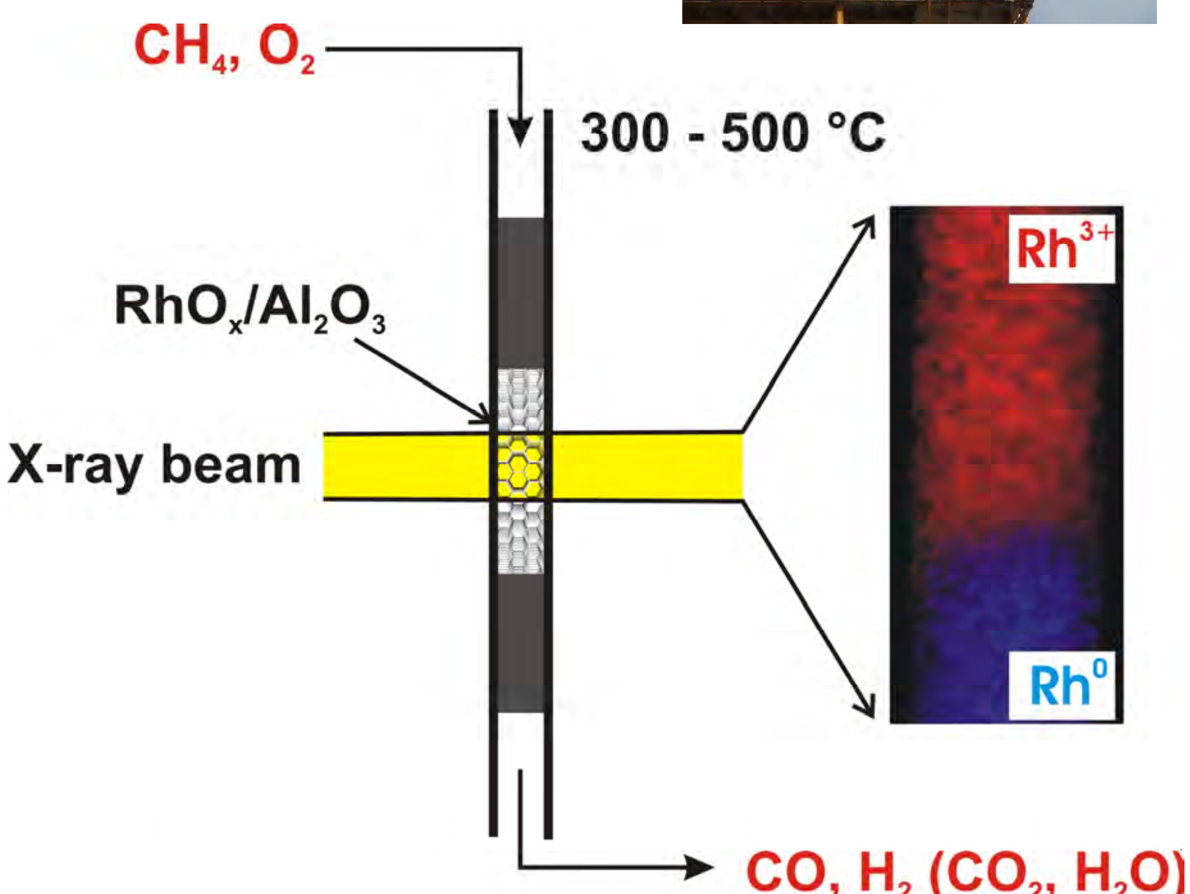

Grunwaldt, et al.,
J. Chem. Phys. B **110,** 8674 (2006)

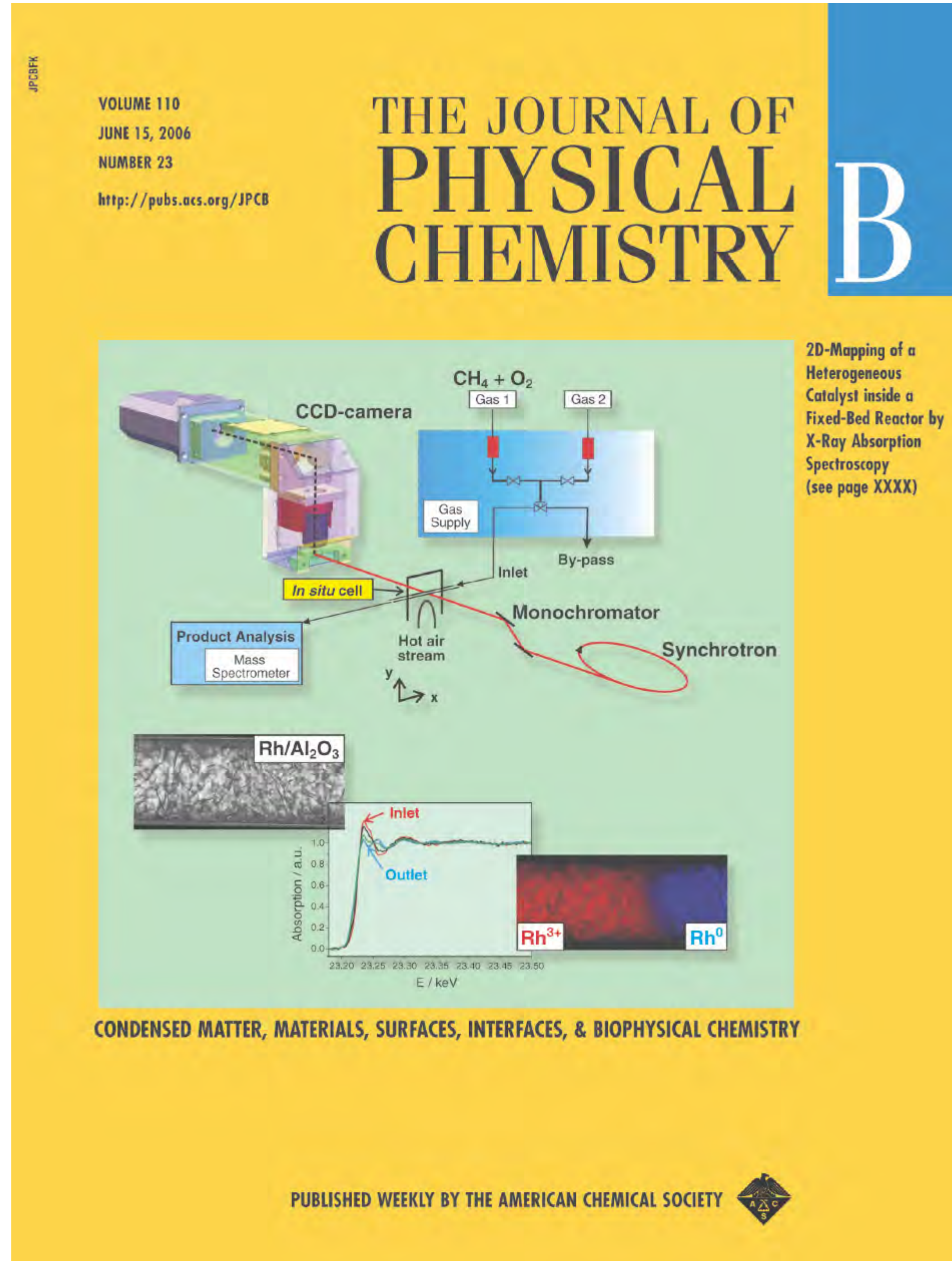

Visualize Catalysts in Action

Methane often wasted during oil production:

First step to convert methane into liquid fuels (syngas production):

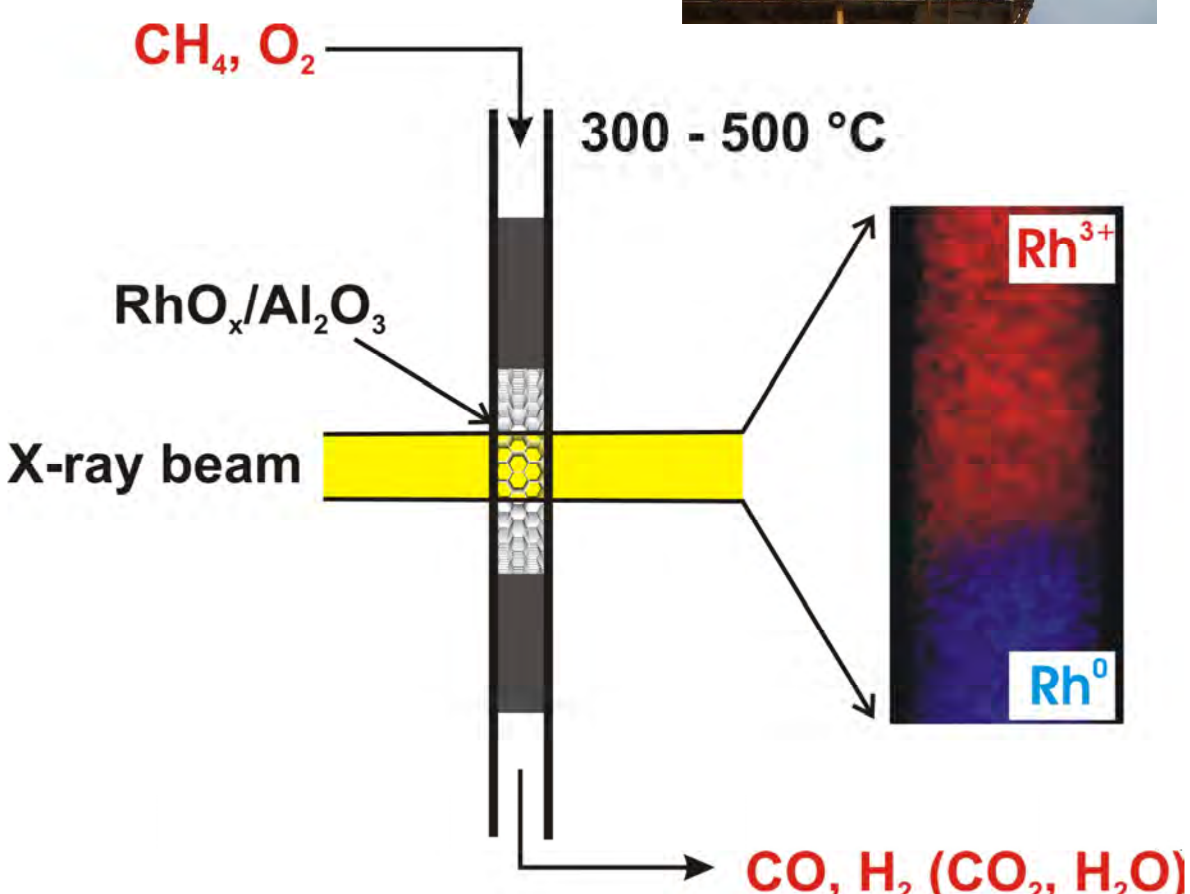

Grunwaldt, et al.,
J. Chem. Phys. B **110,** 8674 (2006)

Combustion of methane:

$$CH_4 + 2O_2 \longrightarrow CO_2 + 2H_2O$$

(exothermal: -801,7kJ/mol)

reforming of methane to H_2:

$$CH_4 + H_2O \xrightarrow{Rh} CO + 3H_2$$

(endothermal: 206.1kJ/mol)

$$CH_4 + CO_2 \xrightarrow{Rh} 2CO + 2H_2$$

(endothermal: 247,5kJ/mol)

potentially other reaction:
direct partial oxidation:

$$2CH_4 + O_2 \xrightarrow{Rh} 2CO + 8H_2$$

(exothermal: -35,5kJ/mol)

X-Ray Absorption: Lambert-Beer Law

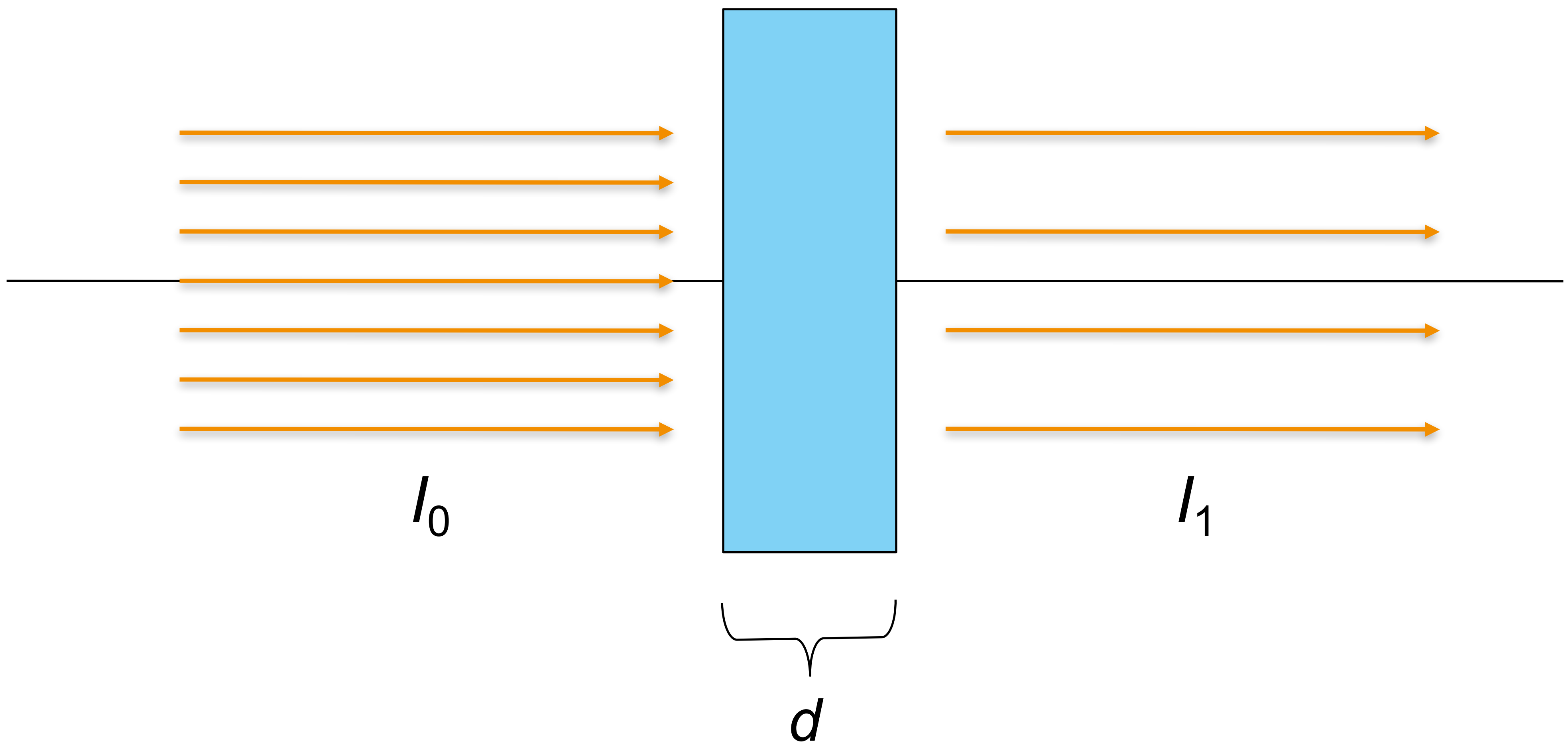

$$I_1(E) = I_0(E) \cdot \exp\left[-\mu(E)d\right]$$

$\mu(E)$: linear attenuation coefficient

$$\mu(E) \cdot d = \ln\left(\frac{I_0}{I_1}\right)$$

Photo Absorption

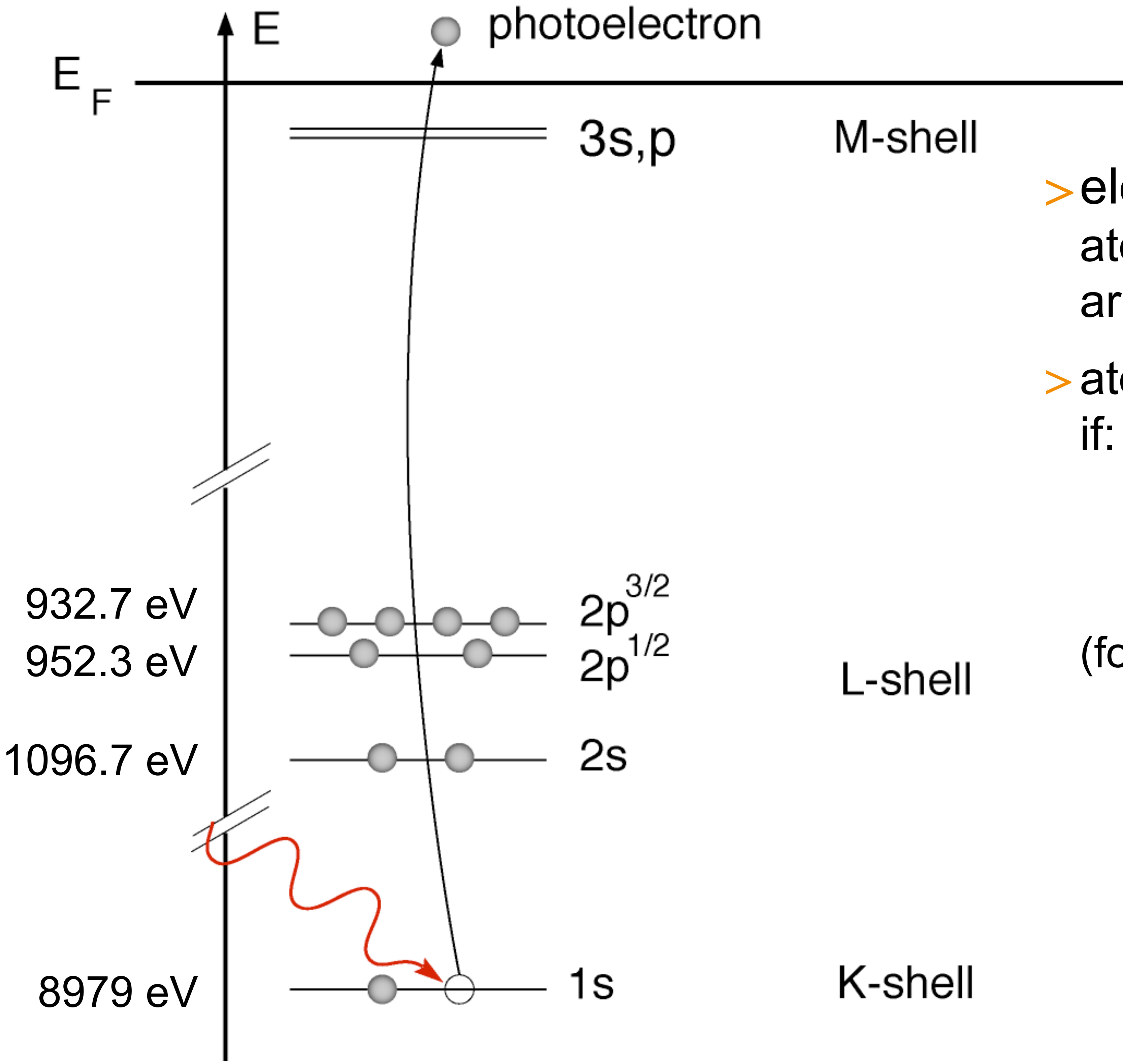

- electrons populate specific atomic states: binding energies are atom specific: K, L, M
- atom can absorb x-ray photon if:

$$E_{\text{photon}} > E_{\text{ionization}}$$

(follows from Pauli principle)

Example: Absorption in Cu & Ag

μ(E): linear attenuation coefficient

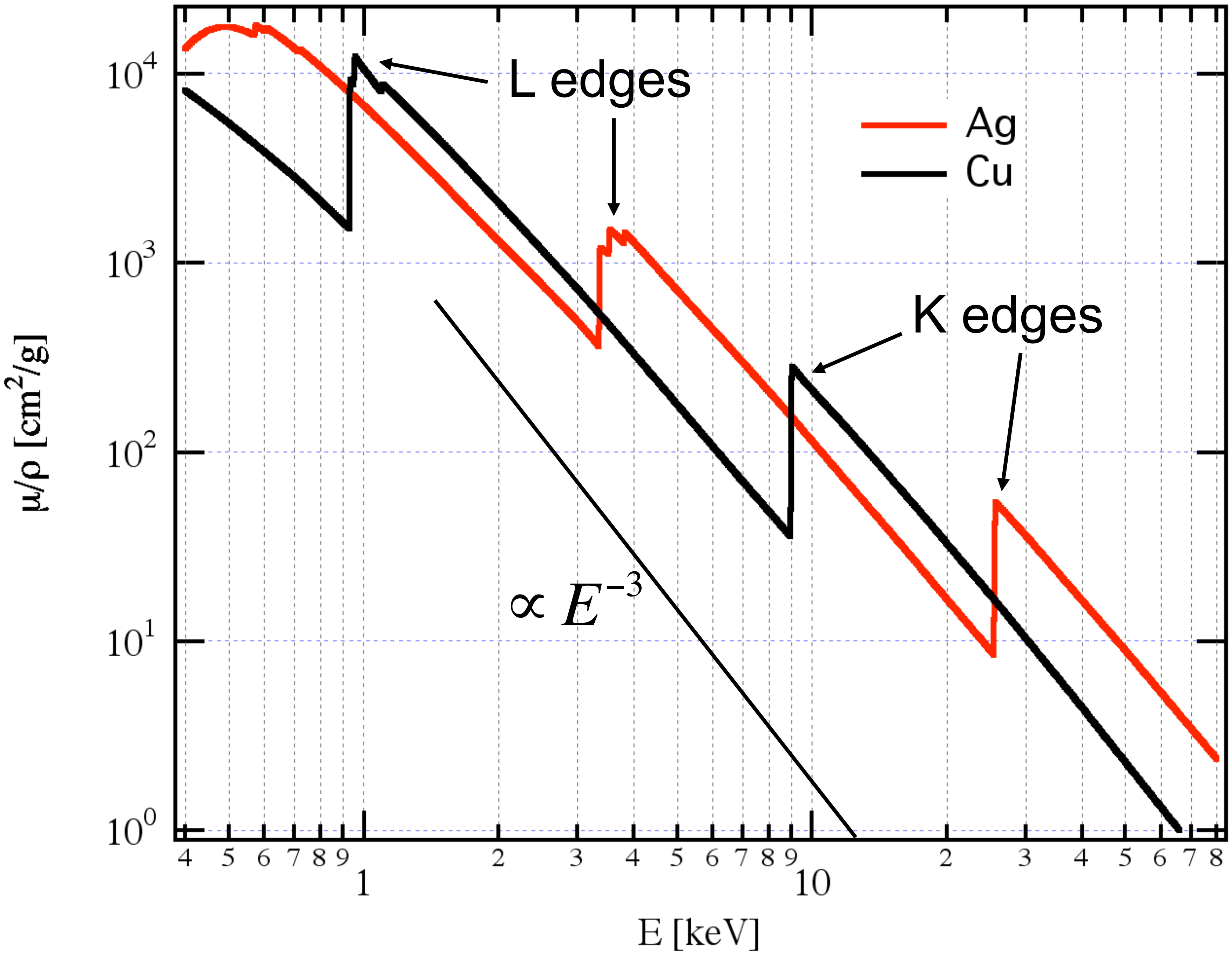

- mainly atomic effect
- strong dependence on x-ray energy:

  $$\propto E^{-2.78}$$

- strong dependence on atomic number:

  $$\propto Z^{2.7}$$

- larges contribution from inner shells

Example: Absorption in Cu

μ(E): linear attenuation coefficient

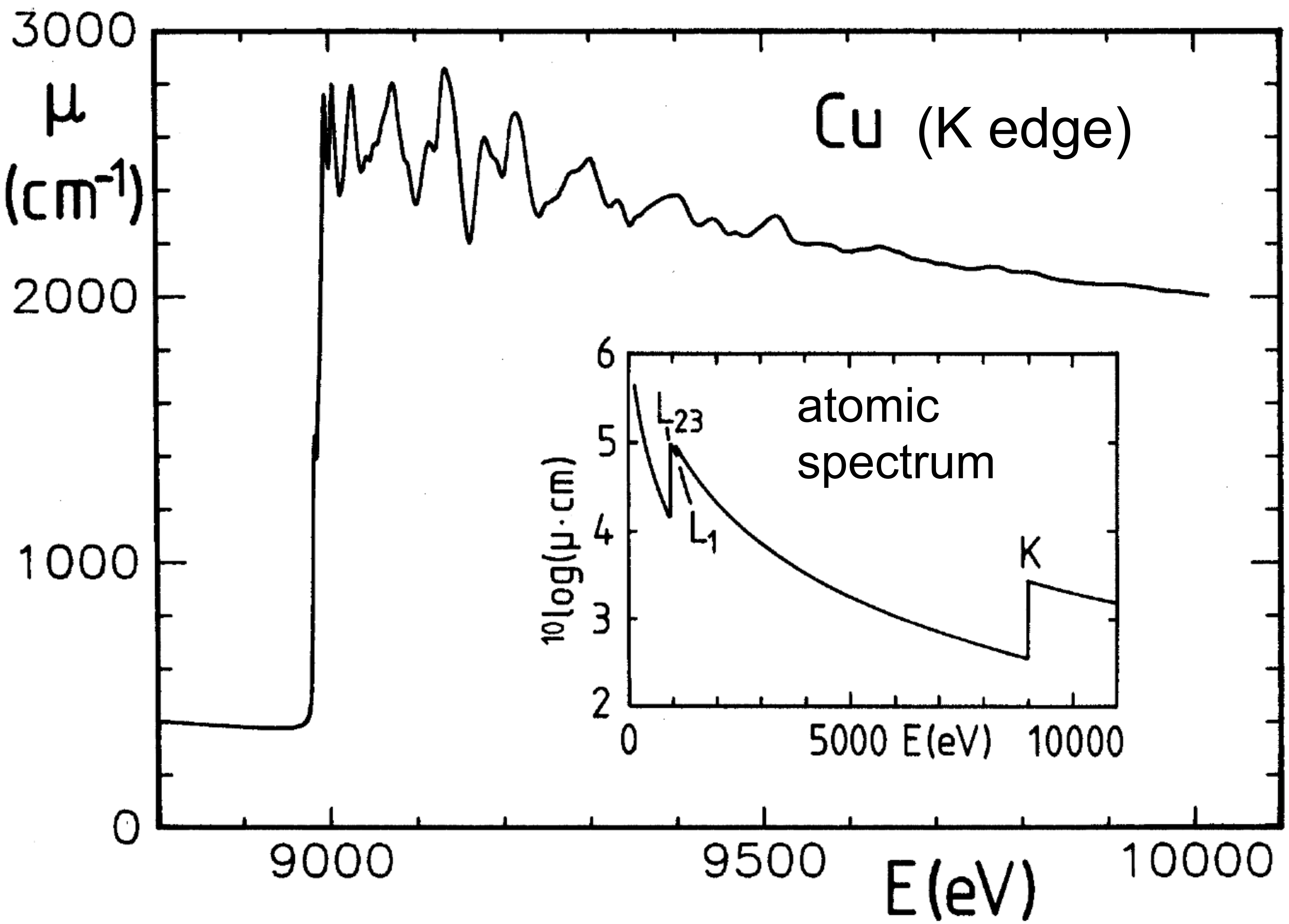

Metallic Cu:

mainly atomic effect

fine structure in solid:
X-ray Absorption Fine Stucture

X-ray Absorption Spectrum

Three characteristic features:

- Energy of absorption edge: oxidation state
- Near-edge region: (XANES: x-ray absorption near edge structure) local, projected density of states
- Extended fine structure: (EXAFS: extended x-ray absorption fine structure) local chemical environment of atomic species

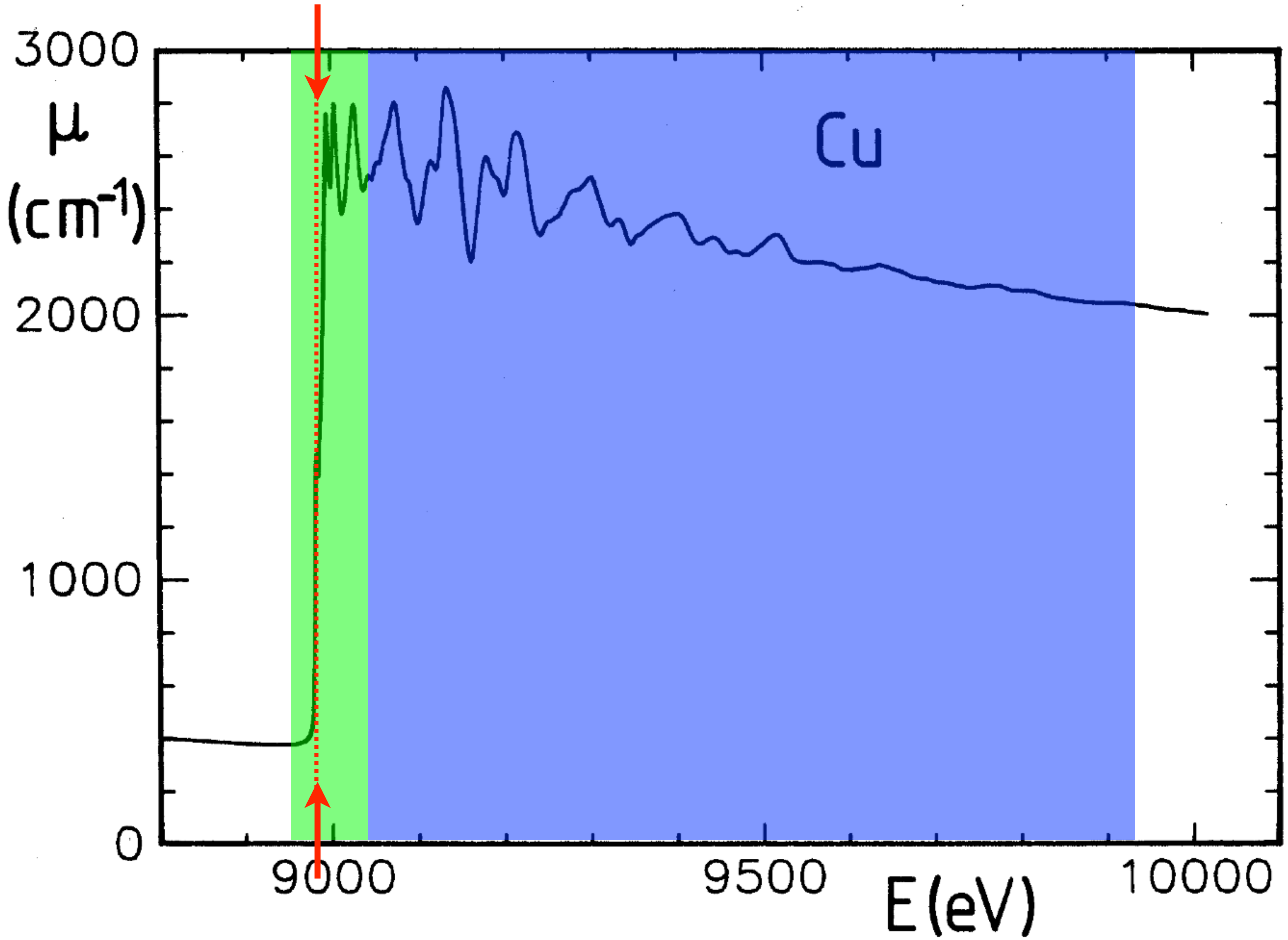

Energy of Absorption Edge

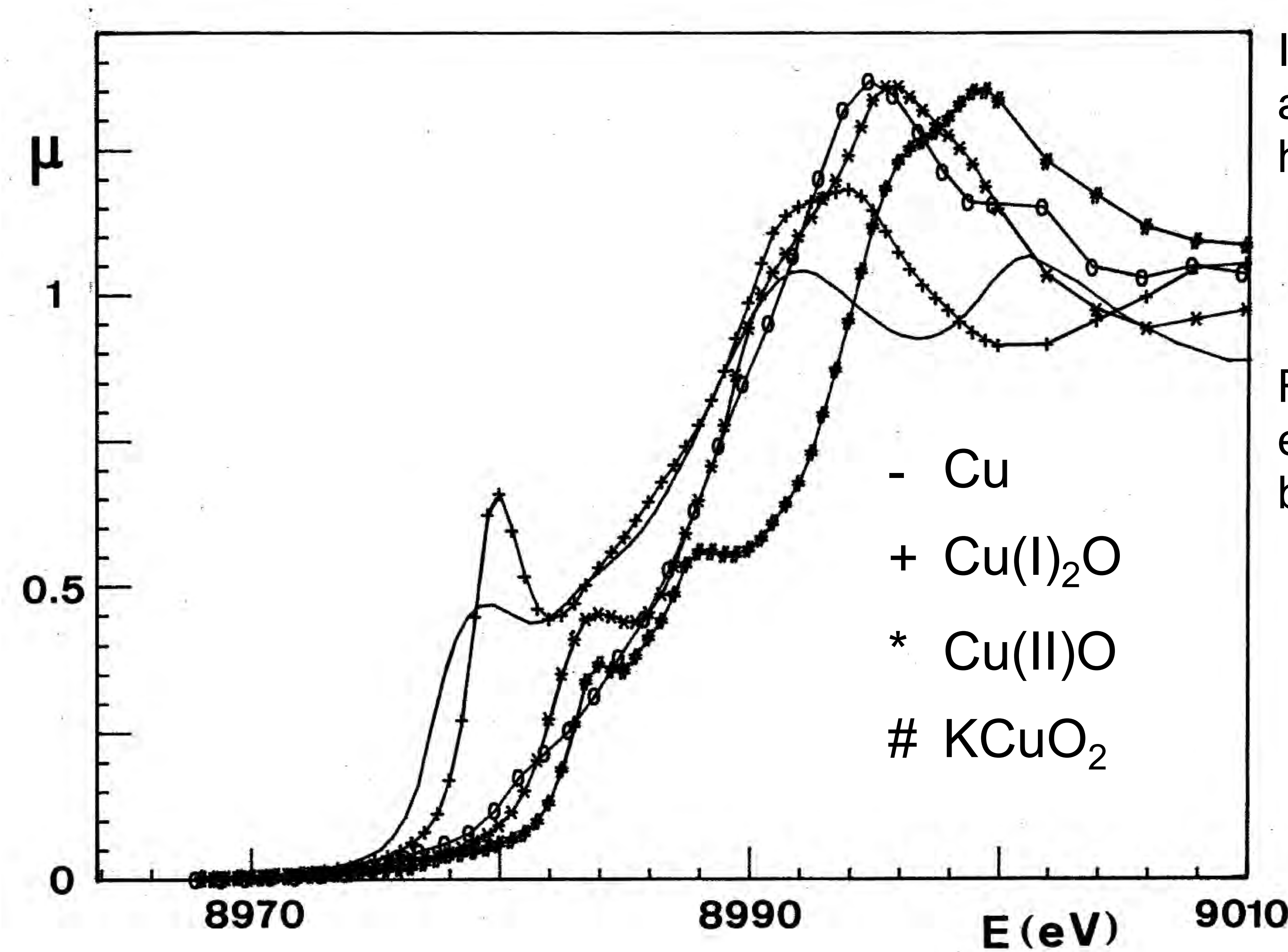

Increasing oxidation state: absorption edge shifts to higher x-ray energies

Reduced screening of electric field of nucleus by valence electrons:

other electrons more tightly bound!

Shape of Near-Edge Spectrum

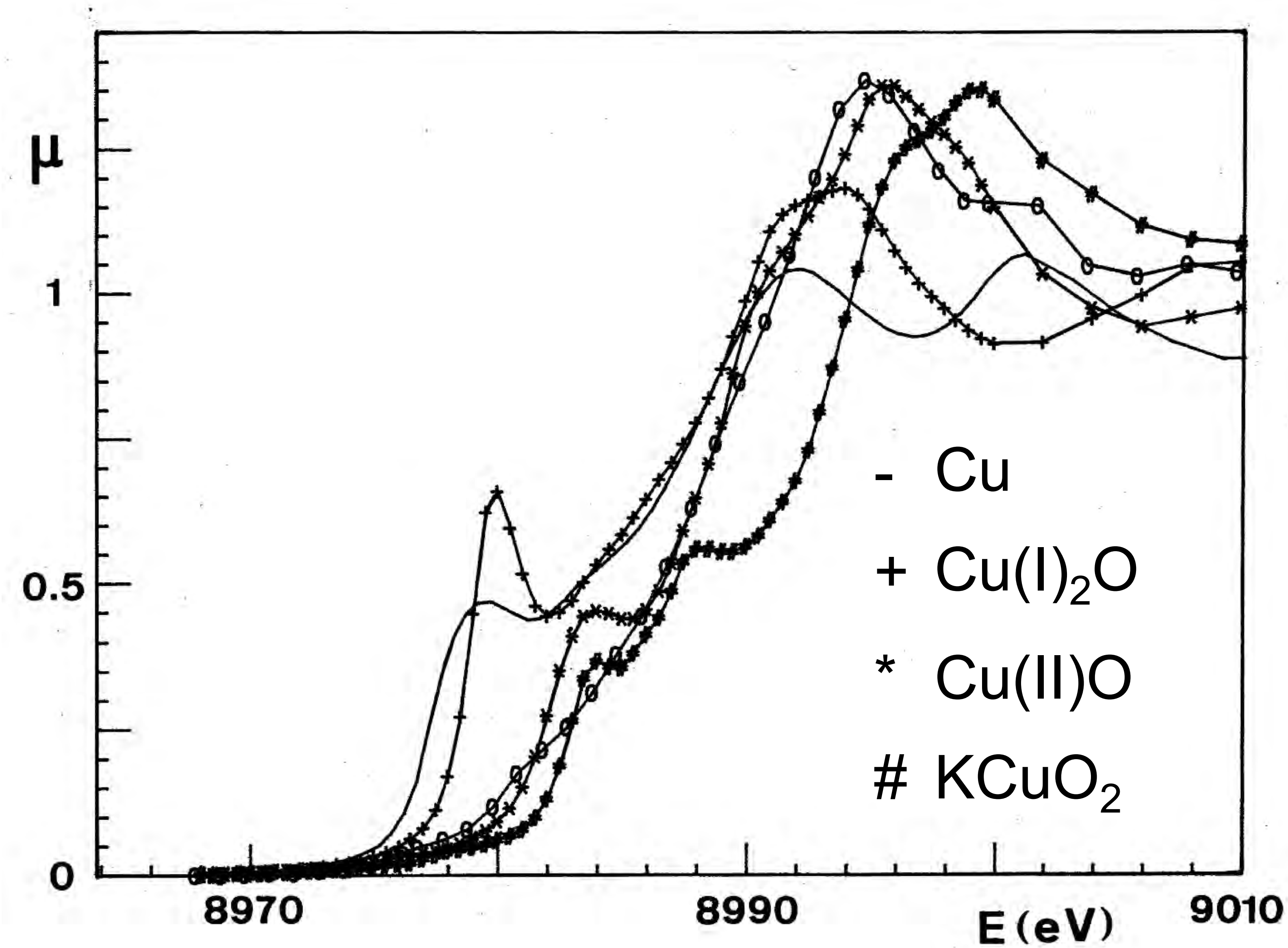

depends on density of states available to photoelectron

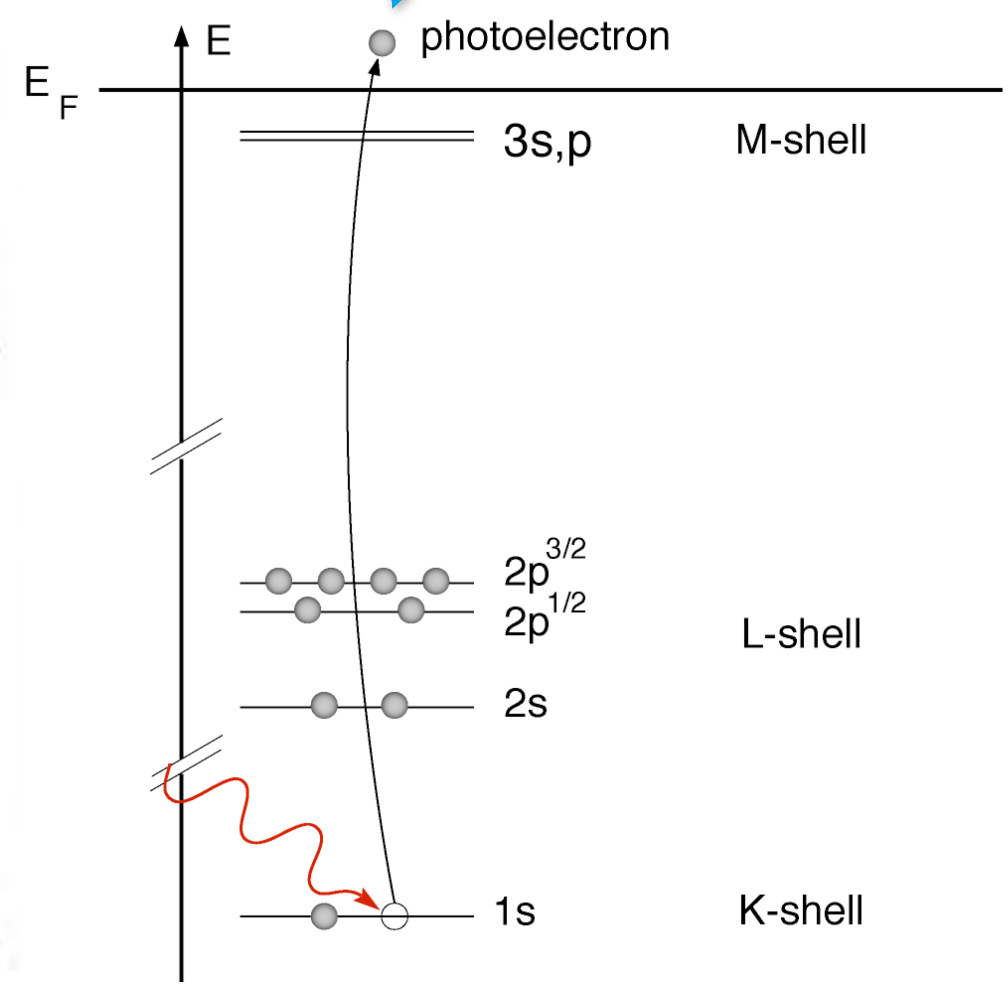

Shape of spectrum:

> can be modeled by methods in theoretical solid state physics

> can be used as „fingerprint“ to identify a given chemical environment

Visualize Catalysts in Action

Methane often wasted during oil production:

First step to convert methane into liquid fuels (syngas production):

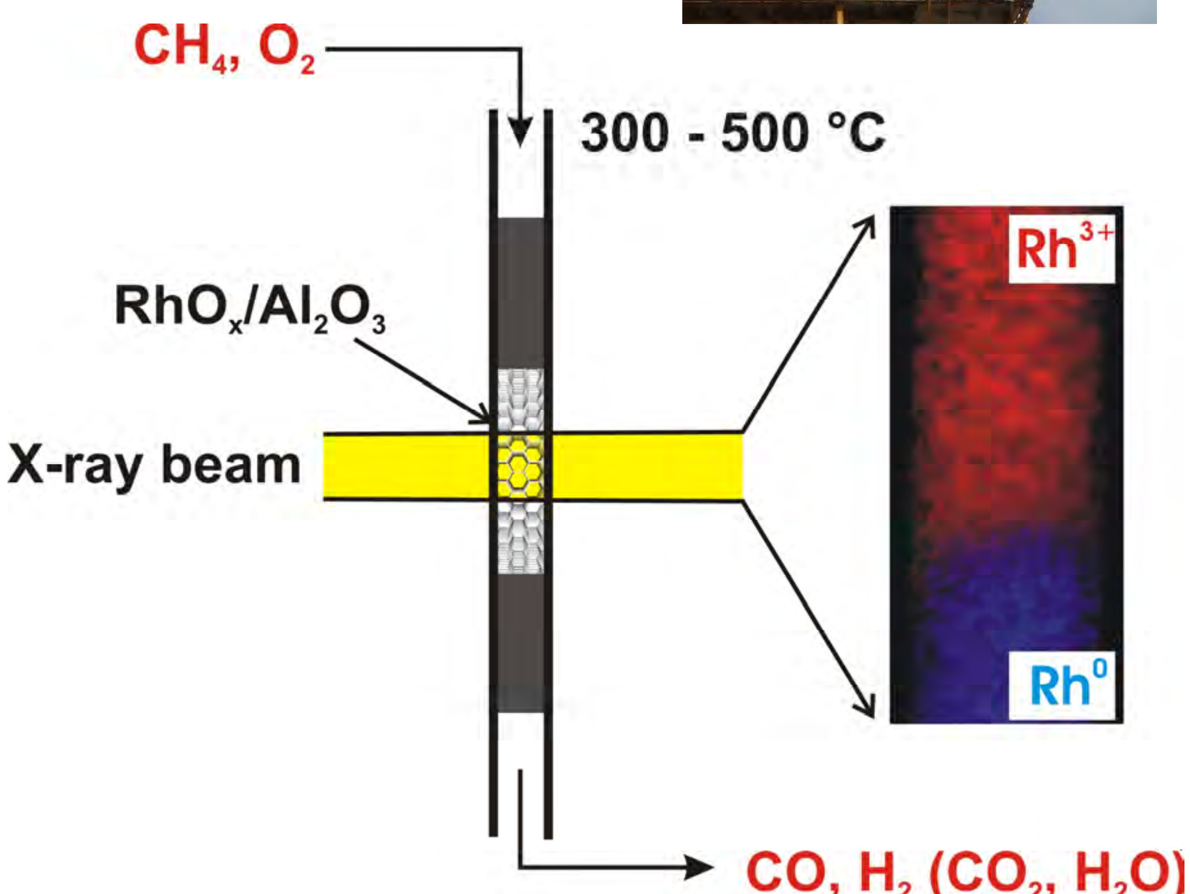

Grunwaldt, et al.,
J. Chem. Phys. B **110,** 8674 (2006)

Combustion of methane:

$$CH_4 + 2O_2 \longrightarrow CO_2 + 2H_2O$$

(exothermal: -801,7kJ/mol)

reforming of methane to H_2:

$$CH_4 + H_2O \xrightarrow{Rh} CO + 3H_2$$

(endothermal: 206.1kJ/mol)

$$CH_4 + CO_2 \xrightarrow{Rh} 2CO + 2H_2$$

(endothermal: 247,5kJ/mol)

potentially other reaction:
direct partial oxidation:

$$2CH_4 + O_2 \xrightarrow{Rh} 2CO + 8H_2$$

(exothermal: -35,5kJ/mol)

Visualize Catalysis

In-situ transmission imaging of catalyst bed inside chemical reactor

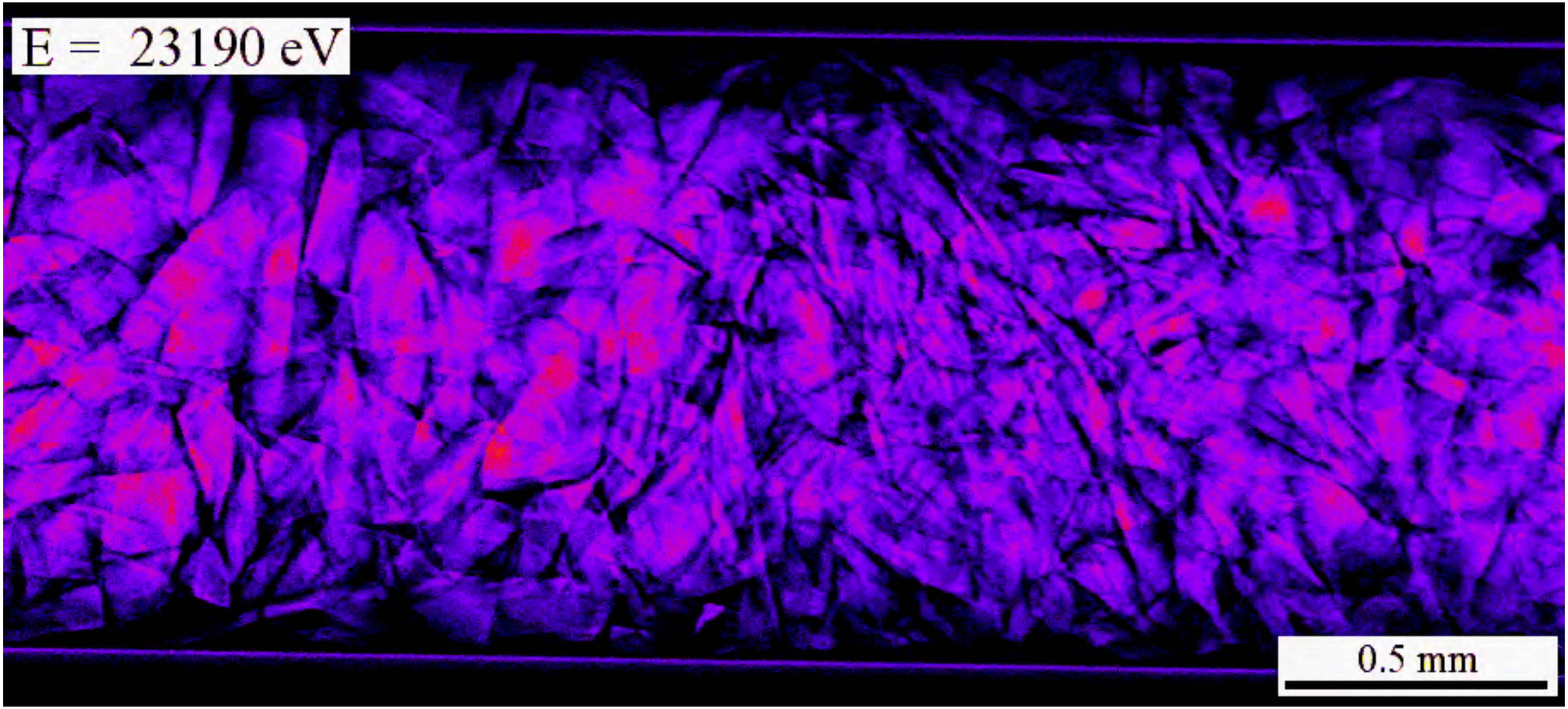

Grunwaldt, et al.,
J. Chem. Phys. B **110,** 8674 (2006)

Visualize Catalysis

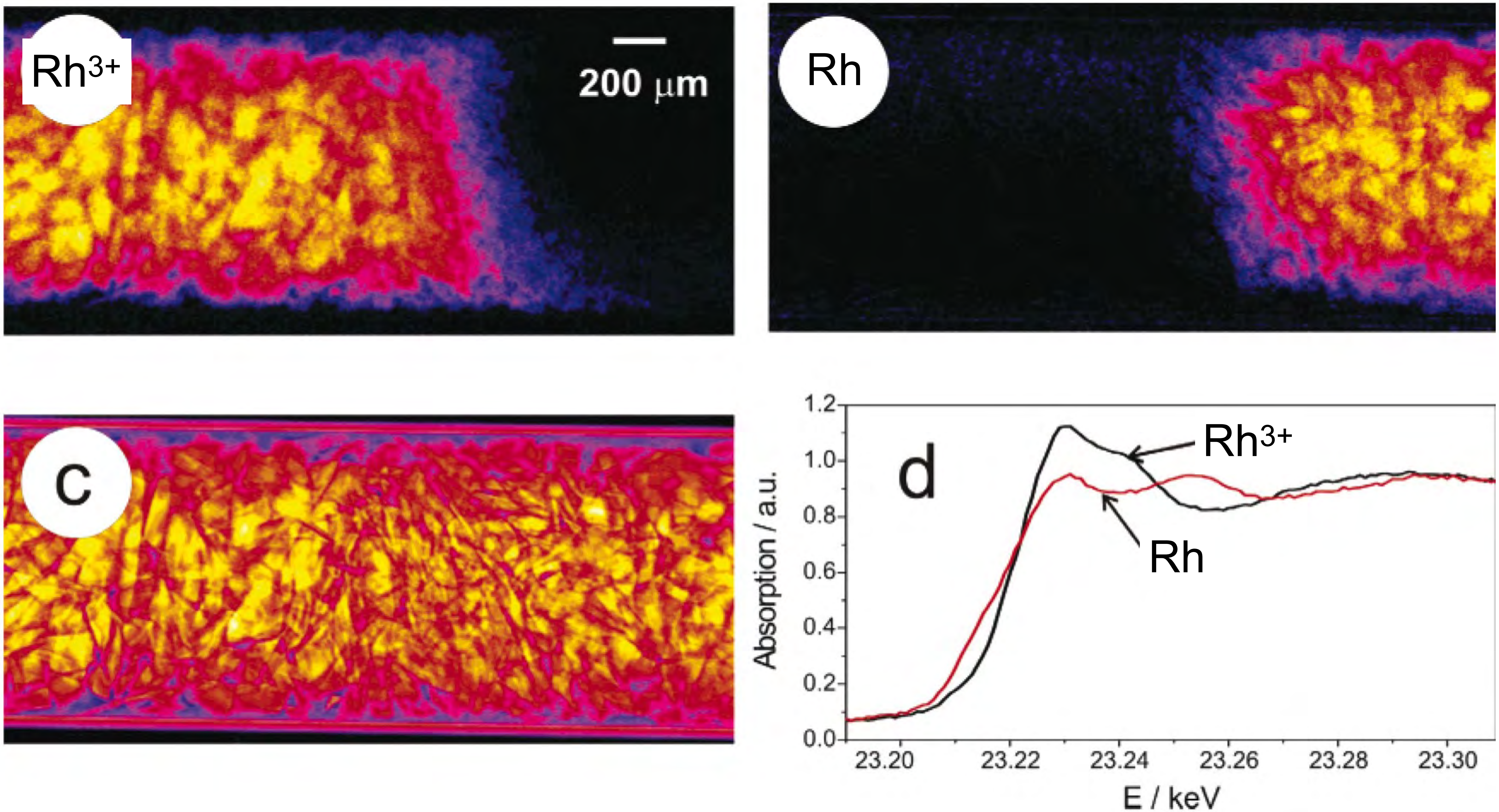

Grunwaldt, et al.,
J. Chem. Phys. B **110,** 8674 (2006)

Visualize Catalysis

$$2\,CH_4 + O_2 \rightarrow 2\,CO + 4\,H_2$$

direction of flow

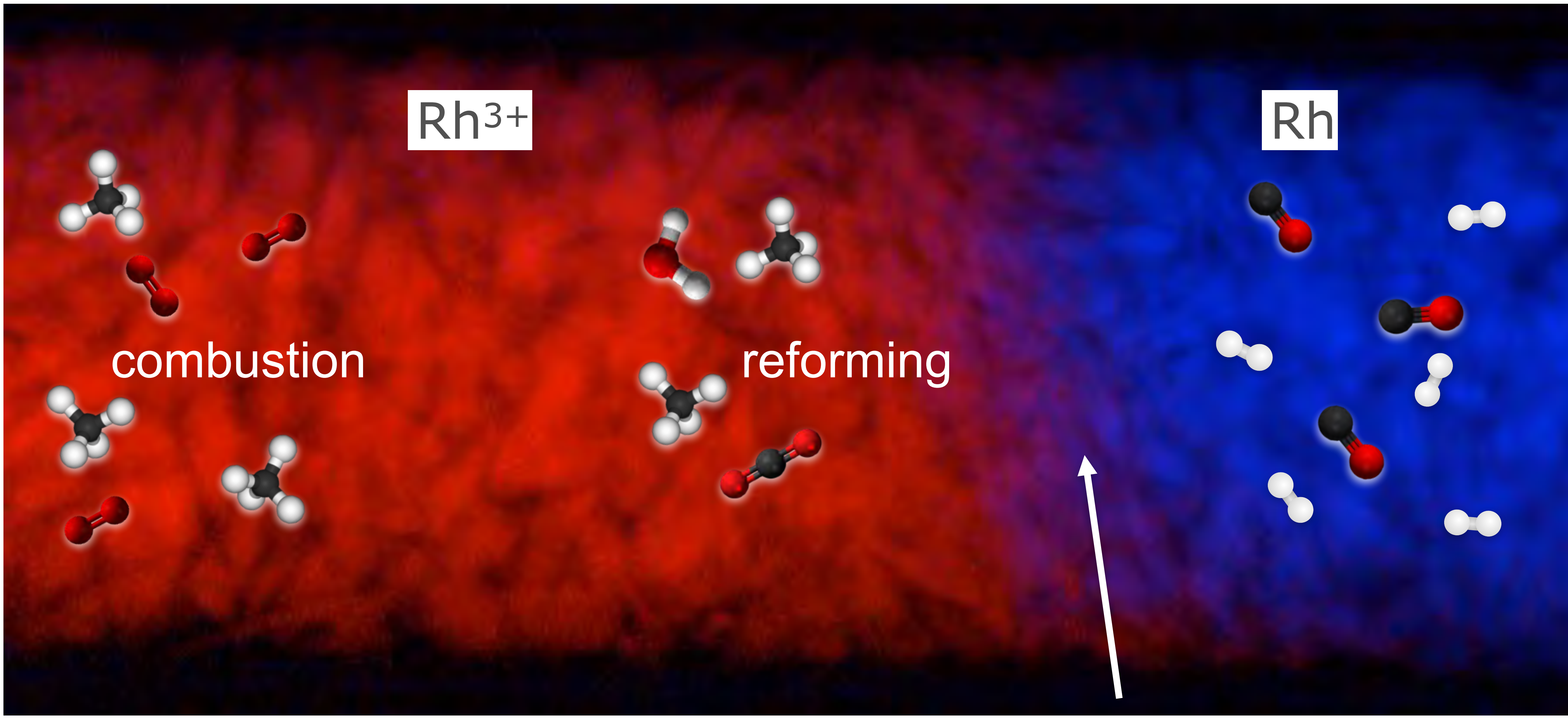

Grunwaldt, et al.,
J. Chem. Phys. B **110,** 8674 (2006)

production of hydrogen
Rh is reduced!

Filming the Ignition of a Catalytic Reaction

Partial oxidation of Methane by reforming

CH_4
O_2

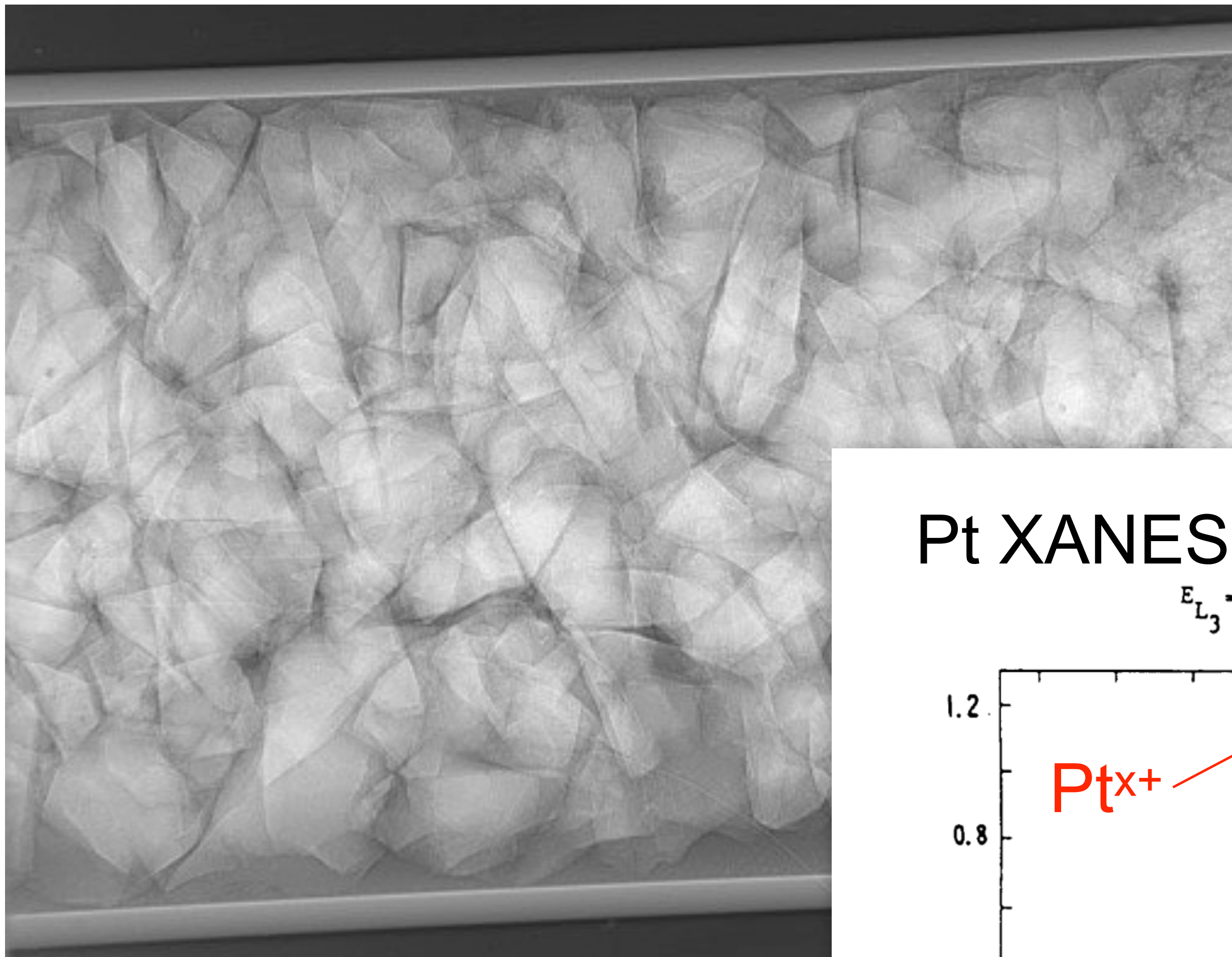

Pt particles on alumina powder in capillary

T ~ 350°C

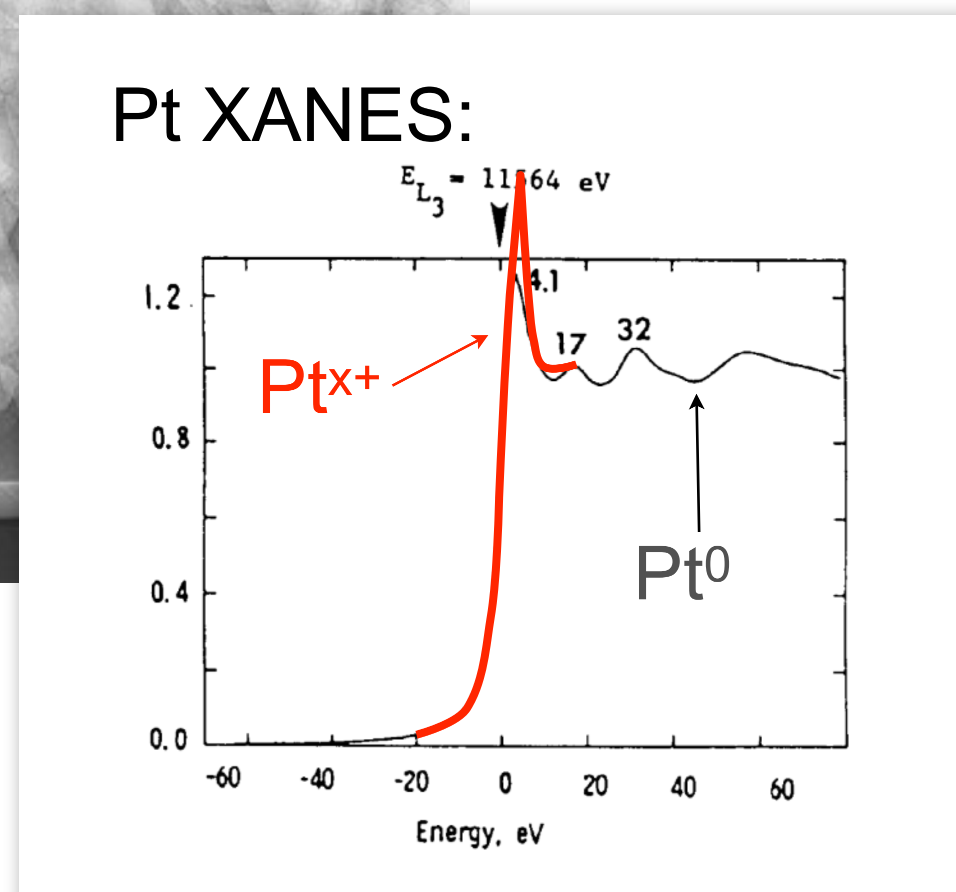

B. Kimmerle, et al.,
J. Phys. Chem. C **113,** 3037 (2009)

Filming the Ignition of a Catalytic Reaction

Partial oxidation of Methane by reforming

Imaging difference compared to oxidized catalyst:

end of
reactor
bed

$\Delta t = 0.25$ s

Pt XANES:

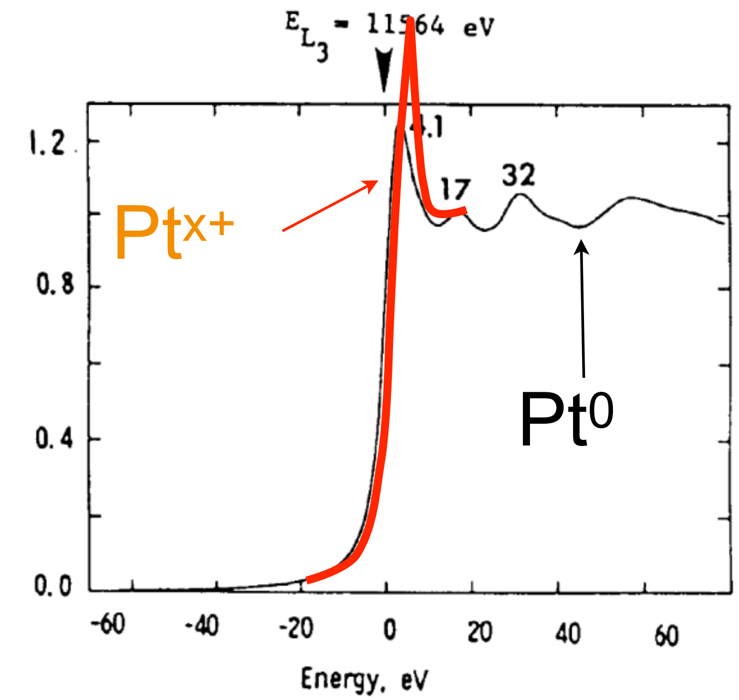

→ Catalyst is being reduced when reforming reaction ignites

B. Kimmerle, et al.,
J. Phys. Chem. C **113,** 3037 (2009)

X-Ray Microscopy Techniques: Full-Field Imaging

Projection imaging:

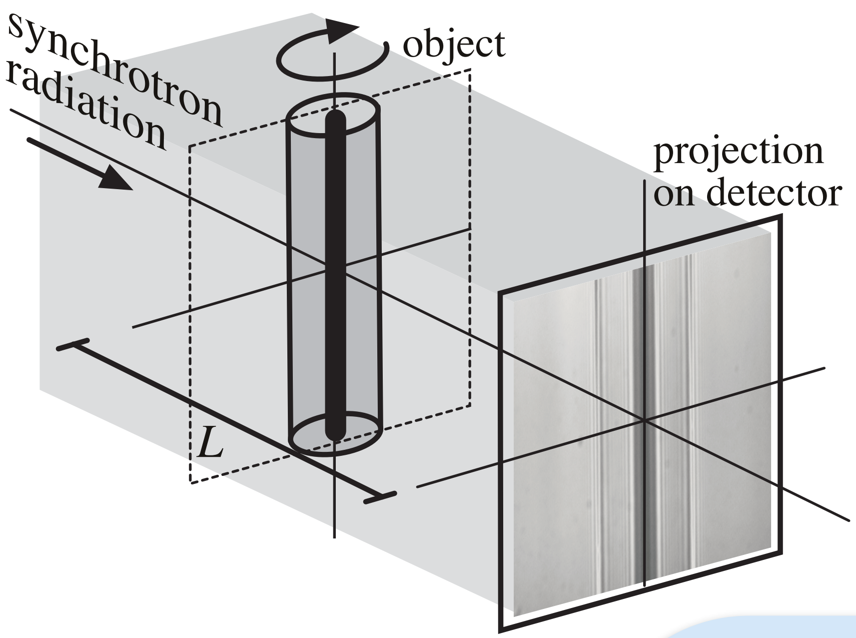

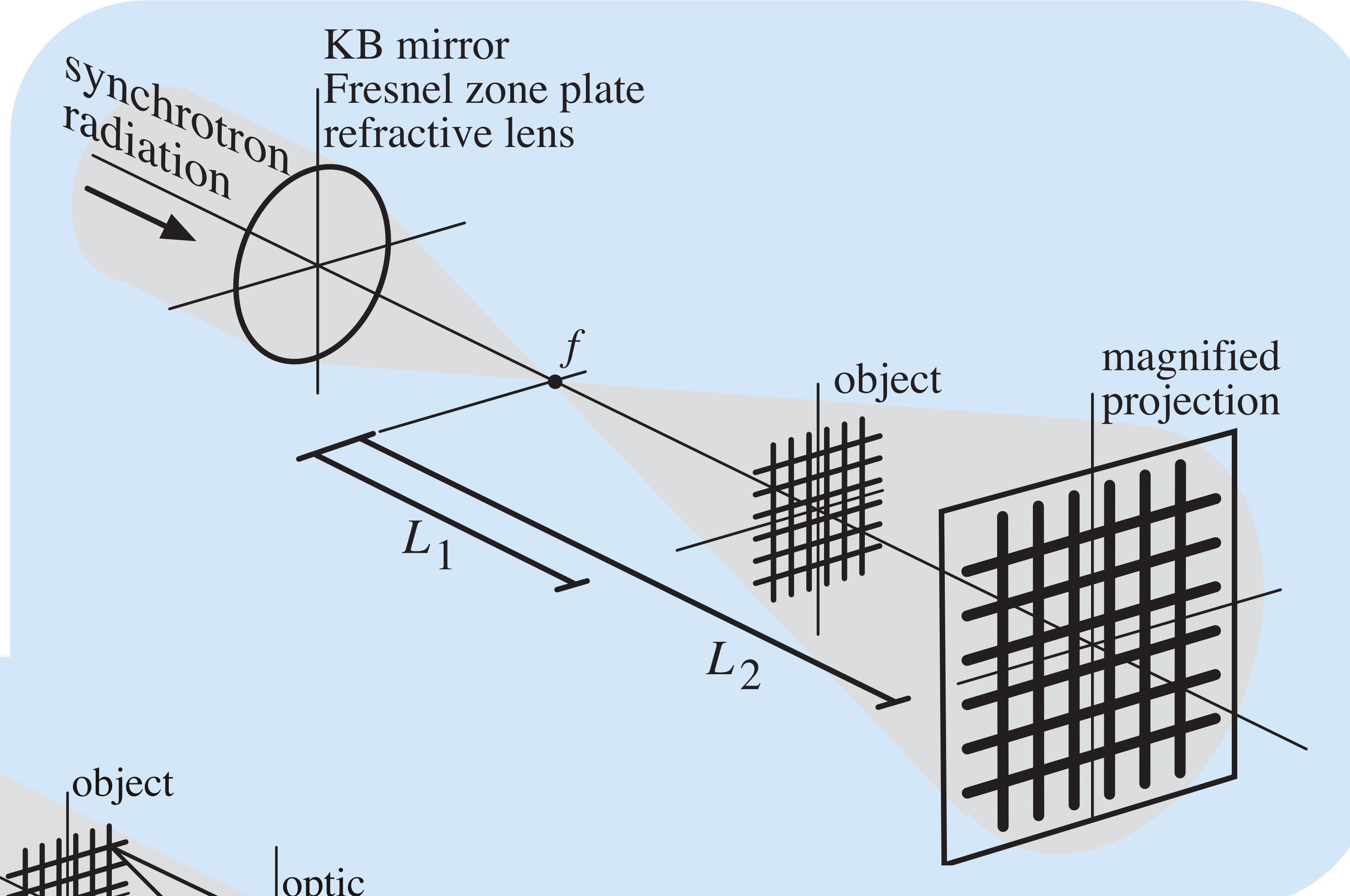

Imaging through objective lens:

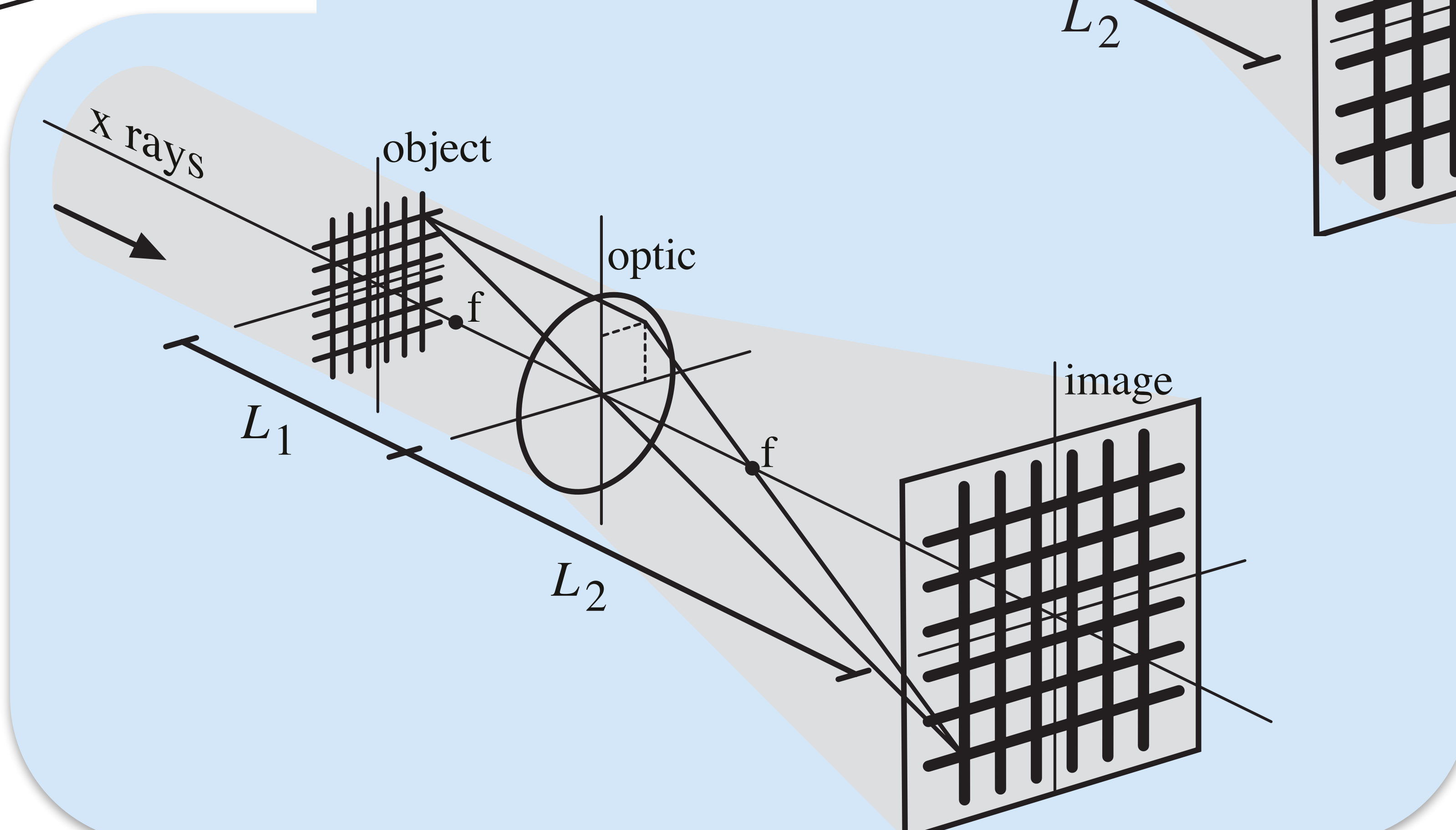

x-rays focused by condensor (aperture matching)

Full-Field X-Ray Microscopy

Magnifying imaging by objective:

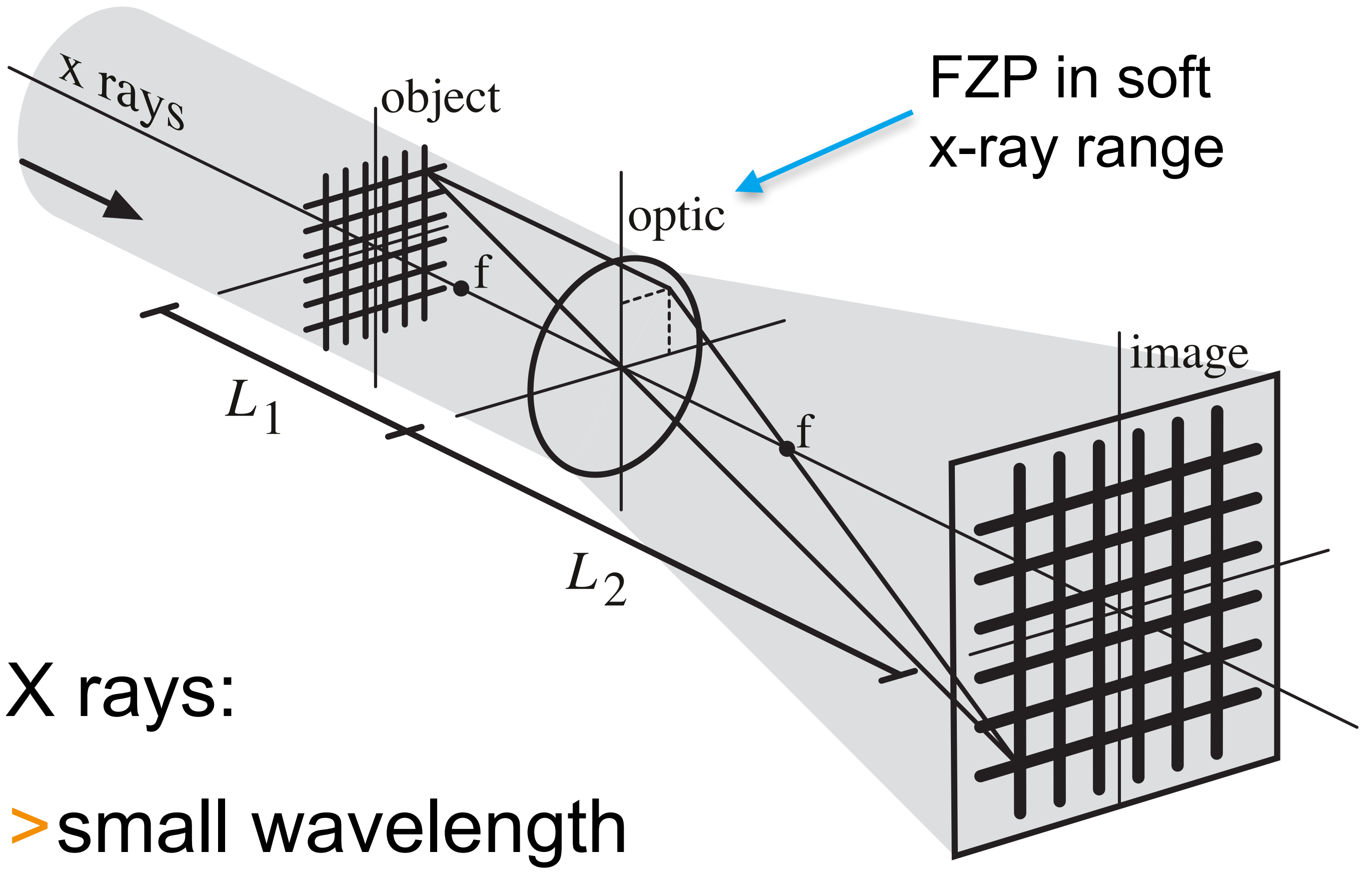

X rays:

- small wavelength
- limited numerical aperture α

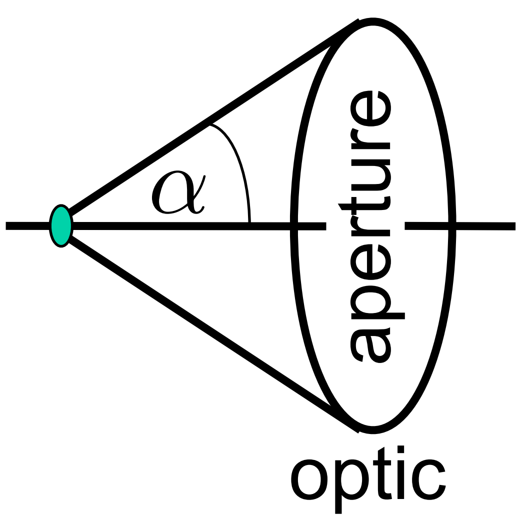

resolution (E. Abbe):

$$d = \frac{\lambda}{2 \sin \alpha}$$

Example: soft x-ray imaging of cells (high contrast in water window)

adenocarcinoma (mouse)

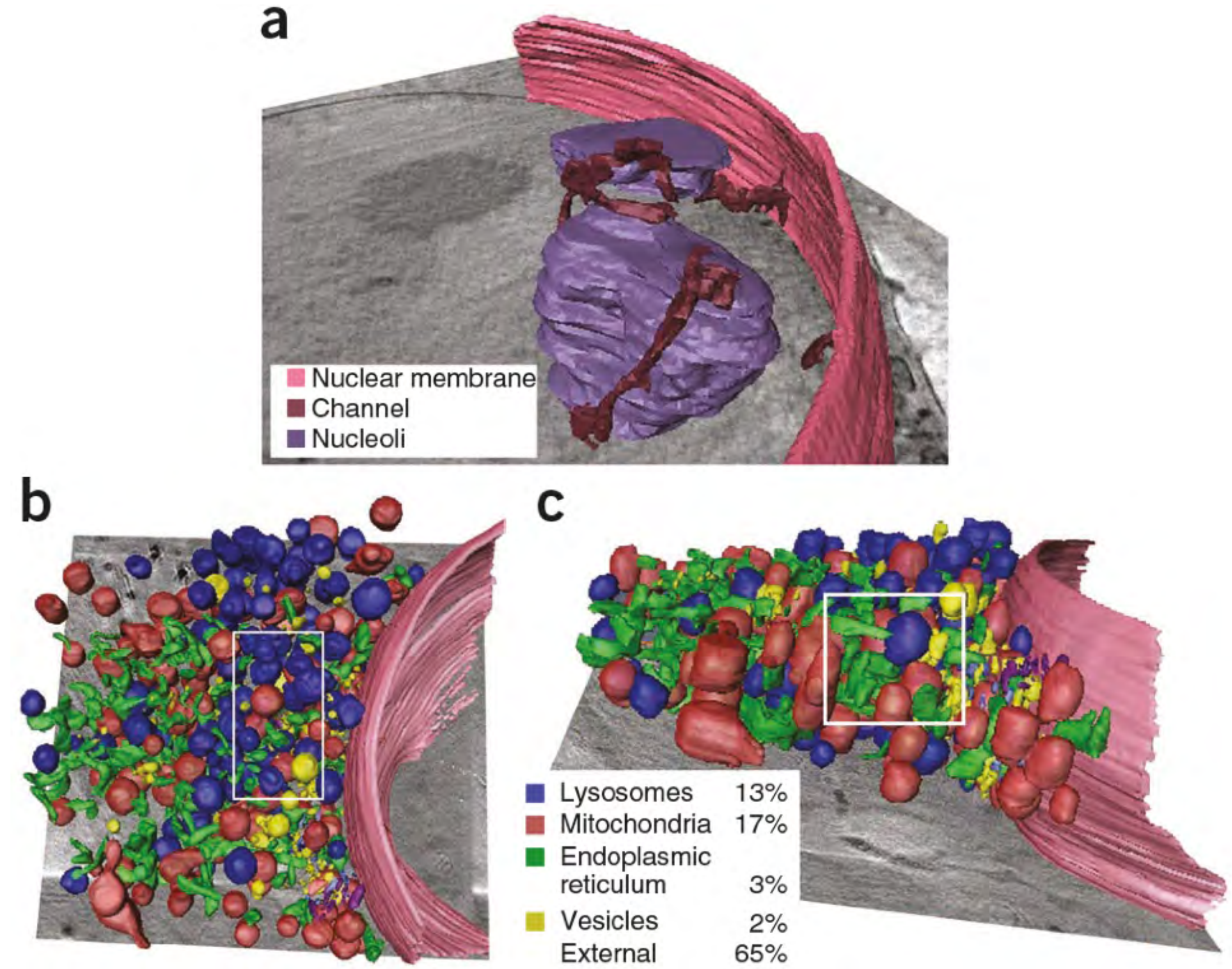

G. Schneider, et al., Nature Methods (2010). BESSY II, HZB

resolution: ca. 70 nm
$(\lambda \approx 2.4\ \mathrm{nm}, \alpha = 3.3^\circ)$

Scanning Microscopy and Tomography: Nanoprobe

X rays are focused onto the sample

raster scan sample through beam:

→ get x-ray analytical information locally and on nanoscale (resolution limited by focus size).

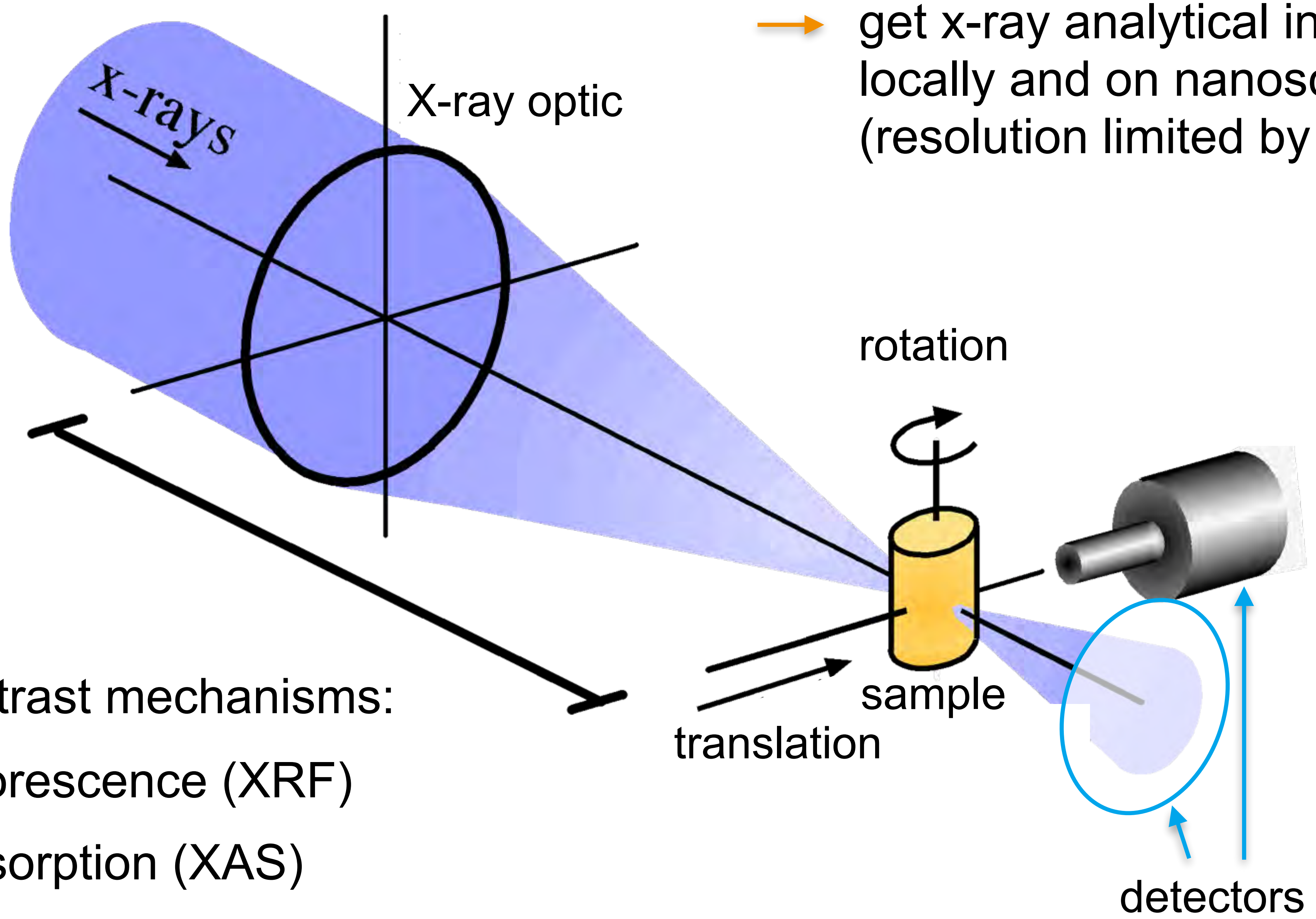

different contrast mechanisms:

- x-ray fluorescence (XRF)
- x-ray absorption (XAS)
- x-ray diffraction (XRD, SAXS, WAXS)
- maybe in future even IXS (RIXS)
- …

X-Ray Scanning Microscopy and Tomography

> Fluorescence microtomography

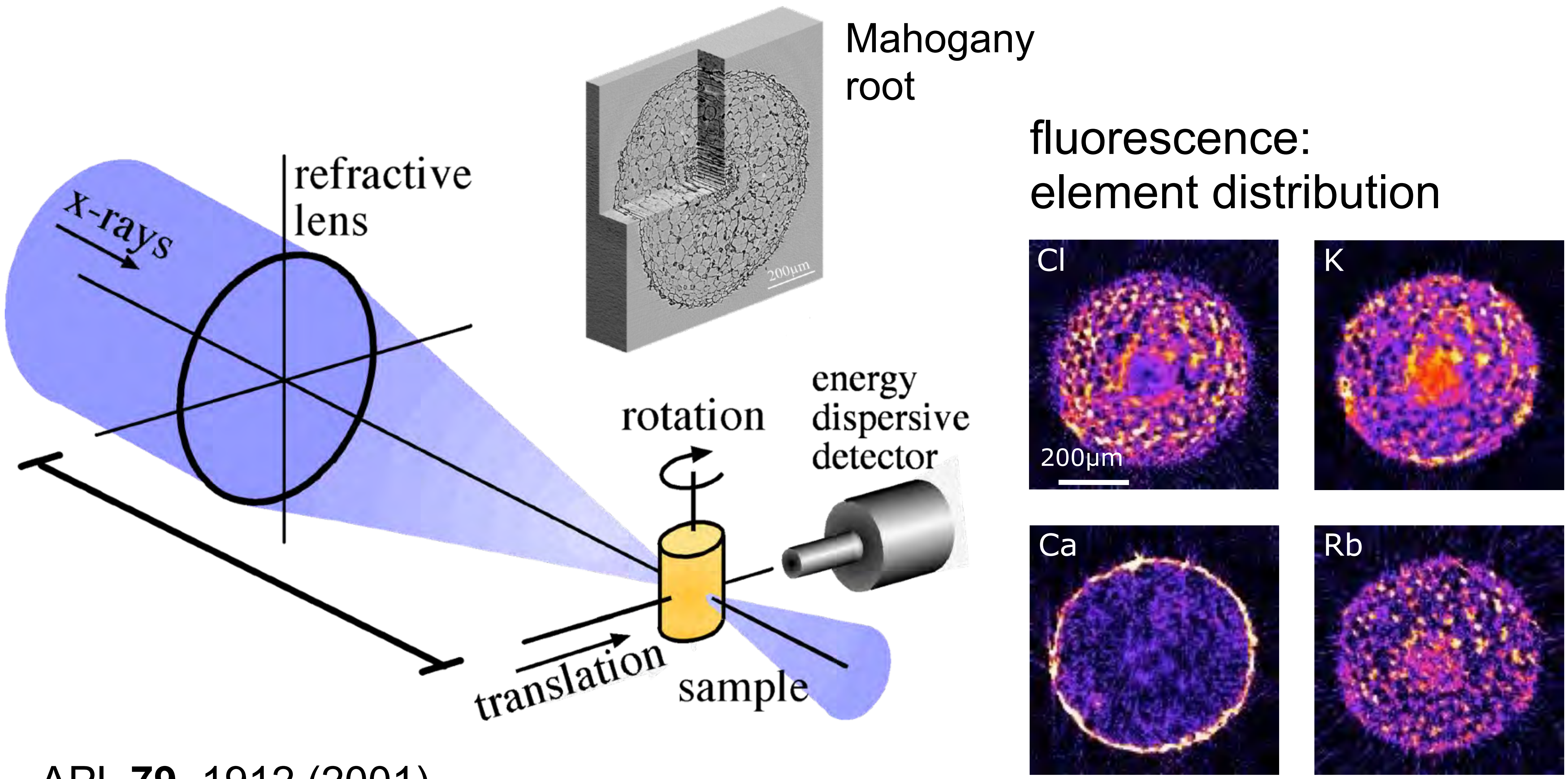

APL **79**, 1912 (2001).

X-Ray Scanning Microscopy and Tomography

> Fluorescence mic

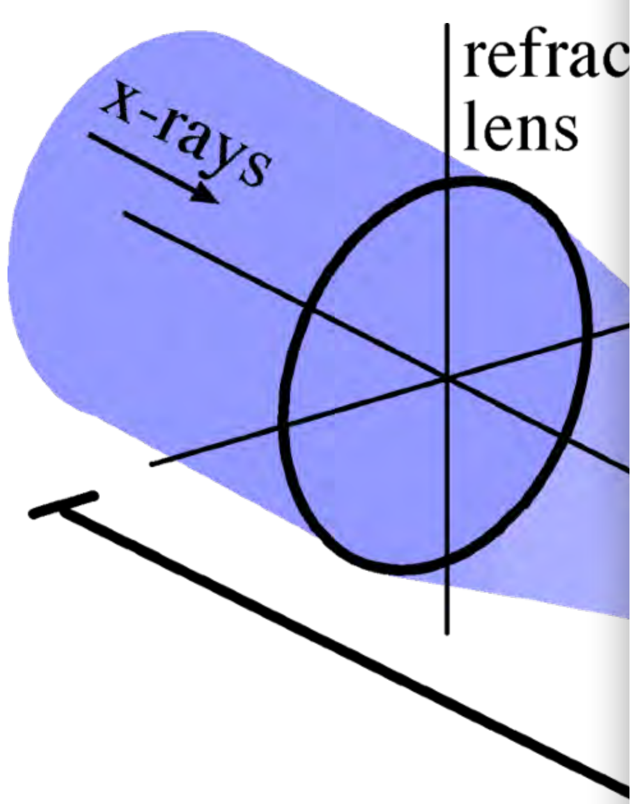

APL **79**, 1912 (200

Full fluorescence tomogram of zebra fish embryo

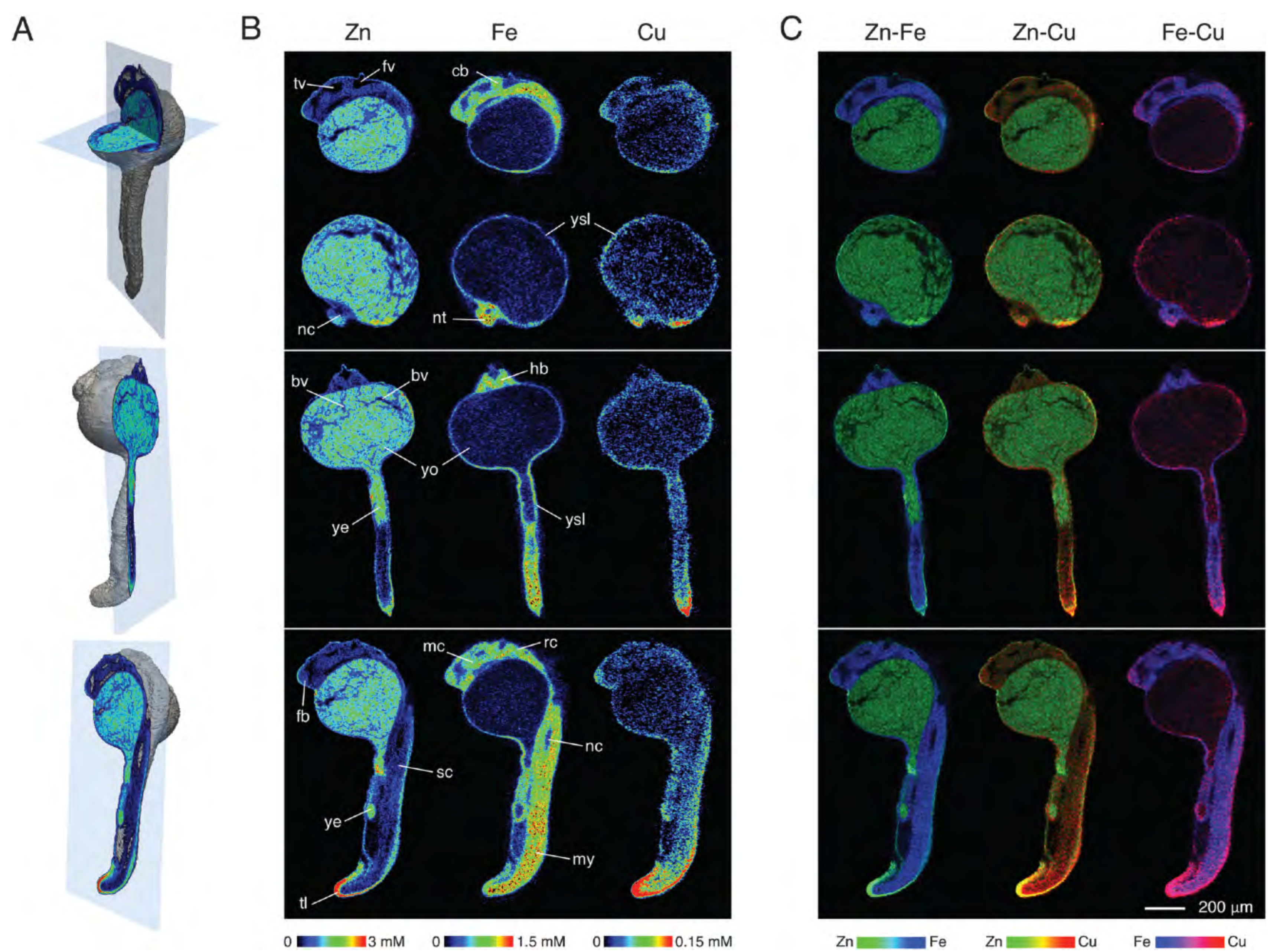

D. Bourassa, et al., Metallomics 6, 1648 (2014).

X-Ray Scanning Microscopy and Tomography

> Fluorescence mic

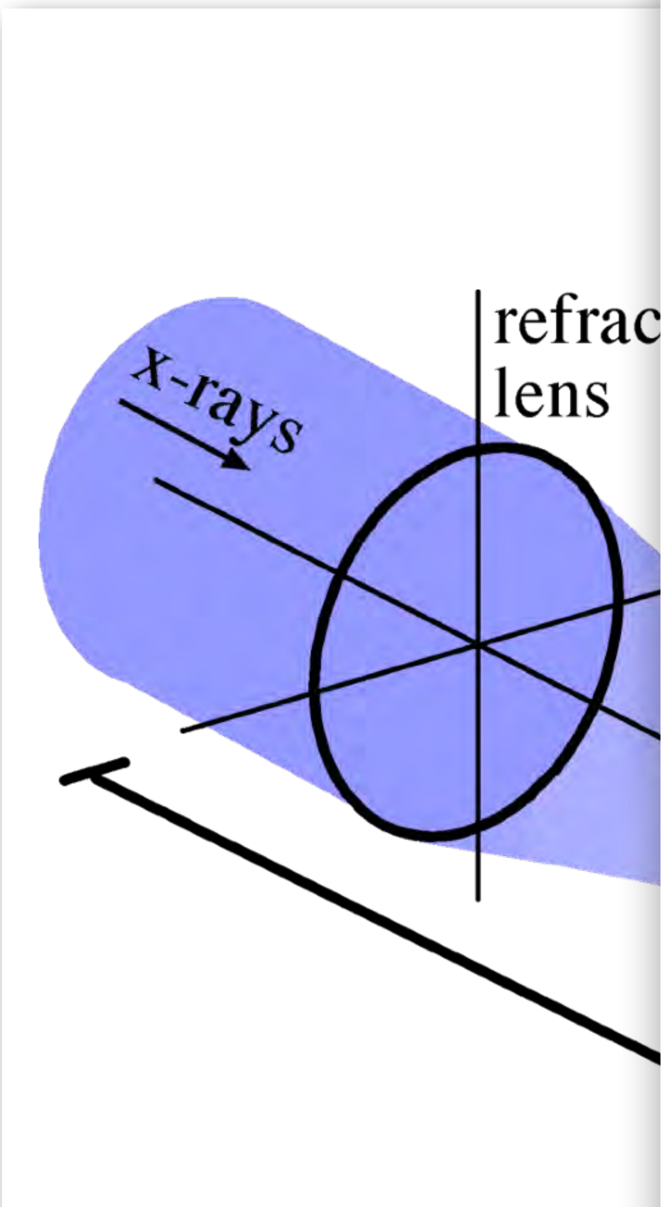

APL **79**, 1912 (200

Full fluorescence tomogram of zebra fish embryo

A

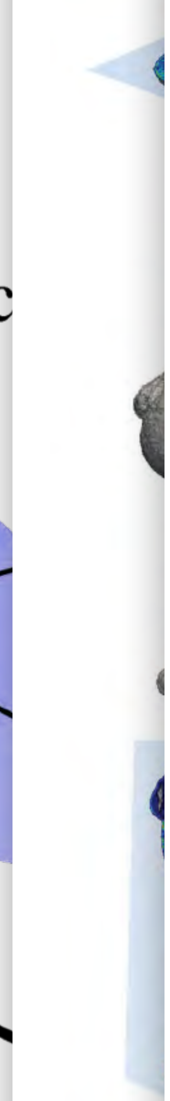

High-resolution fluorescence mapping and tomography

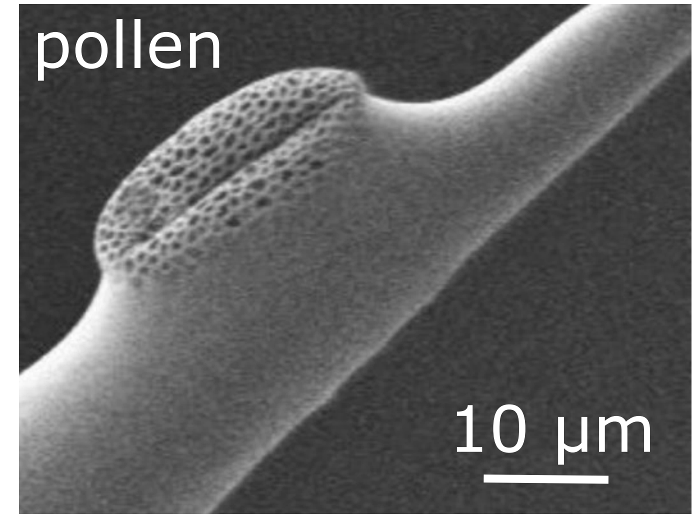

Fluorescence maps

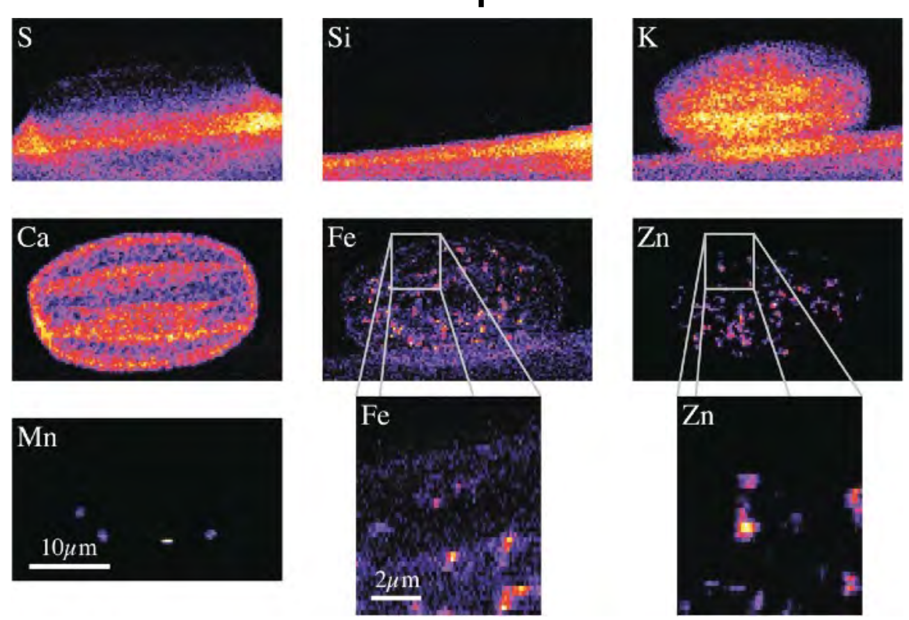

Fluorescence tomogram

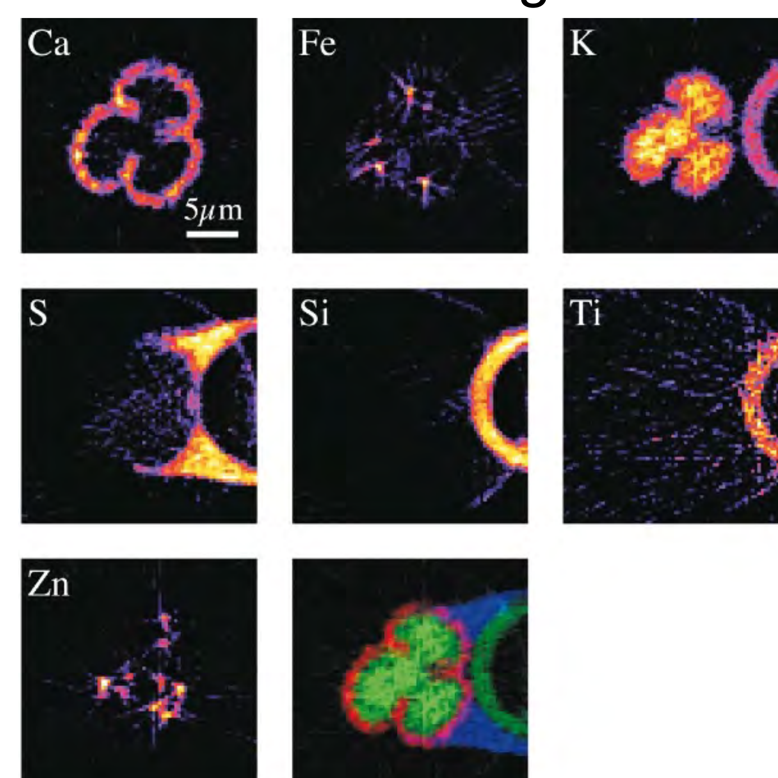

pixel size: 100 nm

W. Schröder, FZ Jülich

X-Ray Scanning Microscopy and Tomography

- Fluorescence microtomography
- Tomographic absorption spectroscopy (XANES tomography)

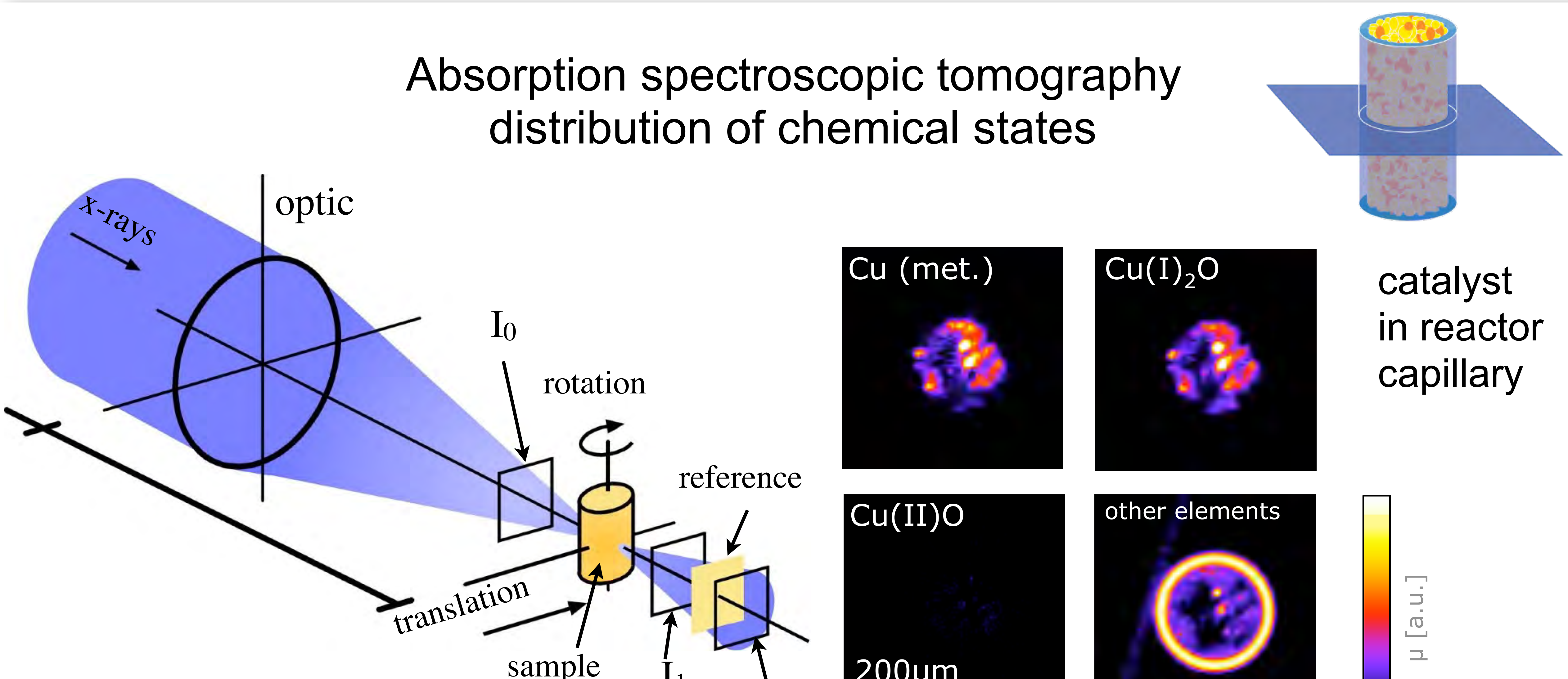

APL **82**, 3360 (2003).

X-Ray Scanning Microscopy and Tomography

- Fluorescence microtomography
- Tomographic absorption spectroscopy (XANES tomography)
- Small-angle x-ray scattering tomography (SAXS tomography)

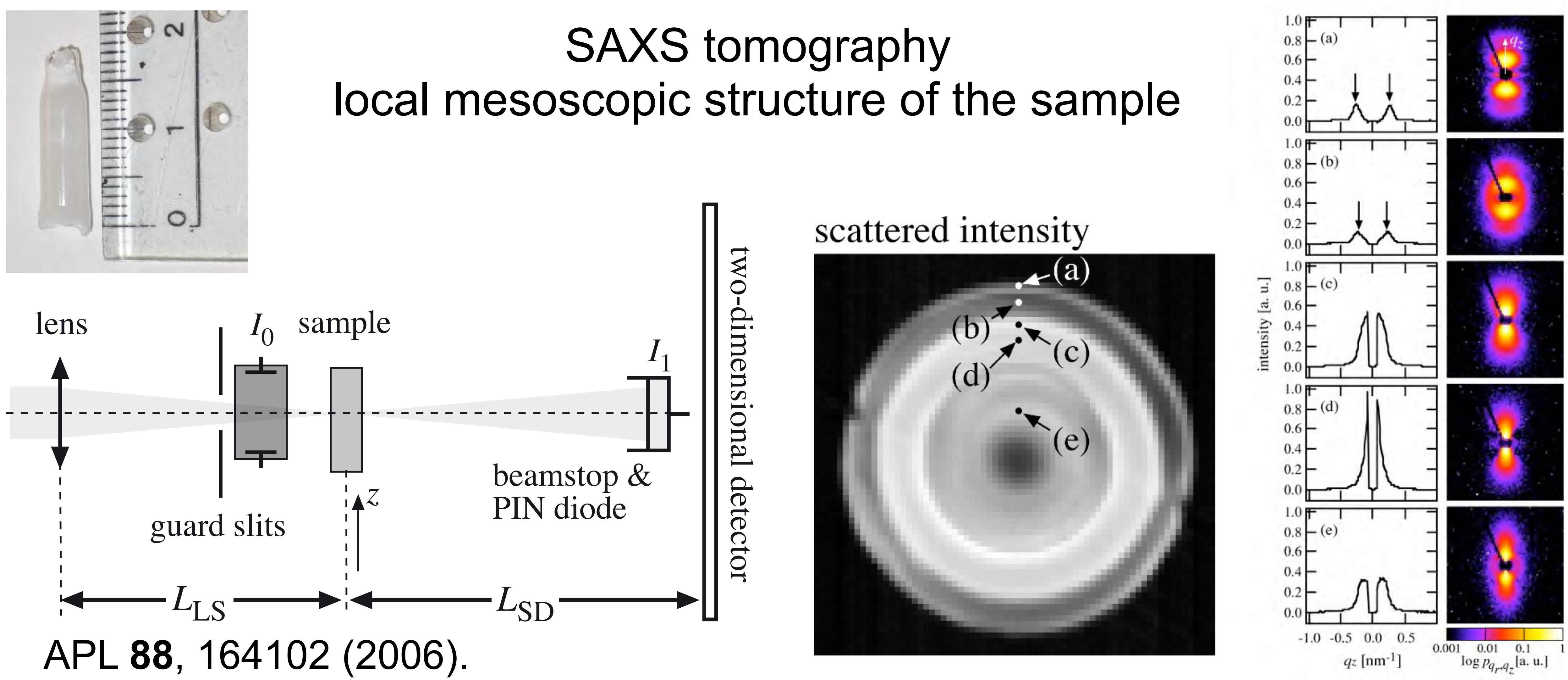

APL **88**, 164102 (2006).

X-Ray Scanning Microscopy and Tomography

- Fluorescence microtomography
- Tomographic absorptic
- Small-angle x-ray scatt

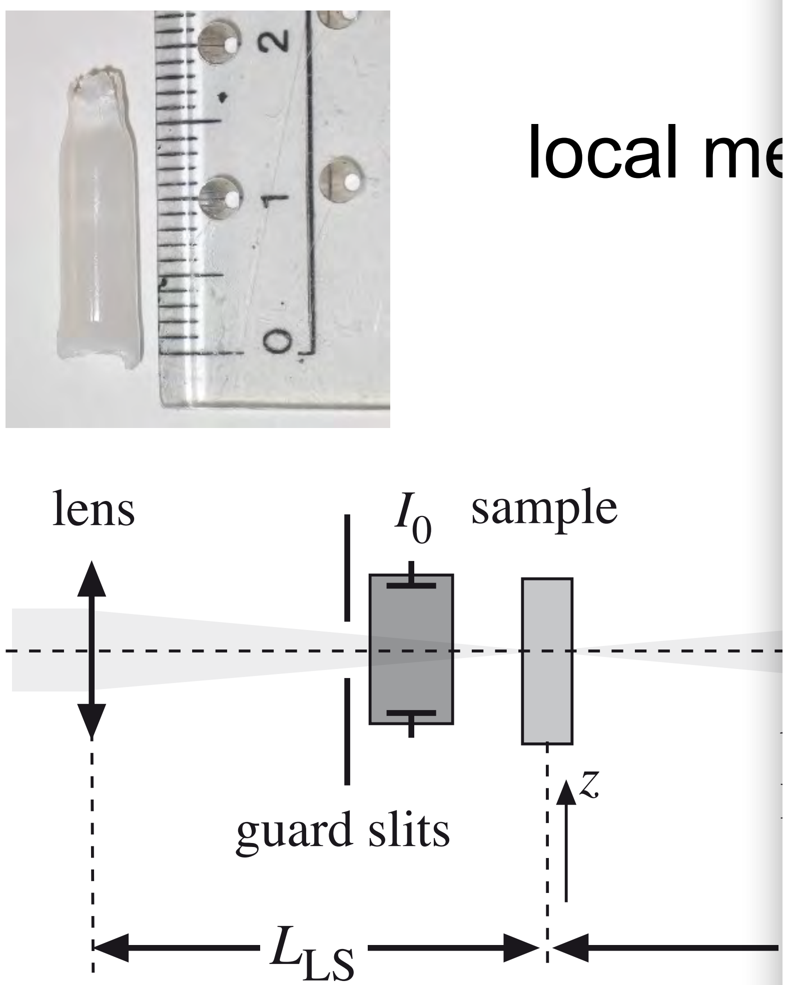

local me

APL **88**, 164102 (2006).

Wide-Angle-X-Ray-Scattering (WAXS) Tomography

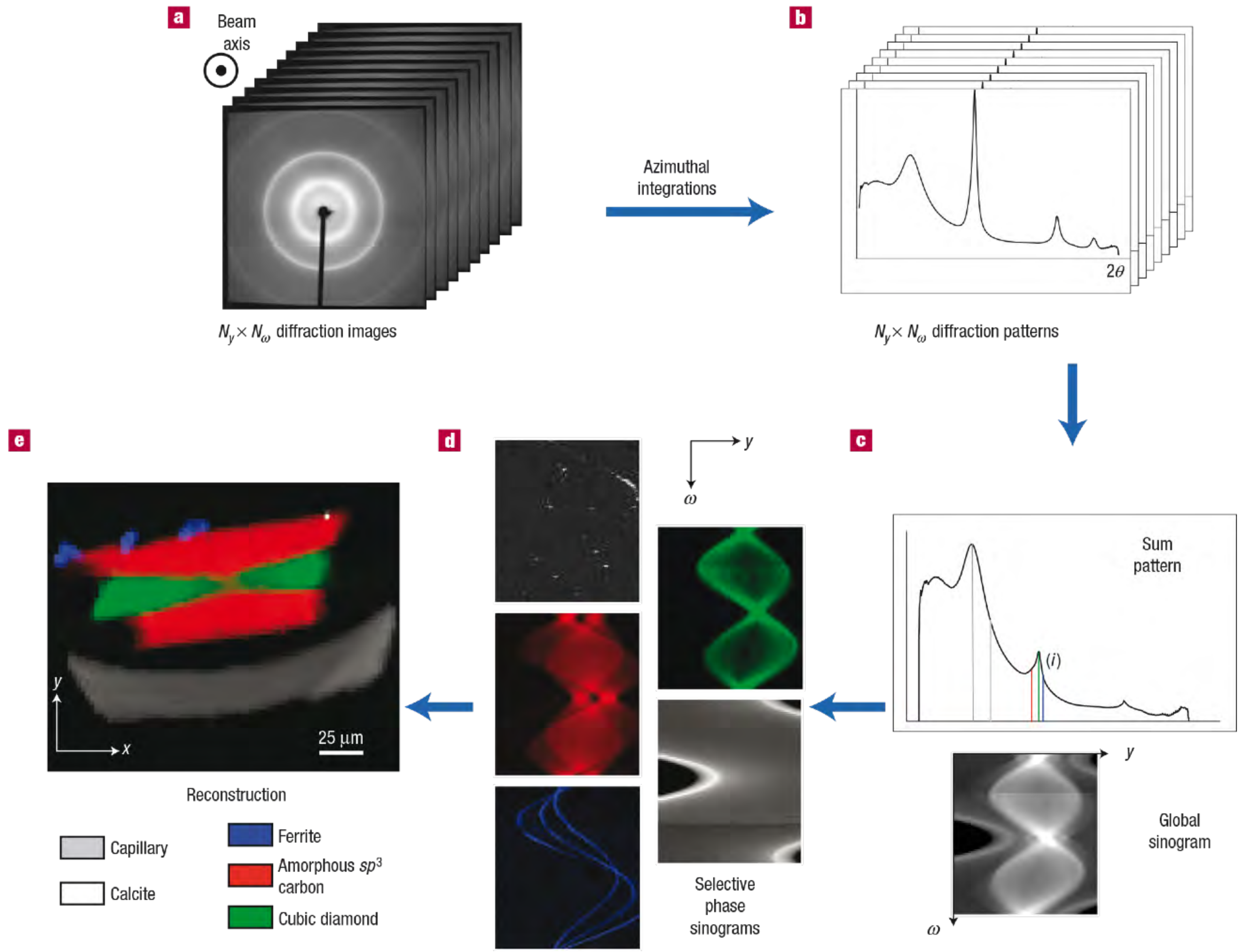

P. Bleuet, et al., Nat. Materials **7**, 468 (2008).

X-Ray Scanning Microscopy and Tomography

- Fluorescence microtomography
- Tomographic absorptic
- Small-angle x-ray scatt

Wide-Angle-X-Ray-Scattering (WAXS) Tomography

3D diffraction microscope (H. Poulsen)

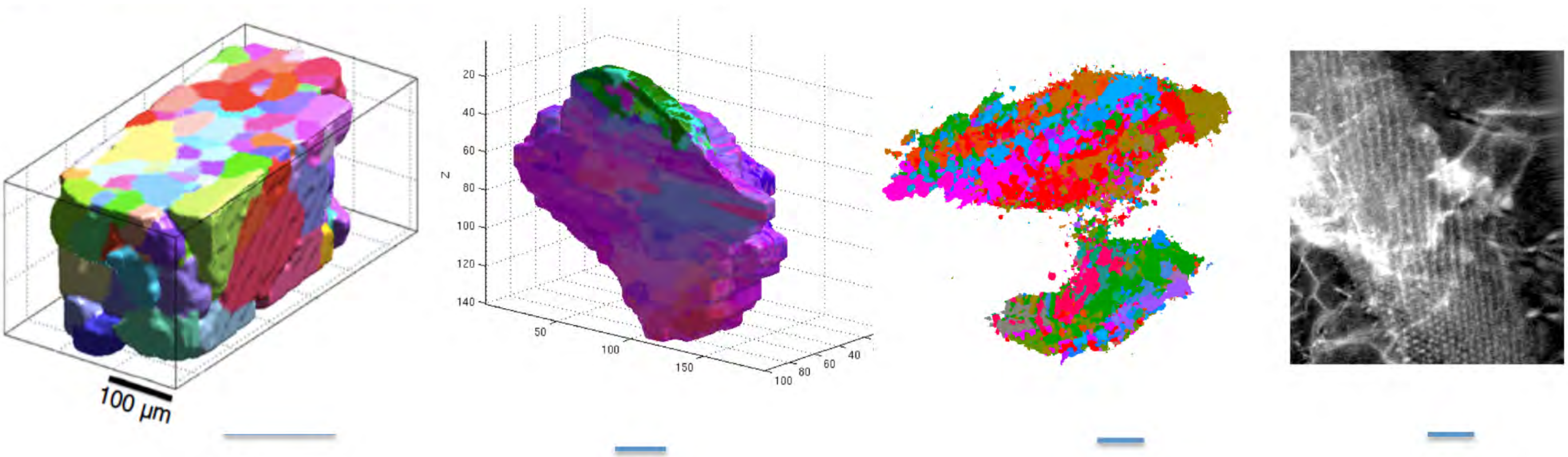

100 μm | 10 μm | 1 μm | 100 nm

Compare 3D movies directly to 3D modelling on "all scales"

Scanning Microscopy with Hard X-Rays

Source is imaged onto the sample to create an intensive micro-/nanobeam:

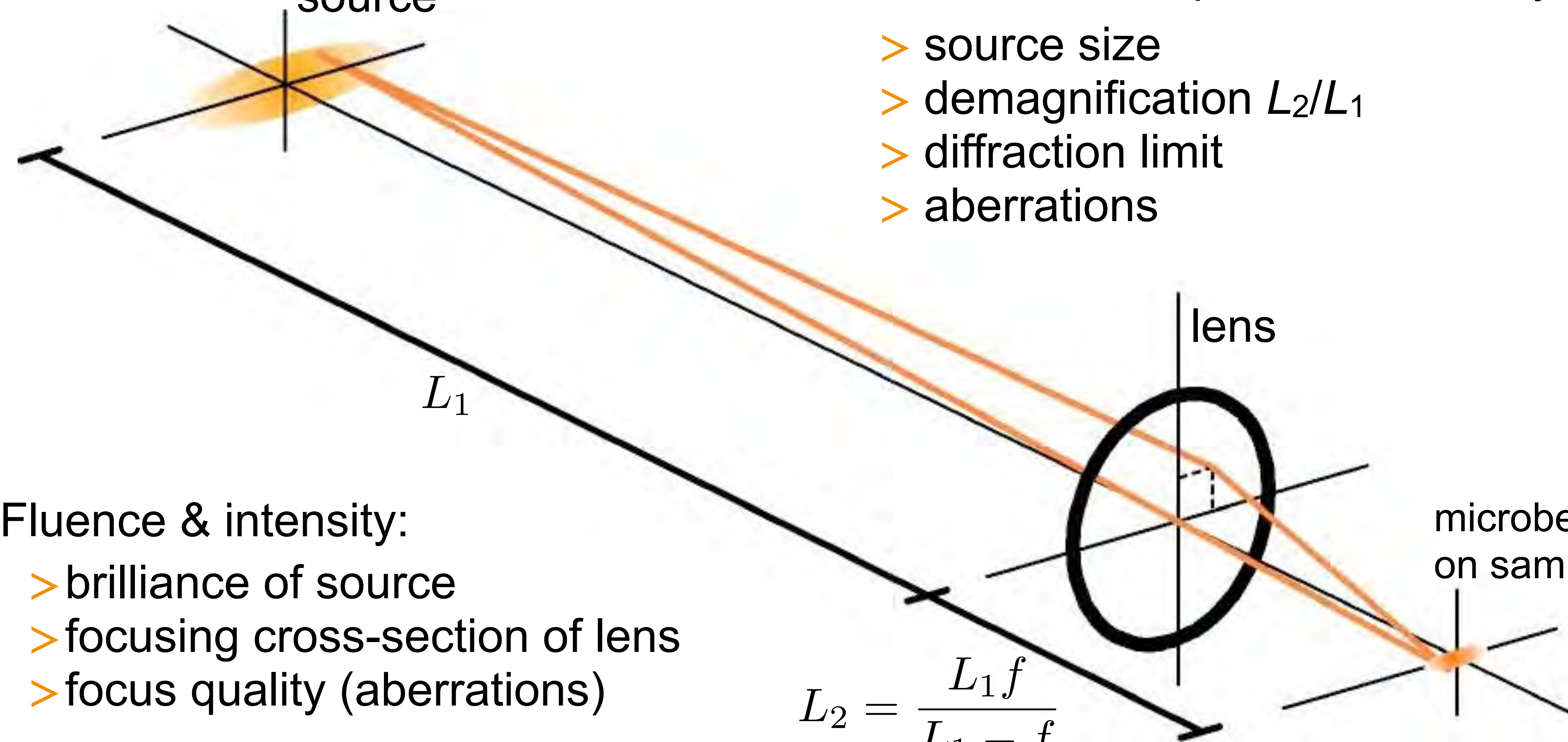

Focus size and shape determined by:

- source size
- demagnification L_2/L_1
- diffraction limit
- aberrations

Fluence & intensity:

- brilliance of source
- focusing cross-section of lens
- focus quality (aberrations)

$$L_2 = \frac{L_1 f}{L_1 - f}$$

Spectral Brightness

10000x more "light" per decade (since 1965)!!

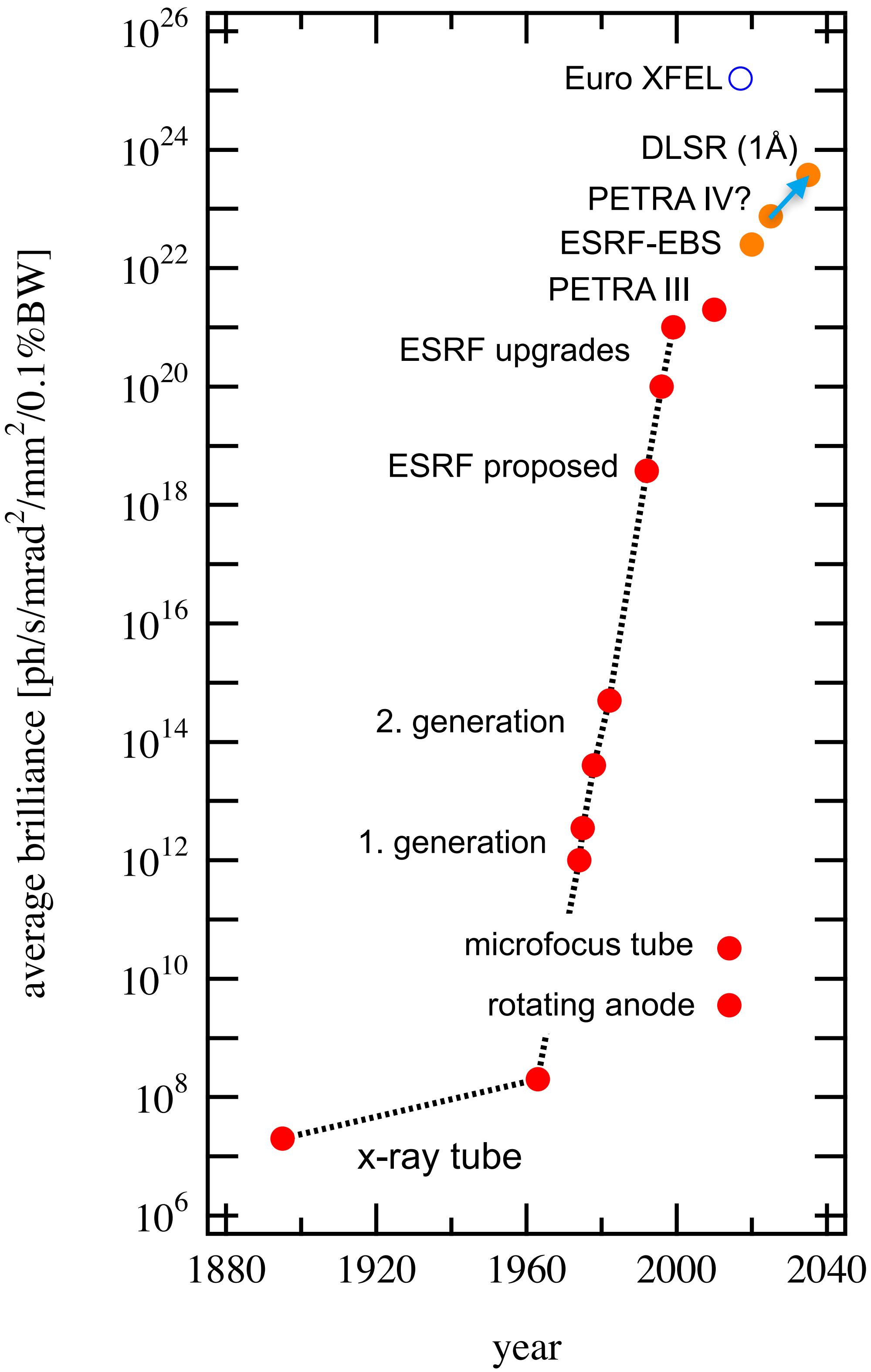

Spectral brightness:

$$B_{\mathrm{sp}} = \frac{F}{\Omega \cdot A \cdot \Delta E / E}$$

Flux per phase-space volume

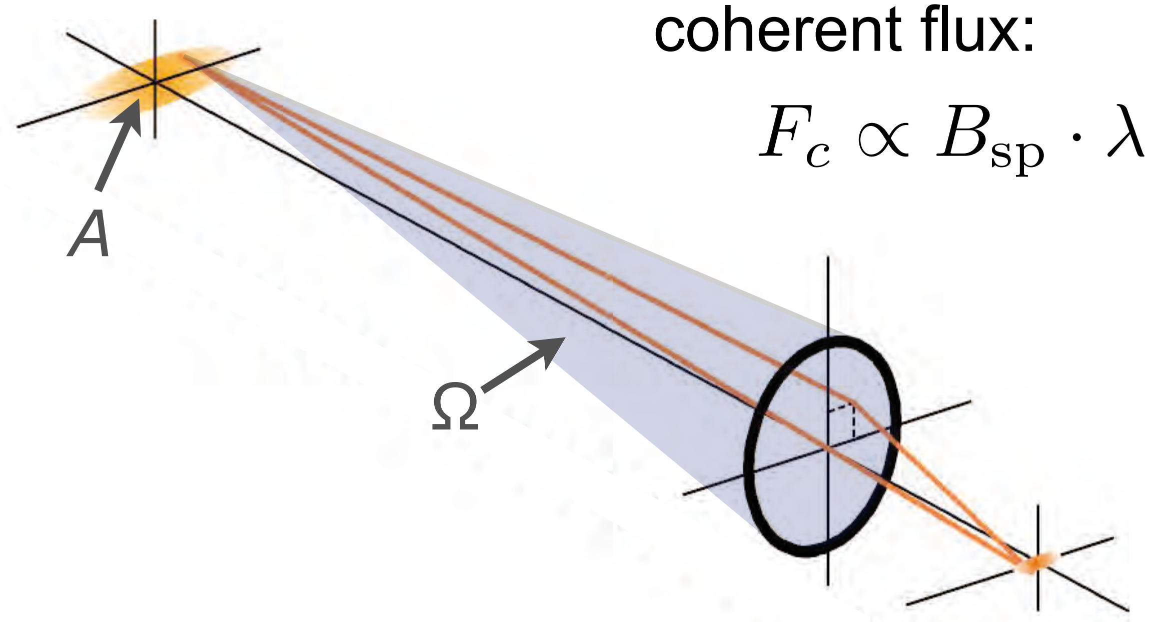

coherent flux:

$$F_c \propto B_{\mathrm{sp}} \cdot \lambda^2 \cdot \frac{\Delta E}{E}$$

Improvements in brightness:

- faster measurements (time resolution)
- nano-imaging (spatial resolution)
- spectroscopy (energy resolution)

Fluorescence Tomography

Example: investigating the ion transport in plants

Fluorescence analysis of plants:

- strong diffusion of elements
- cell structure complicated and delicate

Difficult sample preparation

- cryo sections
- fracture surfaces

ideal:

nondestructive probe of
inner structures of sample

root of Mahogany tree

Fluorescence Tomography

Root of Mahogany tree

element distribution on virtual section through sample

Example:

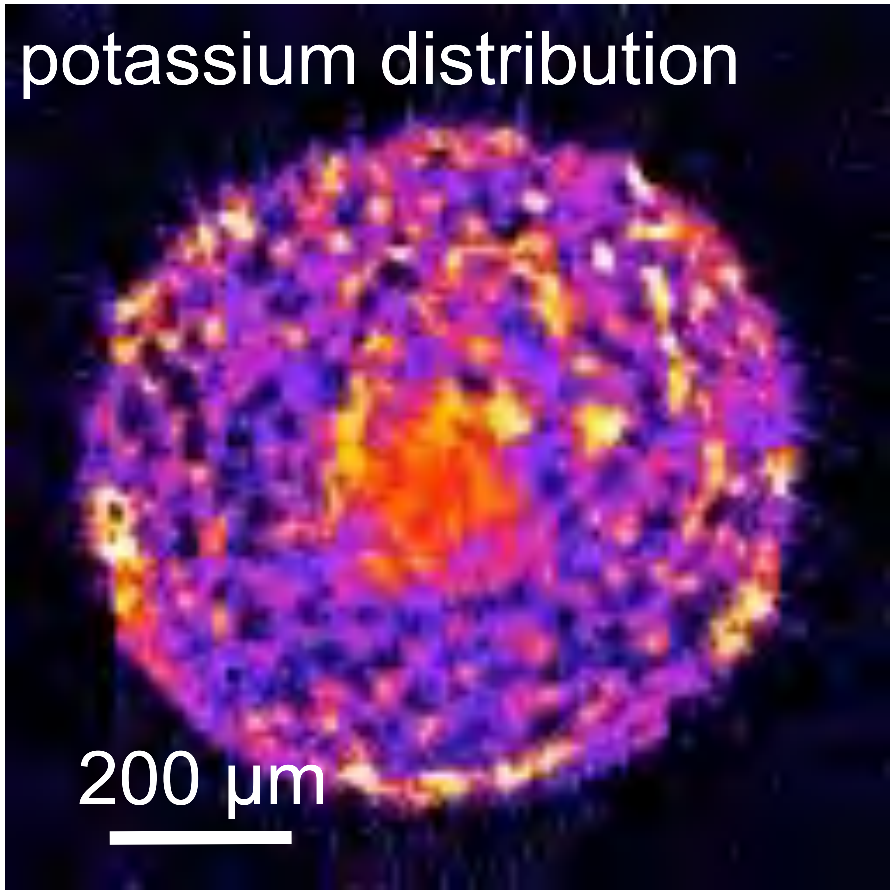

X-ray Fluorescence & Auger Prozess

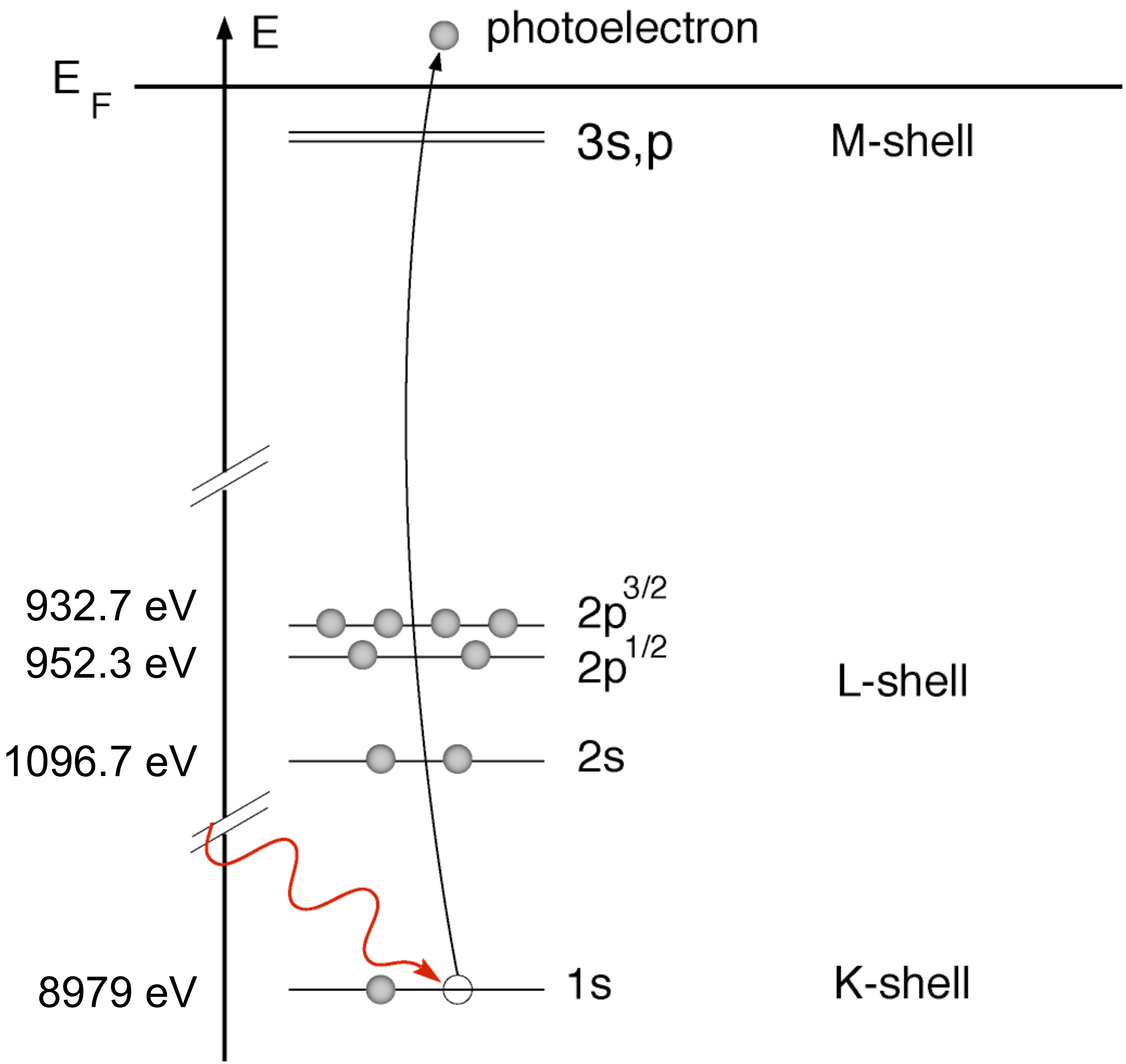

X-ray Absorption

leaves atom in excited state (core hole):

Secondary processes:

- fluorescence

X-ray Fluorescence & Auger Prozess

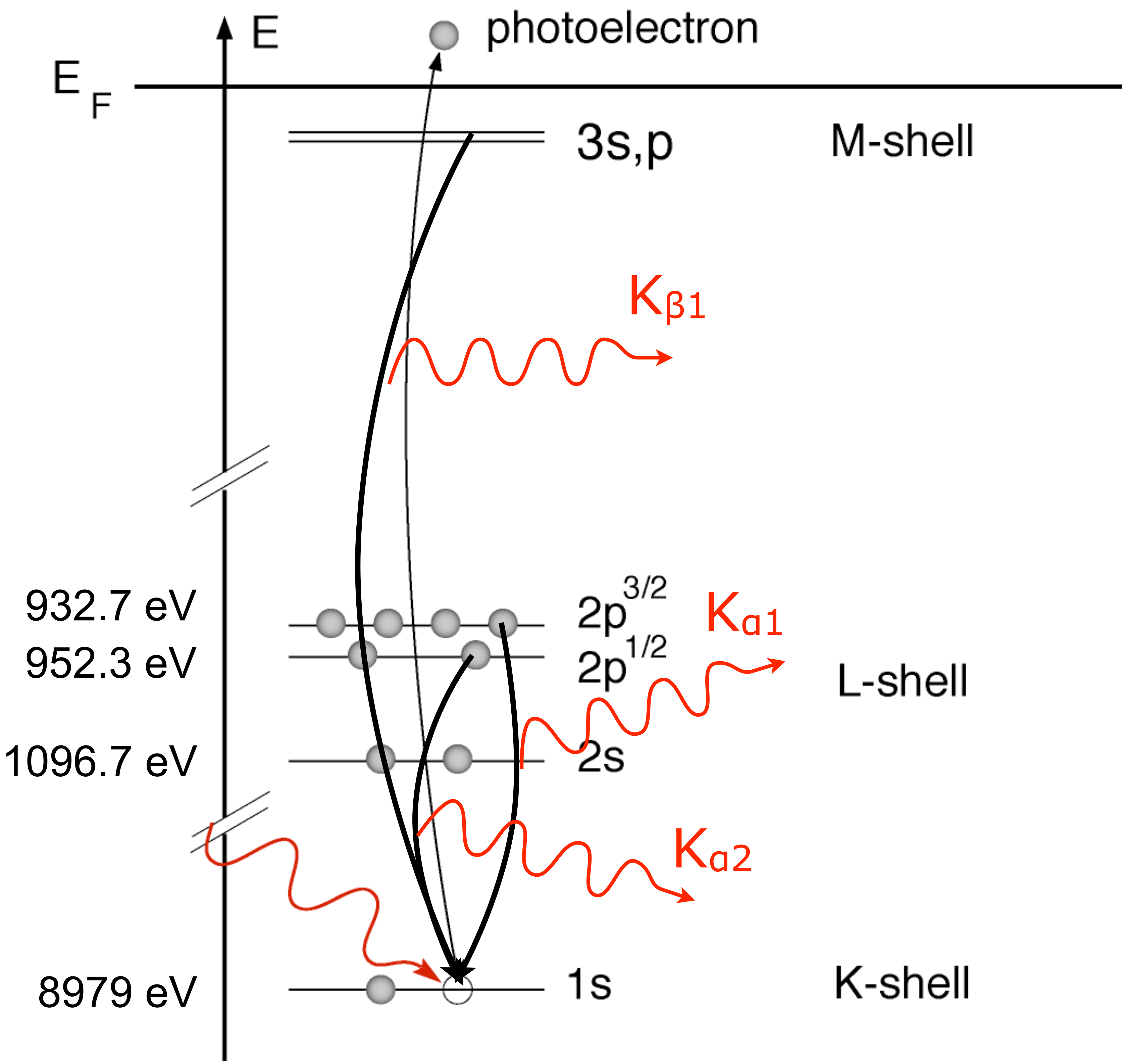

X-ray Absorption

leaves atom in excited state (core hole):

Secondary processes:

> fluorescence

Röntgenfluoreszenz & Augerprozess

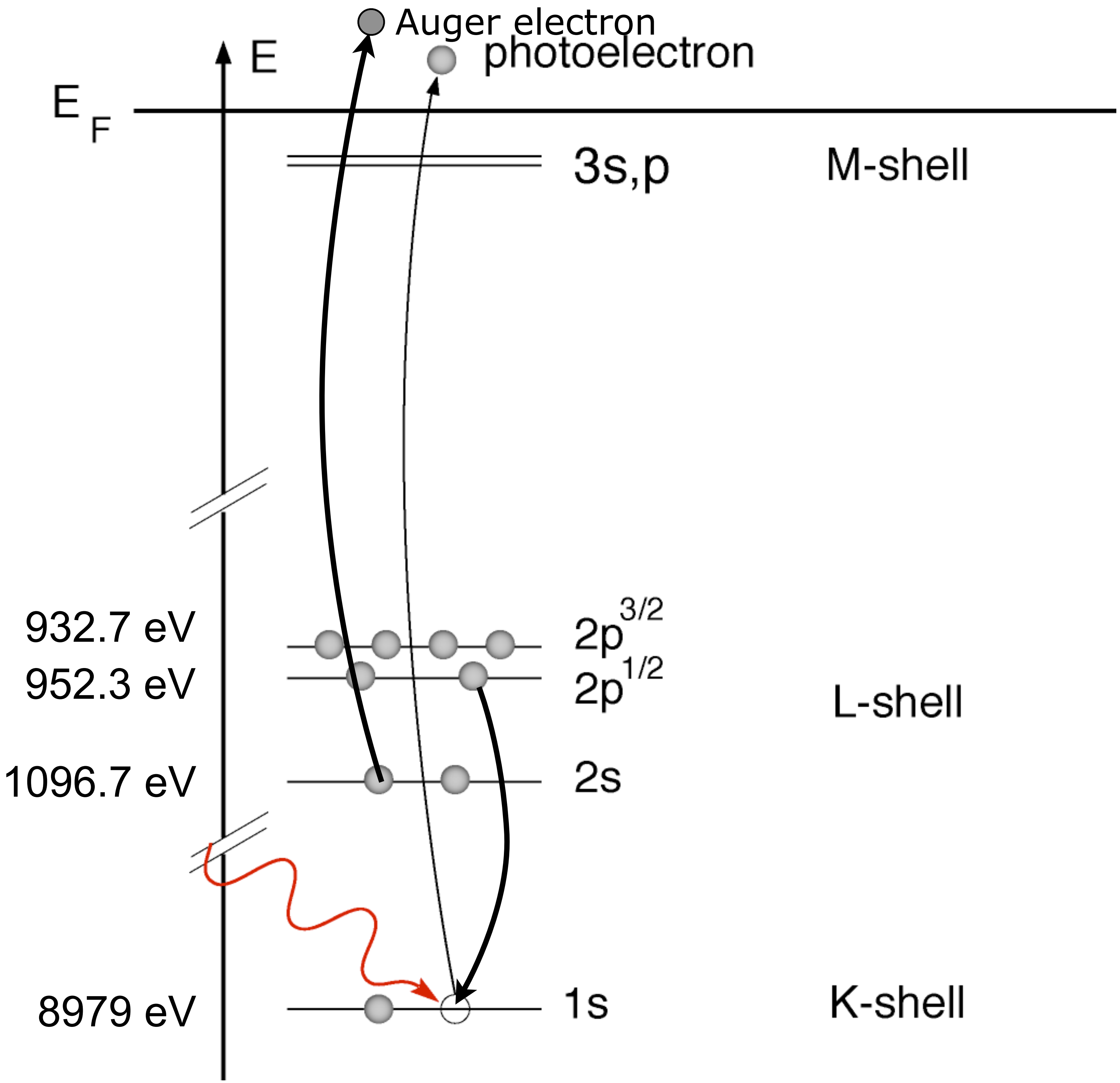

X-ray Absorption

leaves atom in excited state (core hole):

Secondary processes:

- fluorescence
- emission of Auger electron

both processes occur with certain probability

Fluorescence Yield

$1 - \varepsilon =$ Auger yield

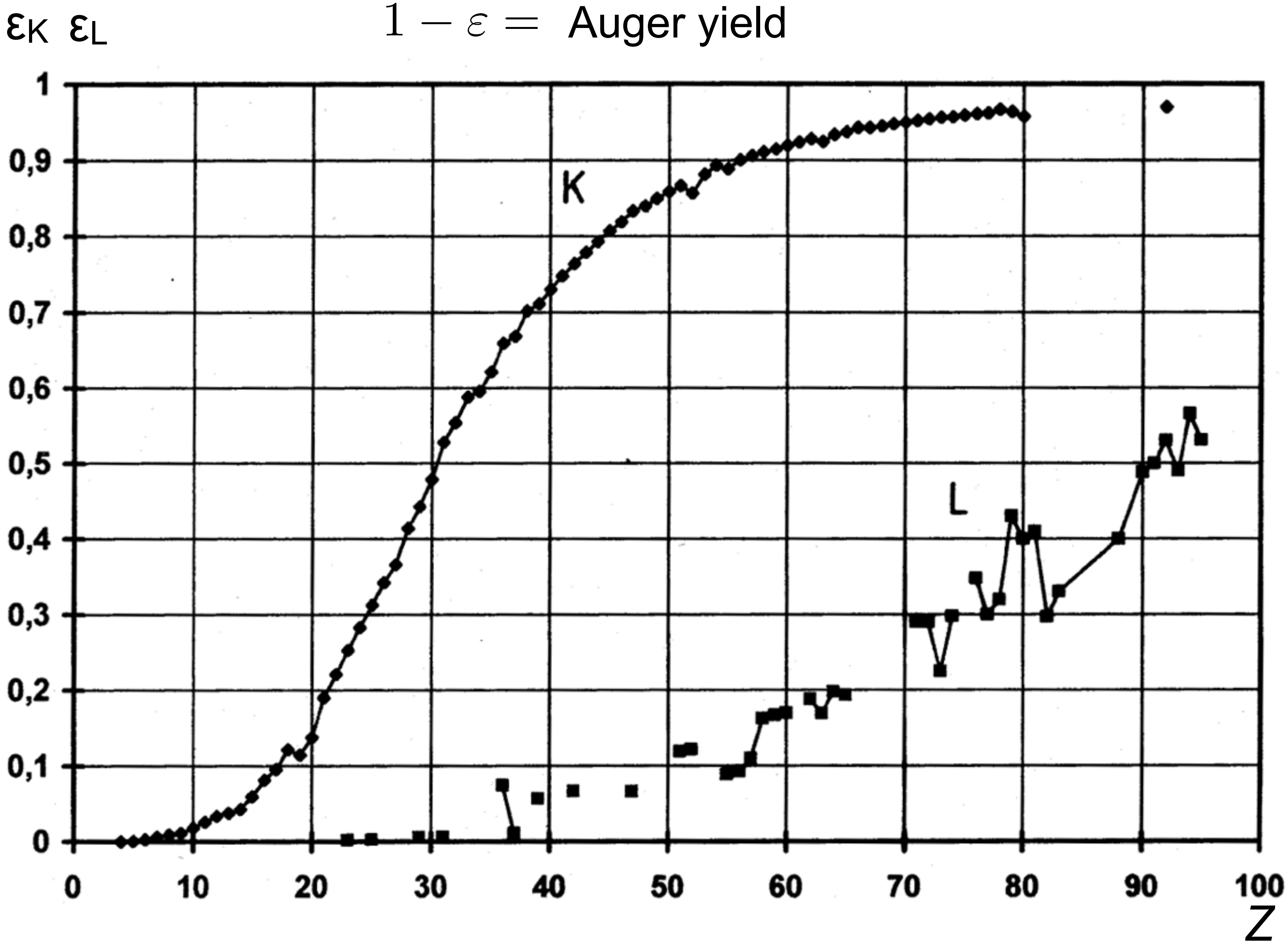

element specific

Fluorescence dominates at higher binding energies for core hole excitation (growing with atomic number Z)

Fluorescence Spectrum

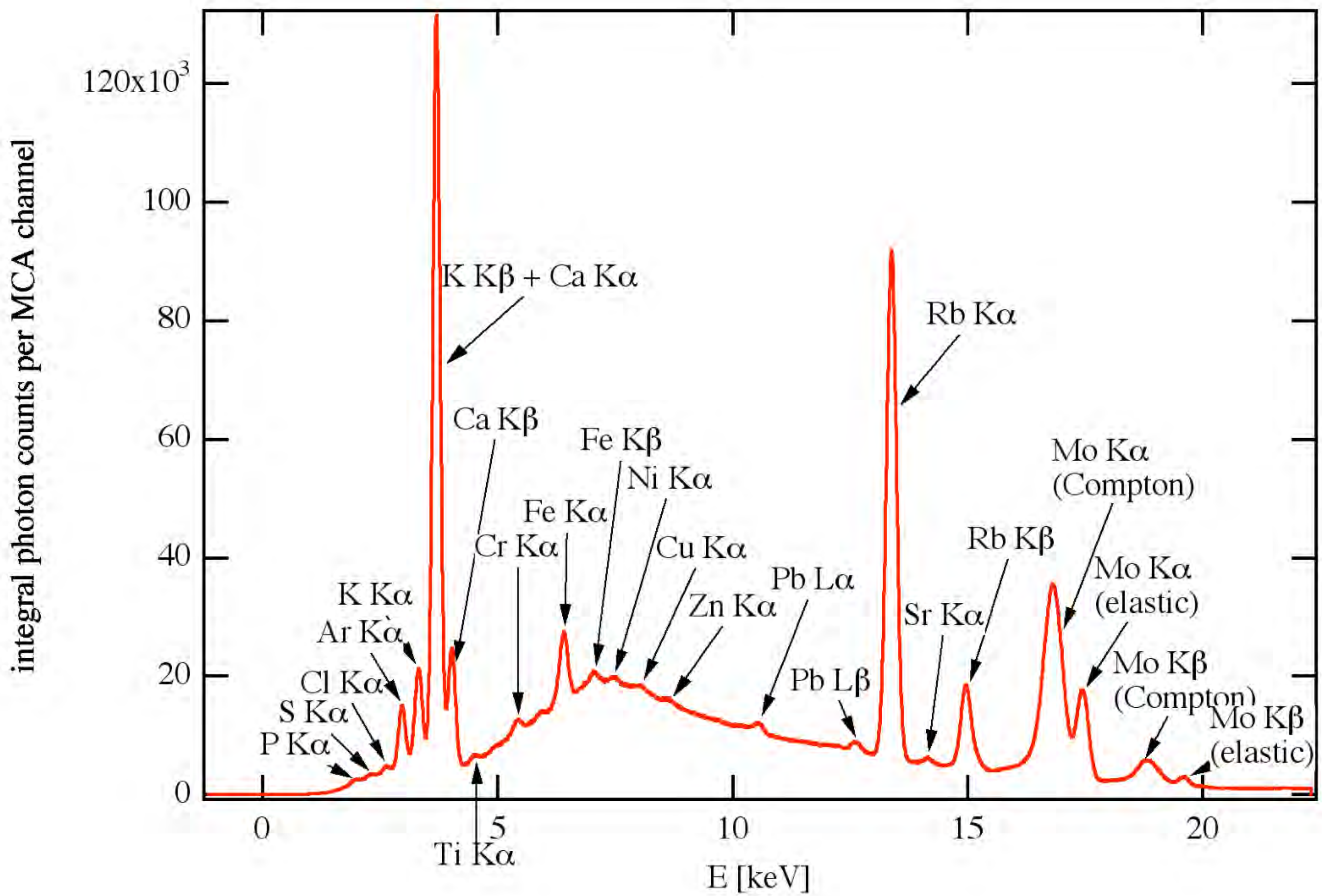

Illuminated atoms emit characteristic fluorescence radiation!

Example spectrum excitation with x-ray tube:

Background due to scattered spectrum of x-ray tube

Limitation of detection limits by background!

Excitation with Monochromatic Synchrotron Radiation

Example: undulator radiation (Si 111 monochrom.): 19.5 keV

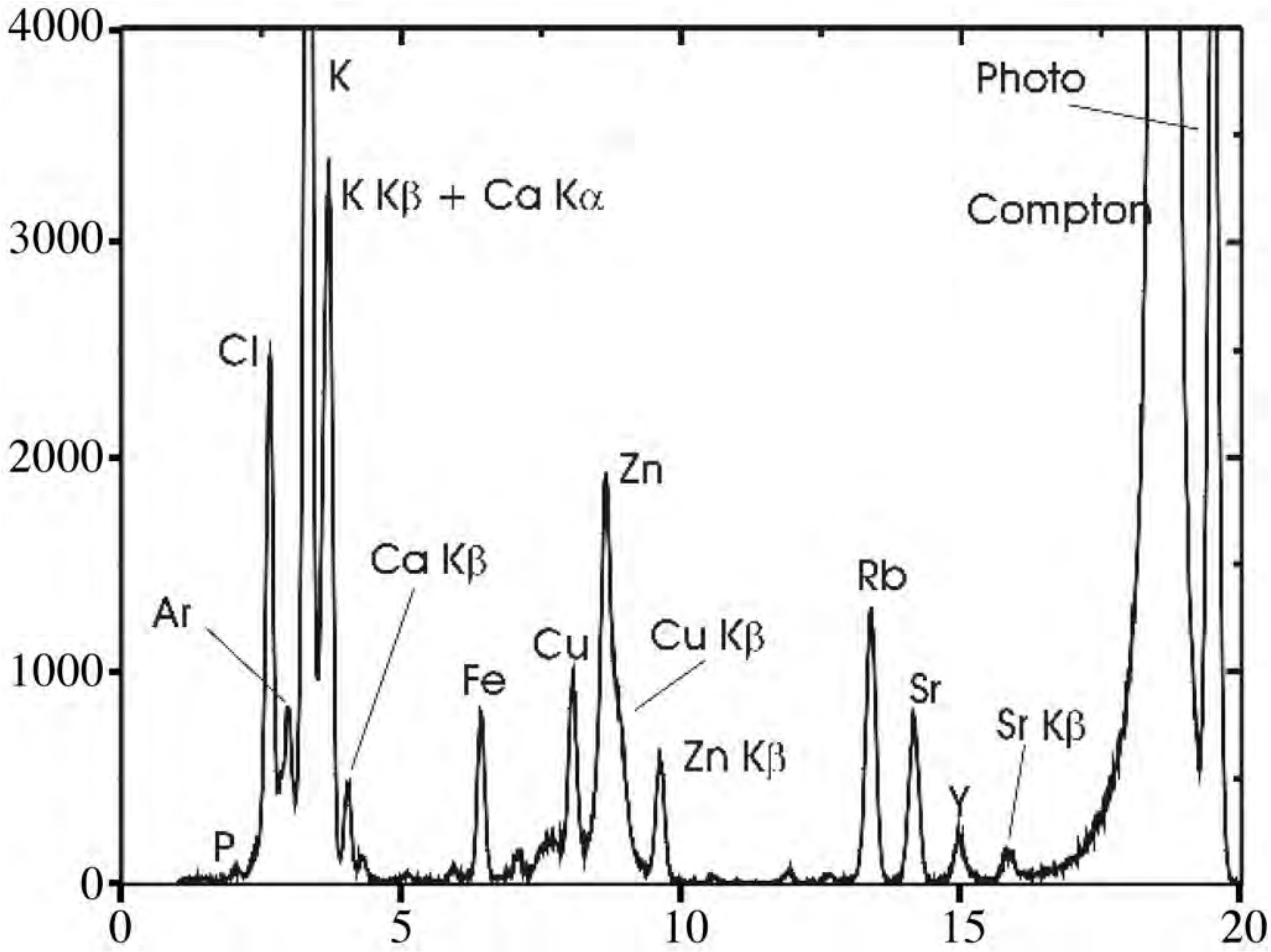

No background due to scattered radiation at fluorescence energy

High signal-to-background ratio!!

very low detection limits possible (ppb-level)!

Scanning Probe: Fluorescence Microtomography

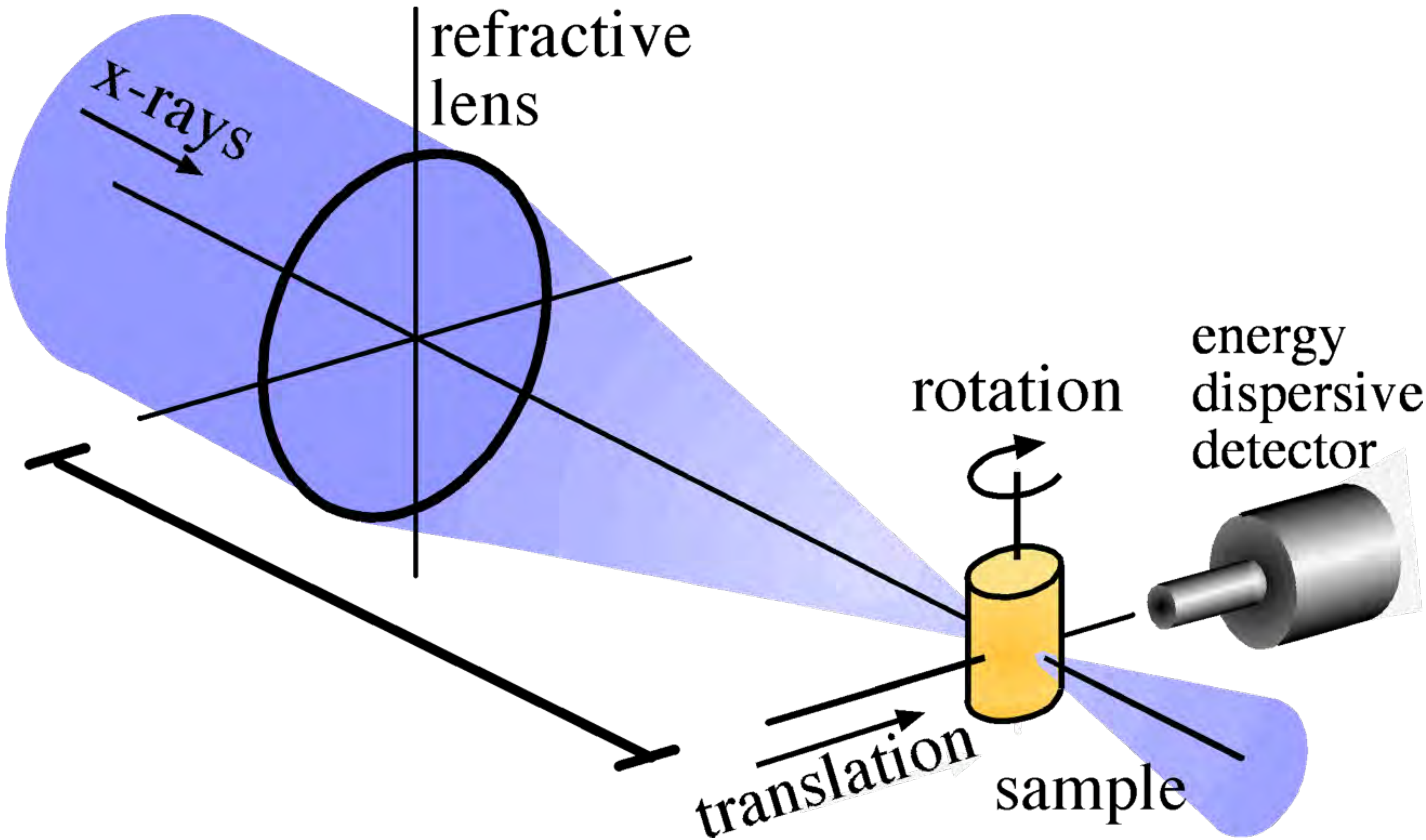

Fluorescence Microtomography

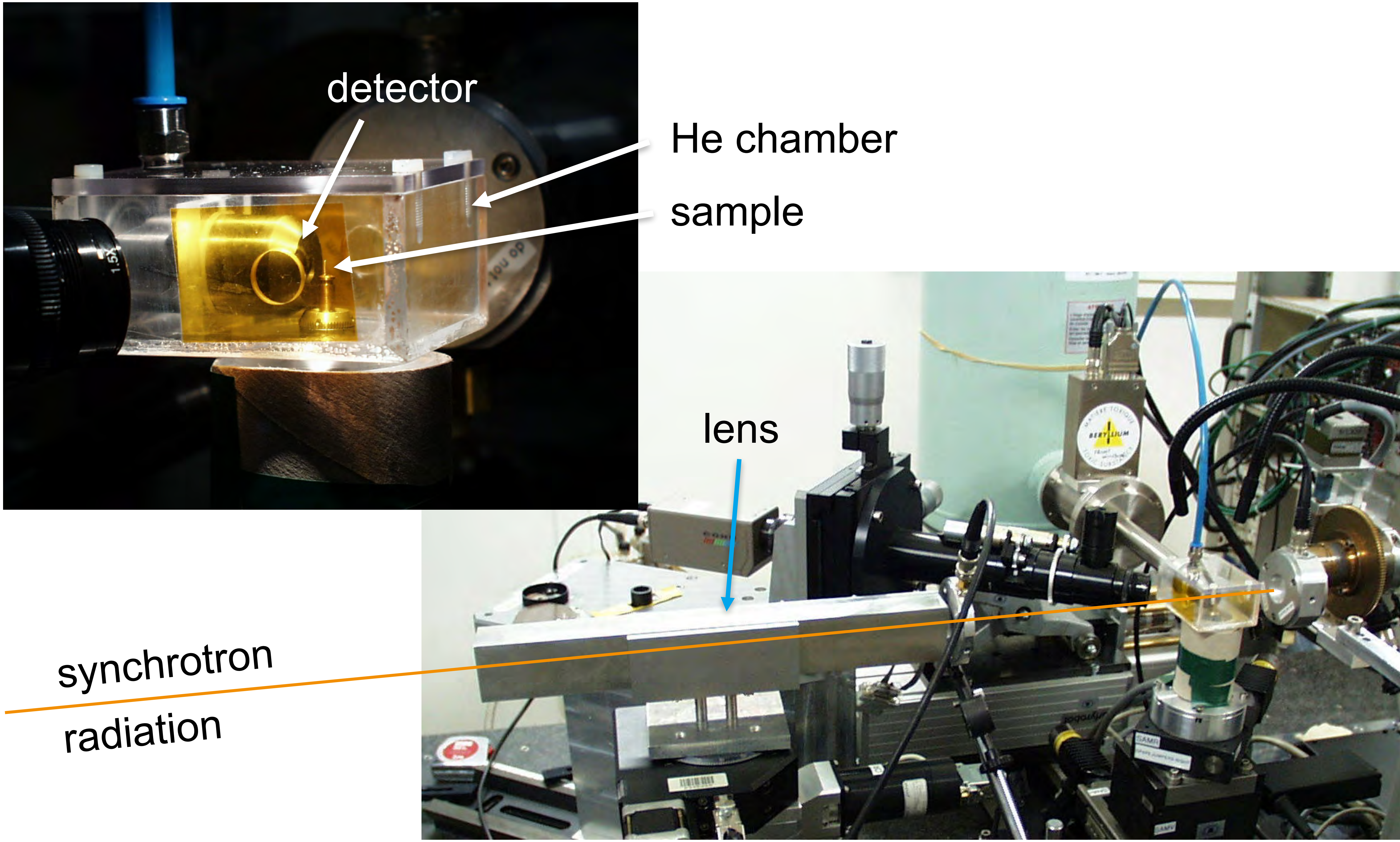

Fluorescence Tomography: Measured Data

Sinograms:

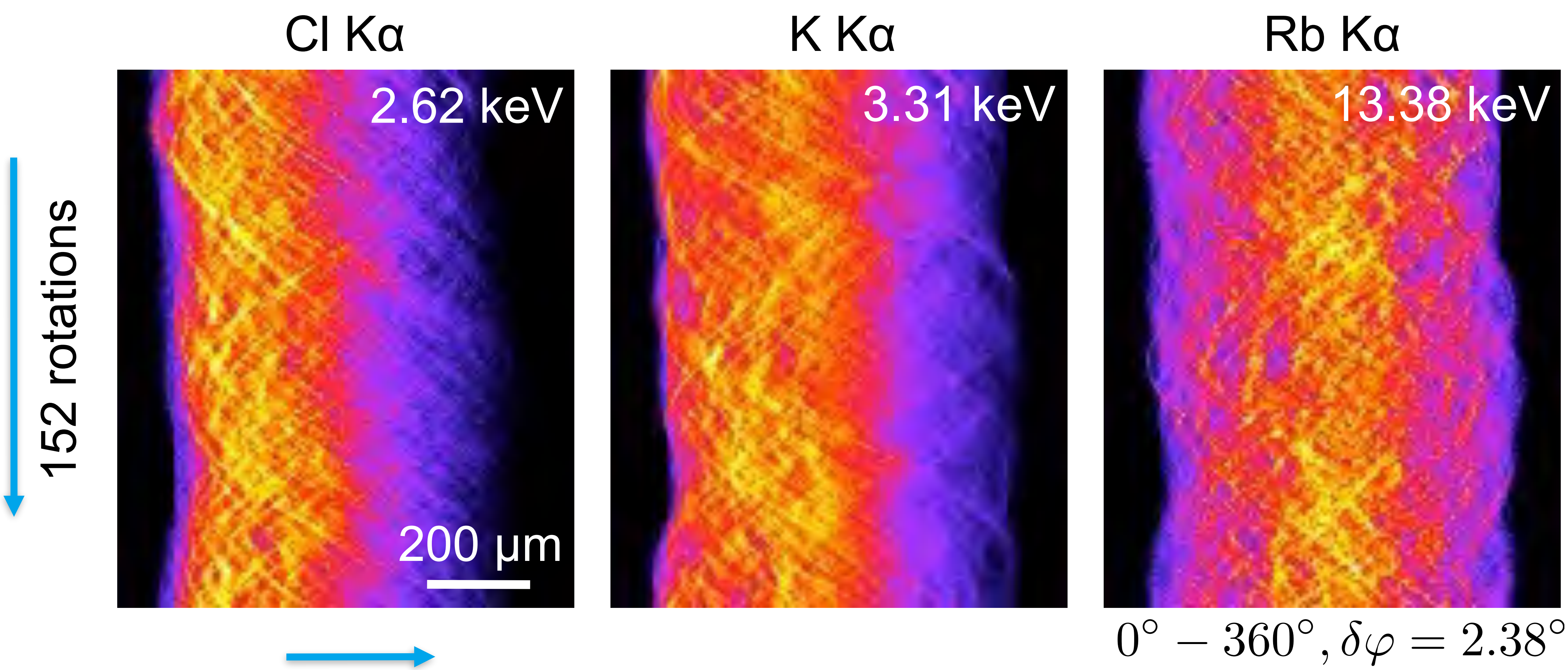

$0^\circ - 360^\circ, \delta\varphi = 2.38^\circ$

translations: 128, 6µm

experimental parameters:

- energy: 19.5 keV
- refractive lens (Al): *N* = 150, f = 45.4 cm, m = 1/127
- beam size: 1.5 x 6µm^2, flux: 1.1 · 10^{10} ph/s

Fluorescence Tomography: Measured Data

Sinograms:

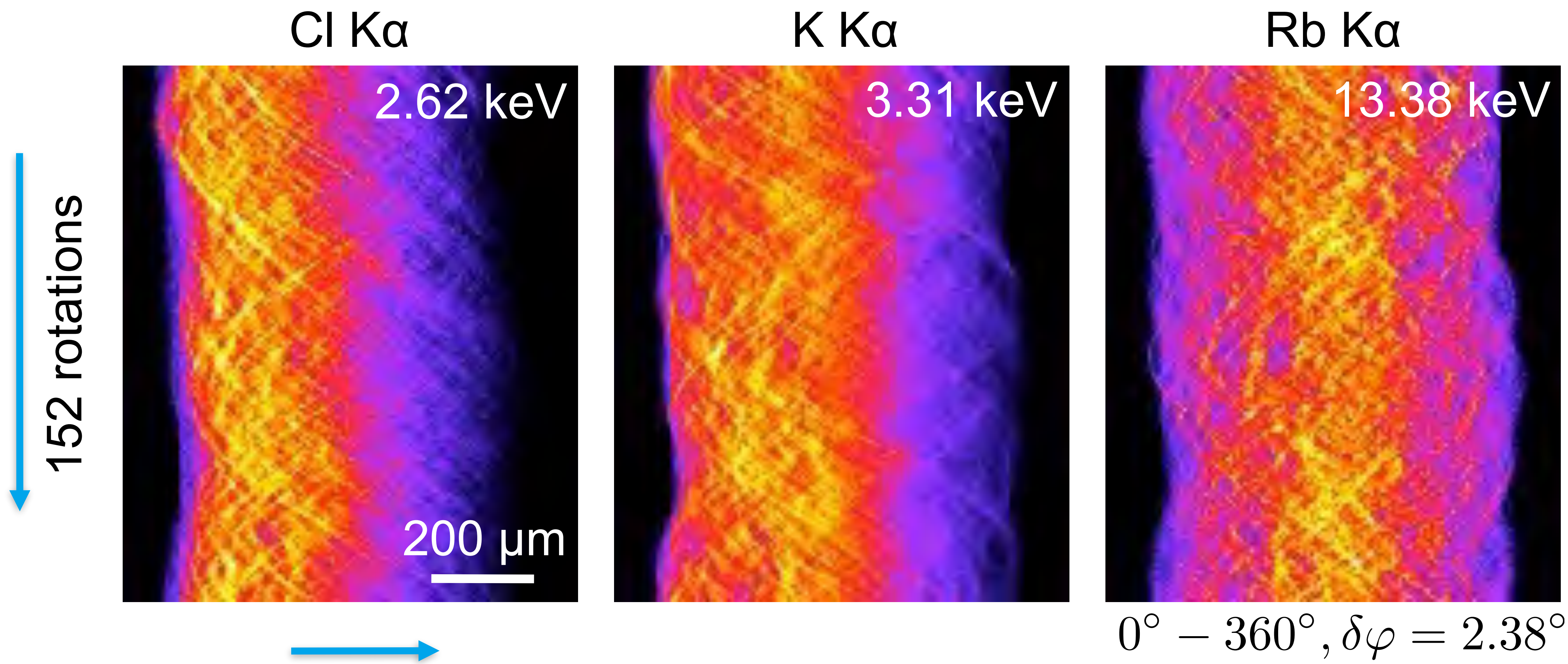

$0^\circ - 360^\circ, \delta\varphi = 2.38^\circ$

translations: 128, 6µm

Symmetry:

$$I_{i\nu}(-r, \varphi + \pi) = I_{i\nu}(r, \varphi)$$

only holds for Rb!
Absorption of fluorescence radiation: asymmetry in sinogram.

Fluorescence Tomography: Model

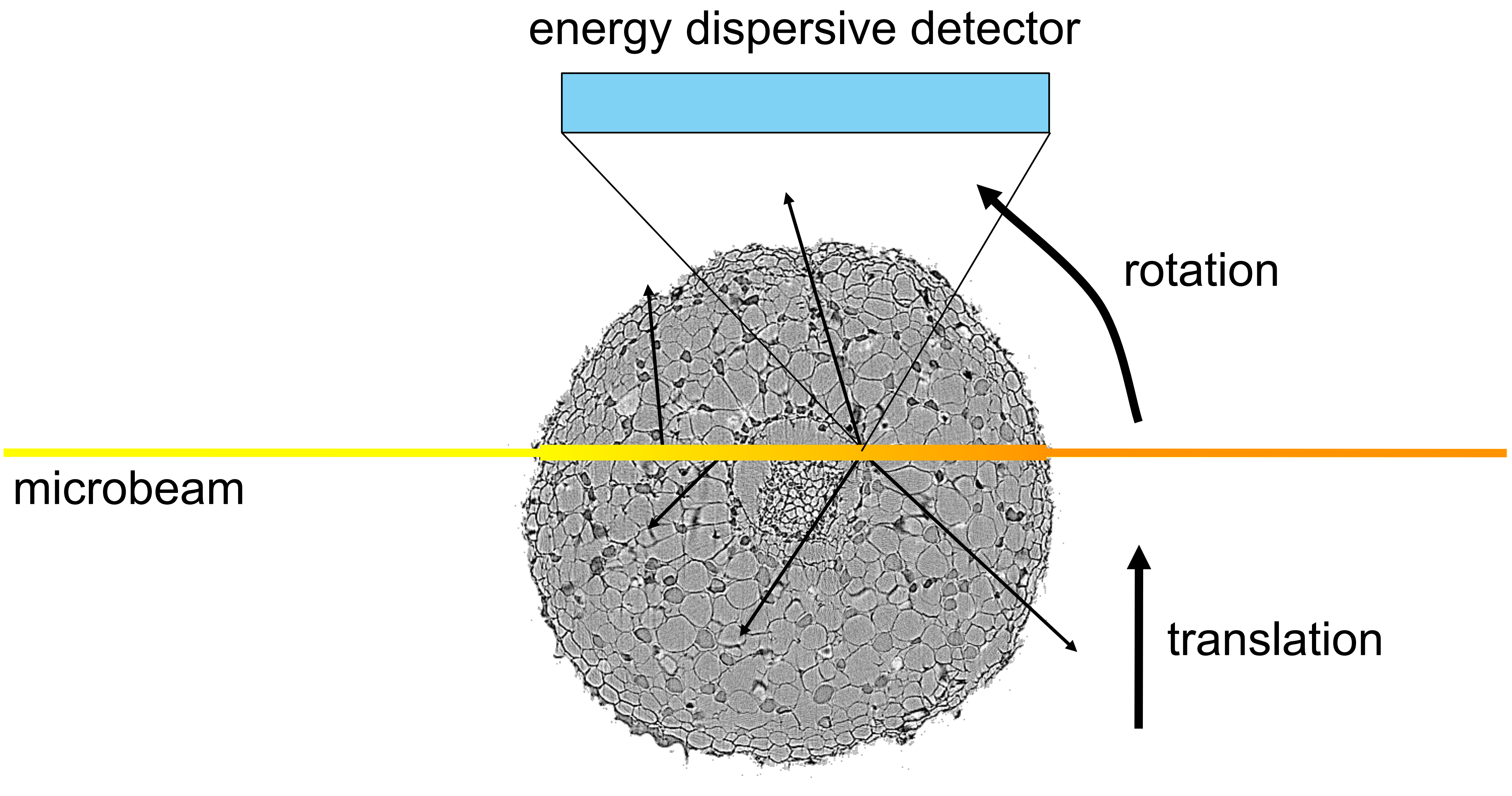

$$I_{i\nu}(r,\varphi) = I_0 \int ds \left[e^{-\int_{-\infty}^{s} ds' \mu_0(x,y)} \cdot p_{i\nu}(x,y) \cdot \int d\gamma e^{-\int dr' \mu_{i\nu}(x,y)} \right]$$

Absorption Correction

Example: potassium distribution in Mahogany root

Disregarding attenuation of fluorescence:

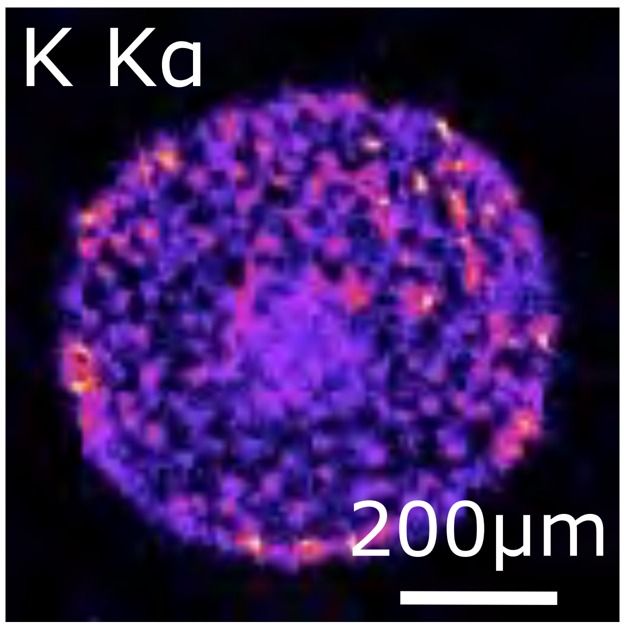

simple tomographic model →

$$\mu_{\mathrm{K\,K}\alpha} = 0$$

reconstructed sinogram

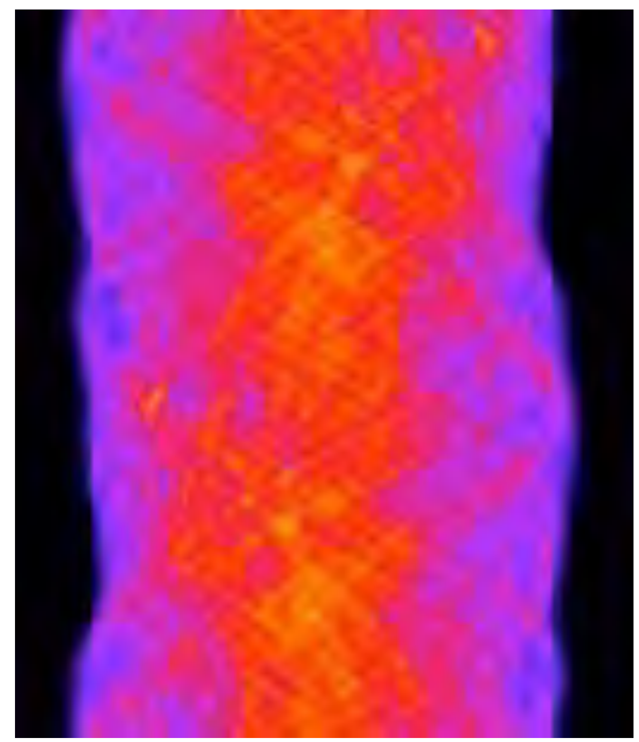

measured sinogram

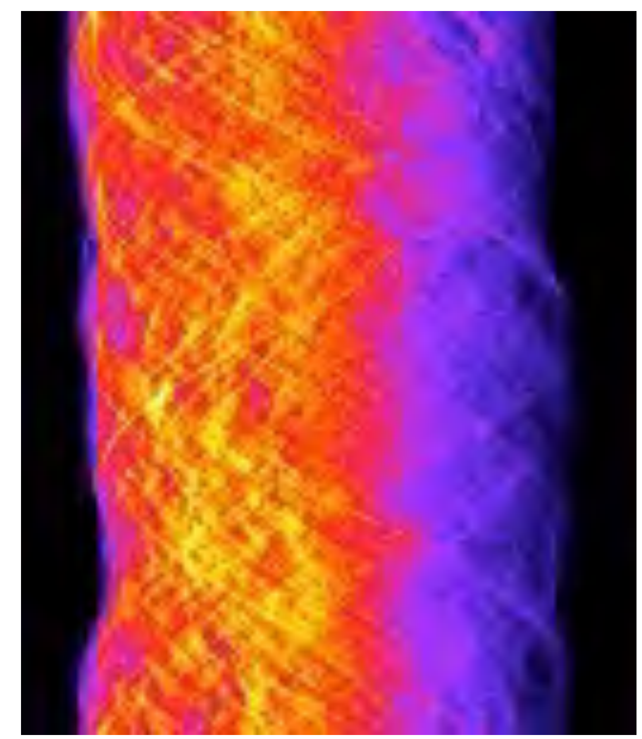

C. Schroer, Appl. Phys. Lett. **79**, 1912 (2001).

Absorption Correction

Example: potassium distribution in Mahogany root

Accounting for attenuation of fluorescence:

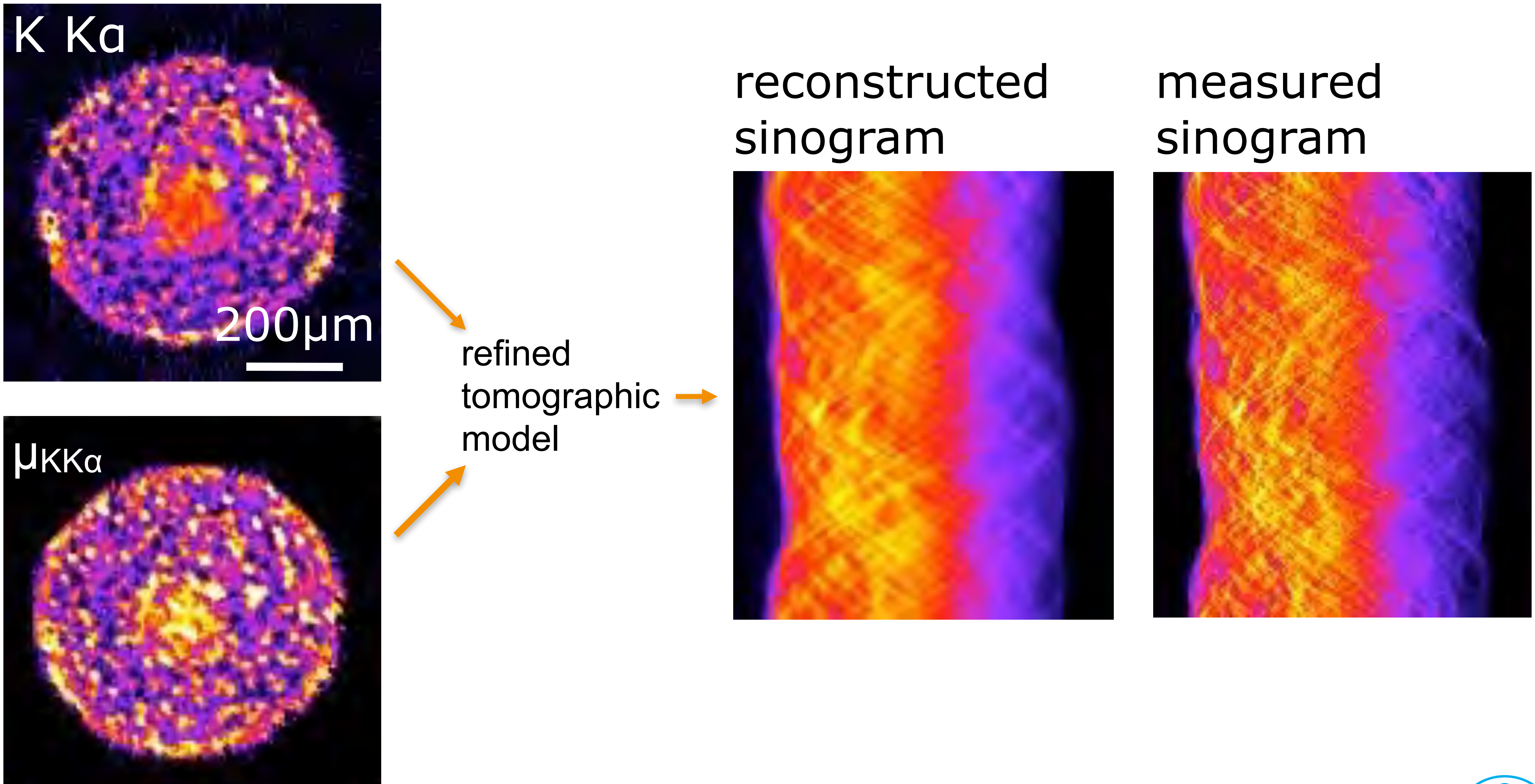

C. Schroer, Appl. Phys. Lett. **79**, 1912 (2001).

Fluorescence Tomography

root of Mahogany tree

pixel size: 6 μm

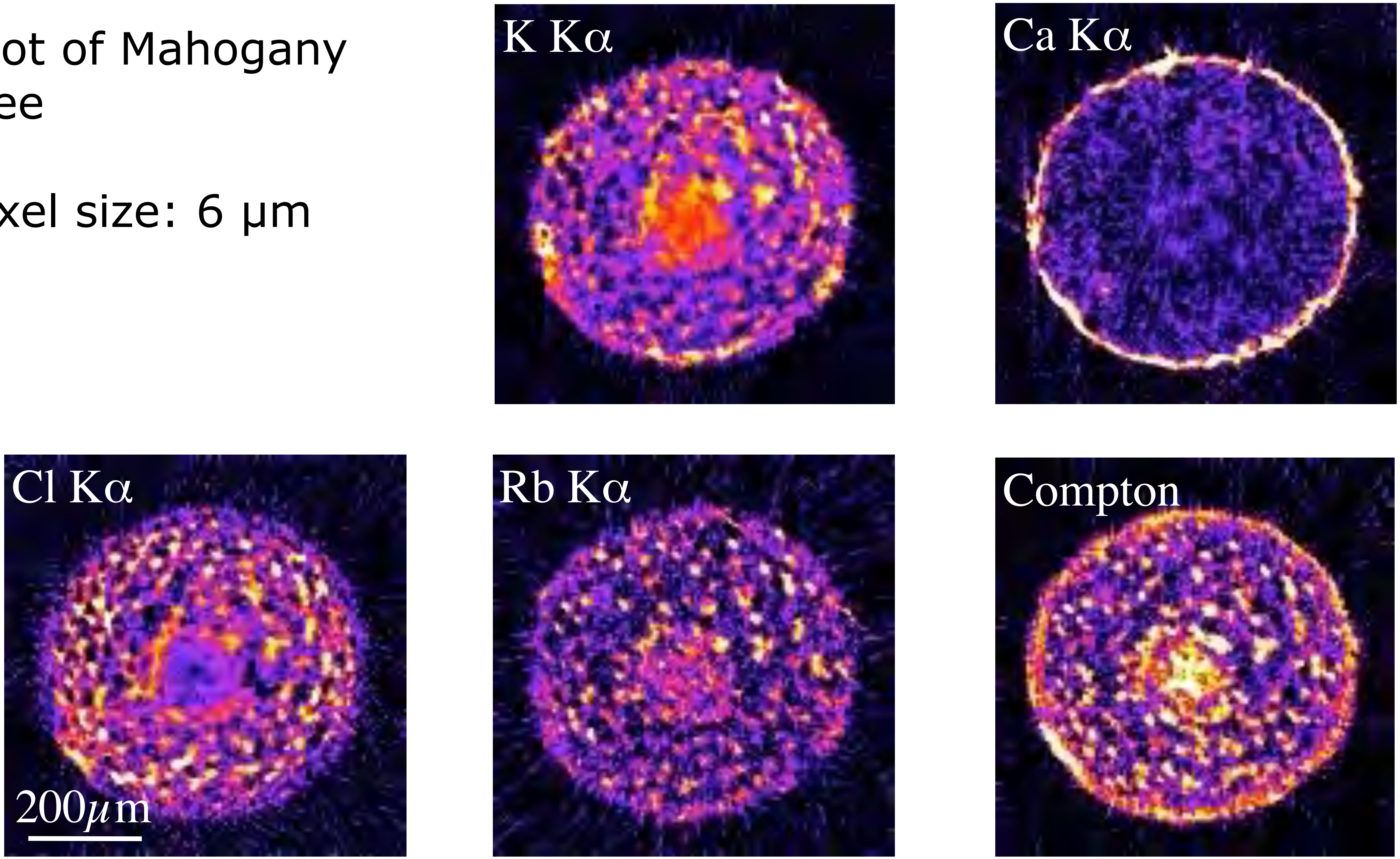

Fluorescence Tomography

Take advantage of:

- large penetration depth of x-rays
- element specific contrast

Compare with structural data from transmission tomogram:

K Kα

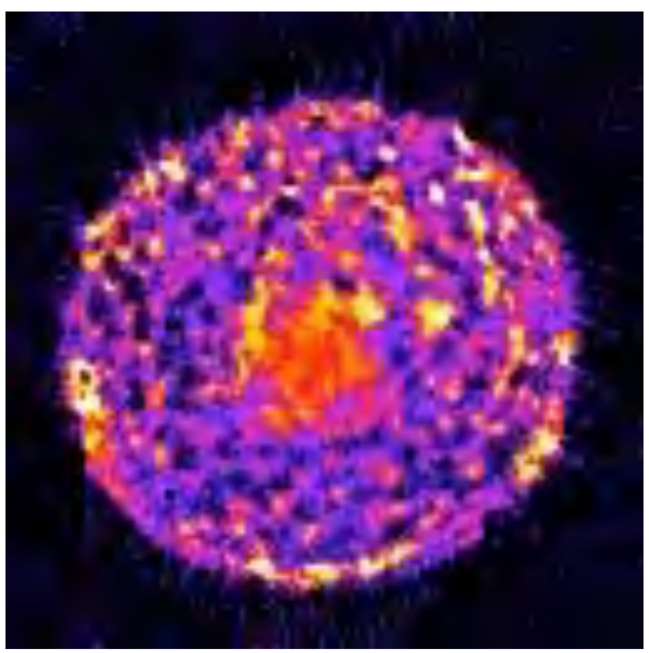

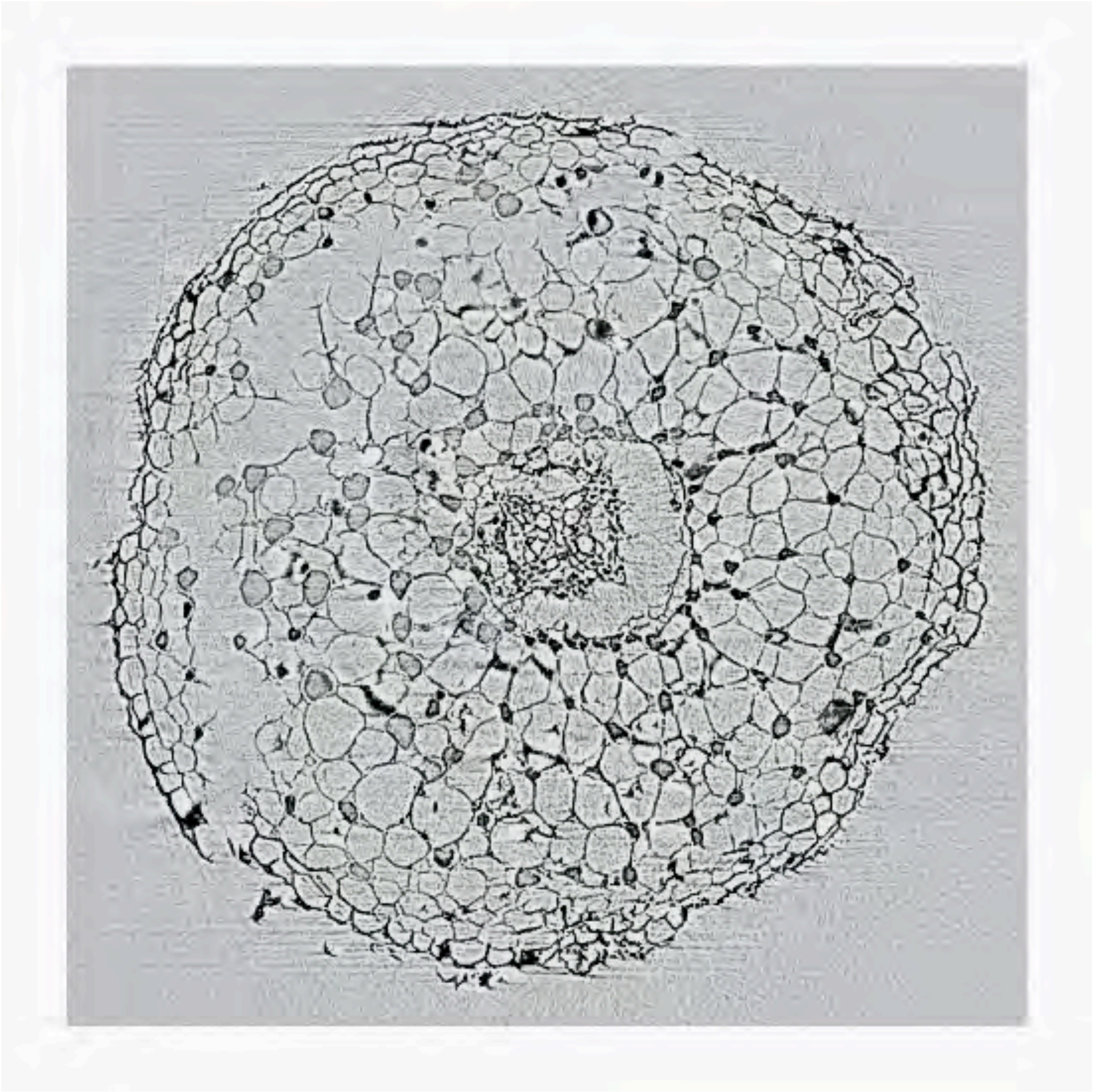

SAXS Tomography: Local Nanostructure

SAXS: **S**mall-**A**ngle **X**-ray **S**cattering

Investigating the local nanostructure on a virtual section through sample

Sample:

Non-destructive investigation of inner structure of sample

virtual section

reconstructed SAXS cross section at each point on the virtual section

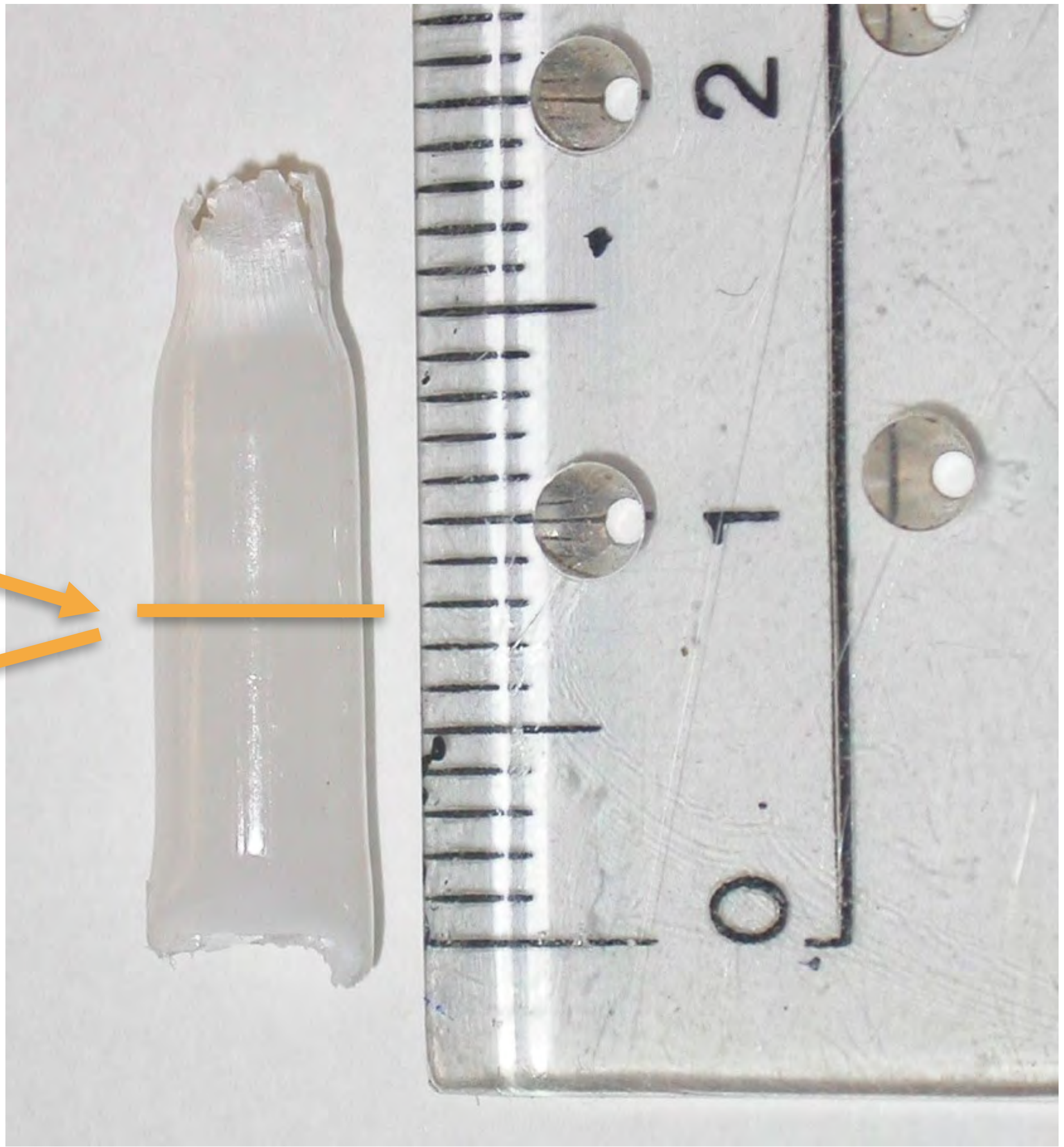

polyethylene rod

C. Schroer, et al., Appl. Phys. Lett. **88**, 164102 (2006)

Tomographic Small-Angle X-Ray Scattering

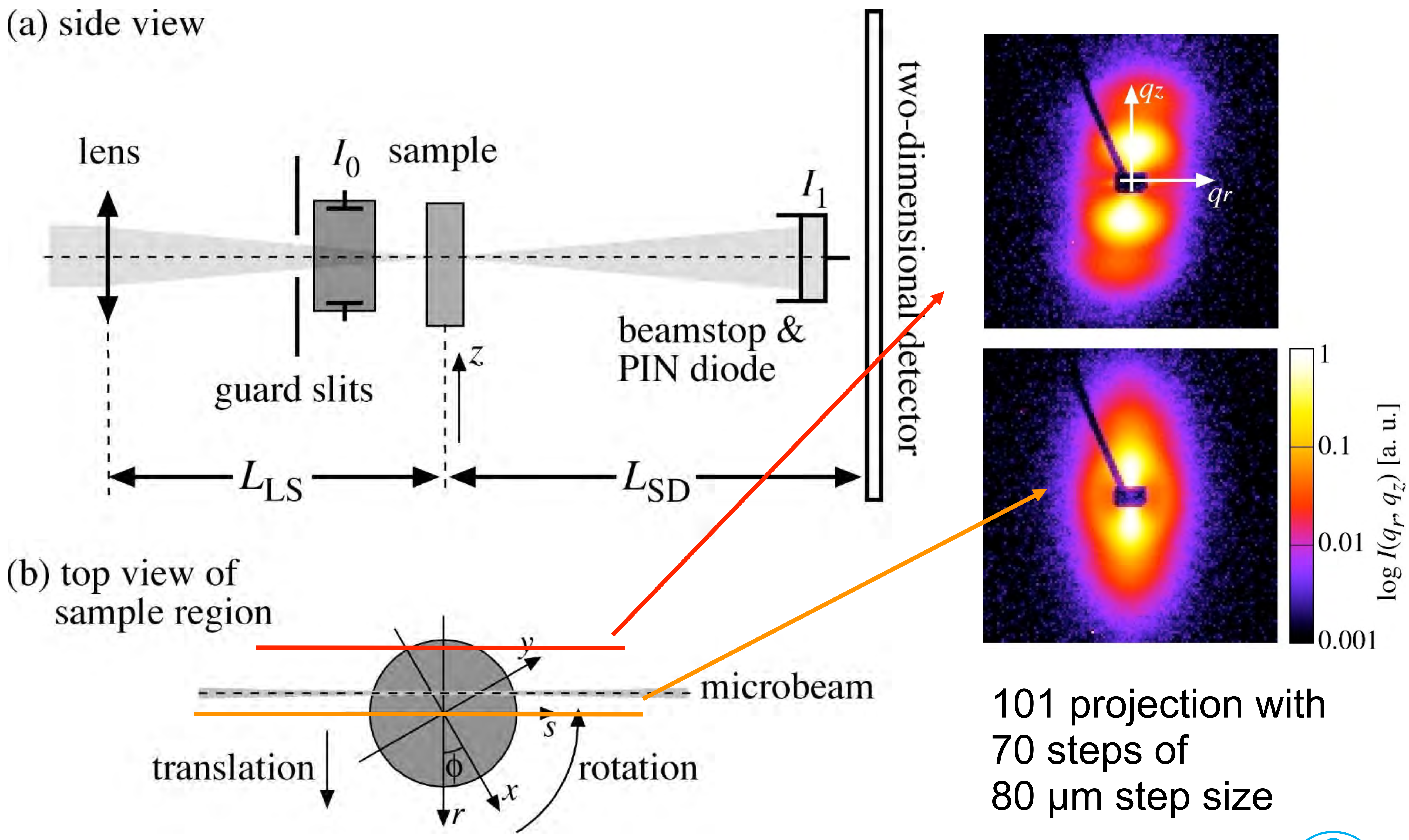

101 projection with
70 steps of
80 µm step size

SAXS Tomography at Beamline BW4 at DORIS III

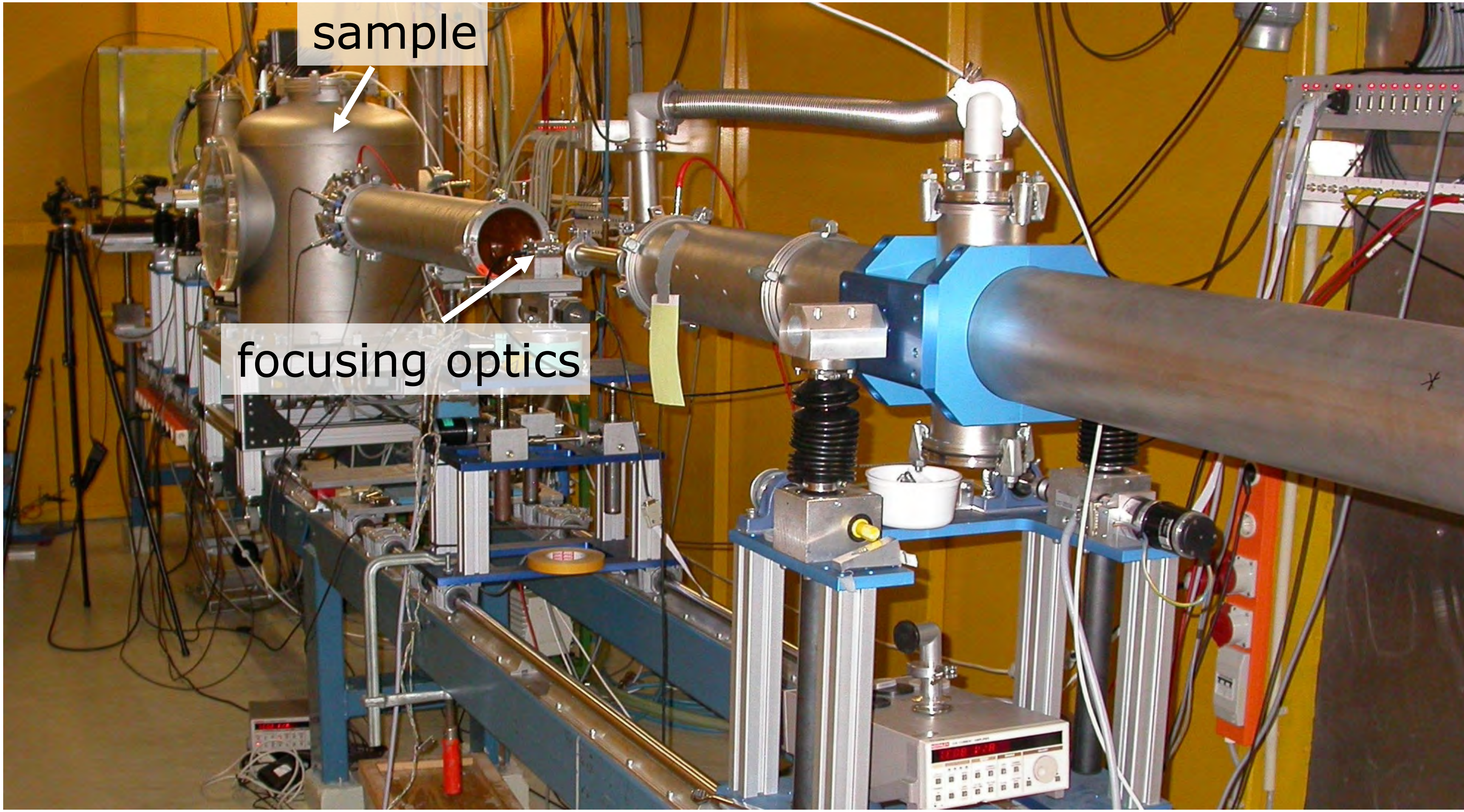

SAXS Tomography at Beamline BW4 at DORIS III

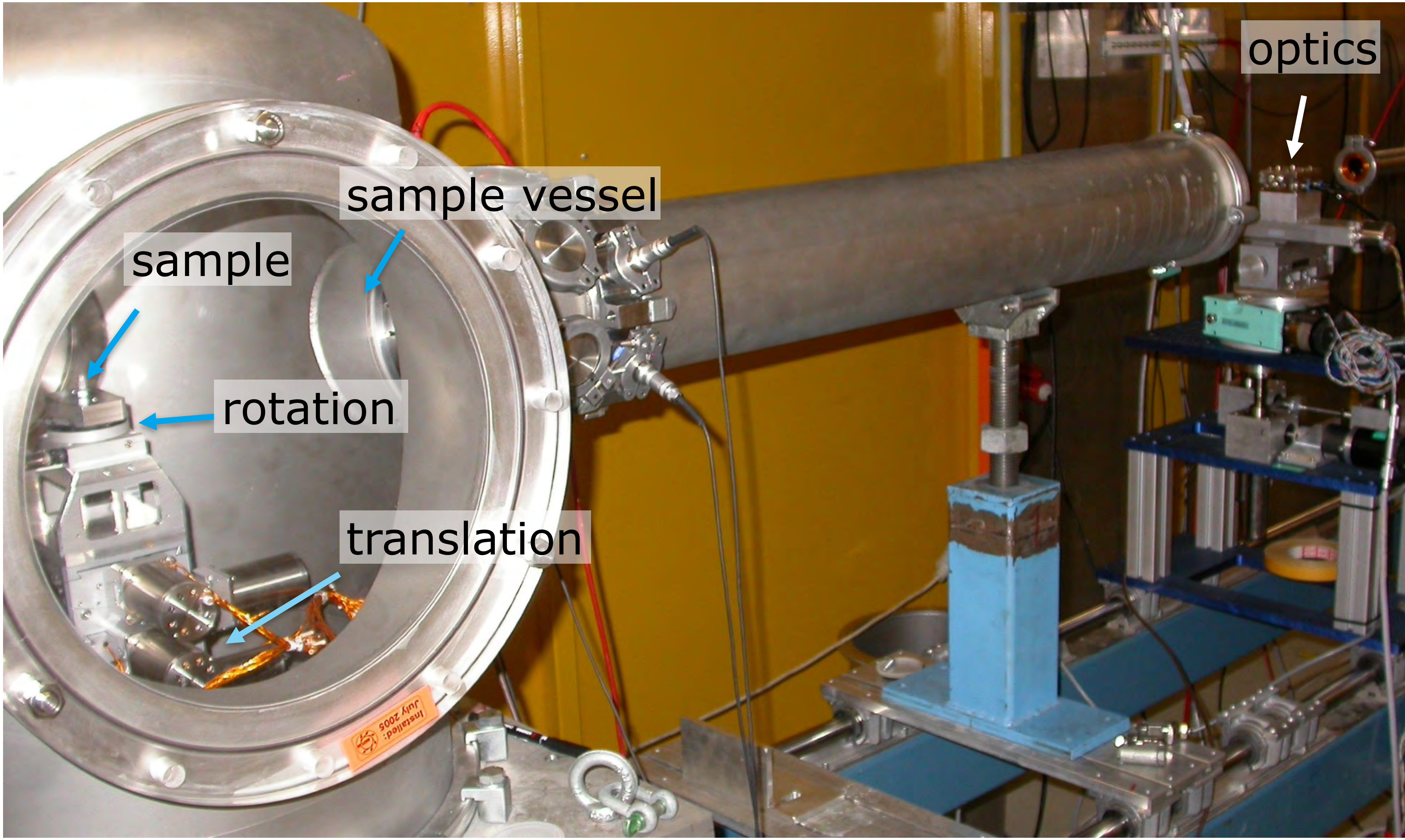

SAXS Tomography at Beamline BW4 at DORIS III

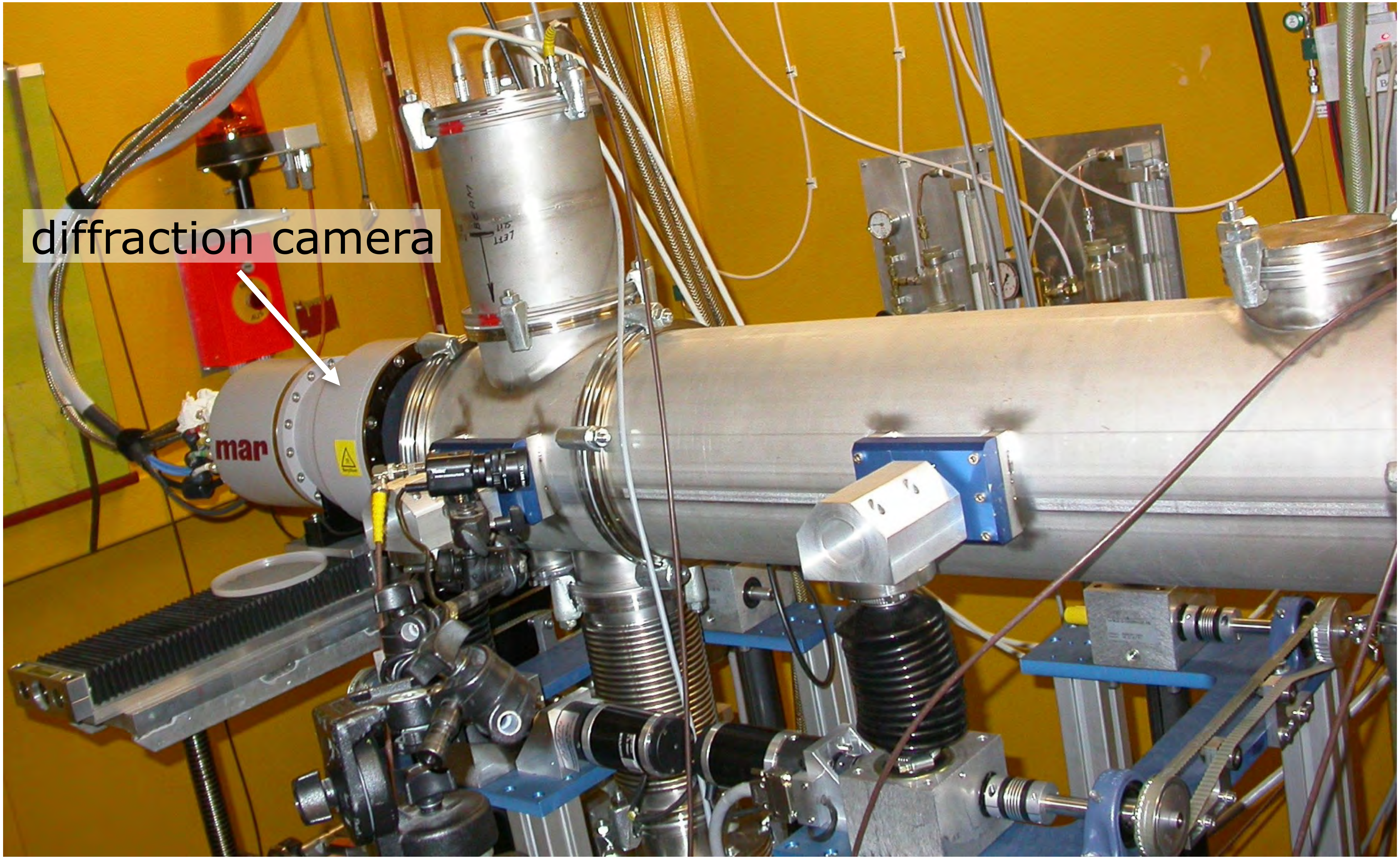

SAXS Tomography

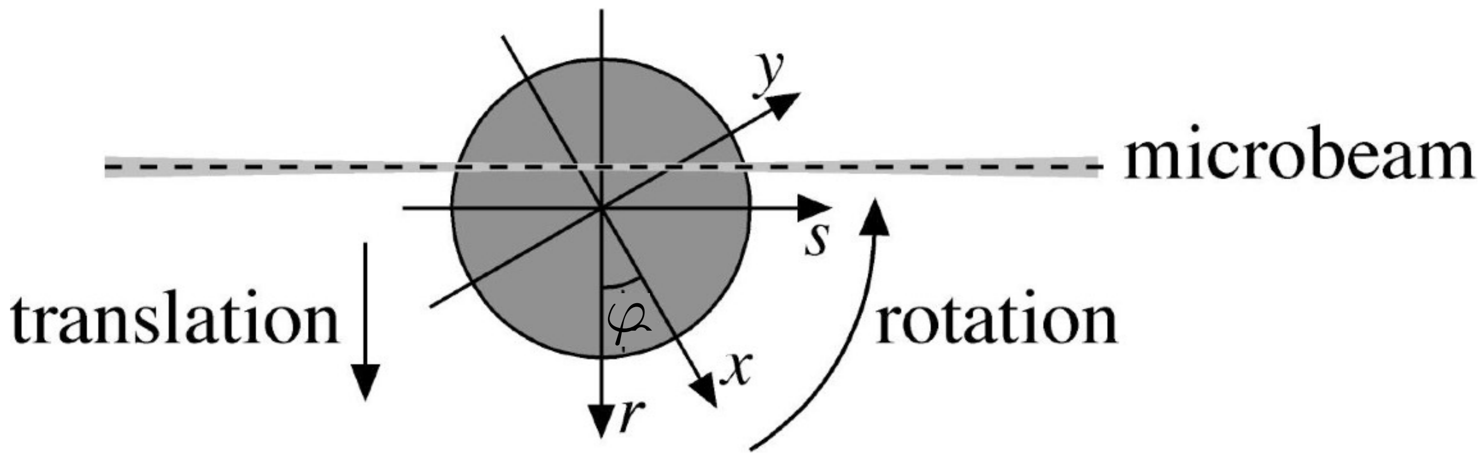

Transmitted beam:

$$I_1(r,\varphi) = I_0 \exp\left\{-\int ds'\mu\left[x(s',r),y(s',r)\right]\right\}$$

Standard tomography:

homogeneous density (polyethylene):

$$\rho = \left[0.88 \pm 0.04\right] \mathrm{g/cm^3}$$

attenuation

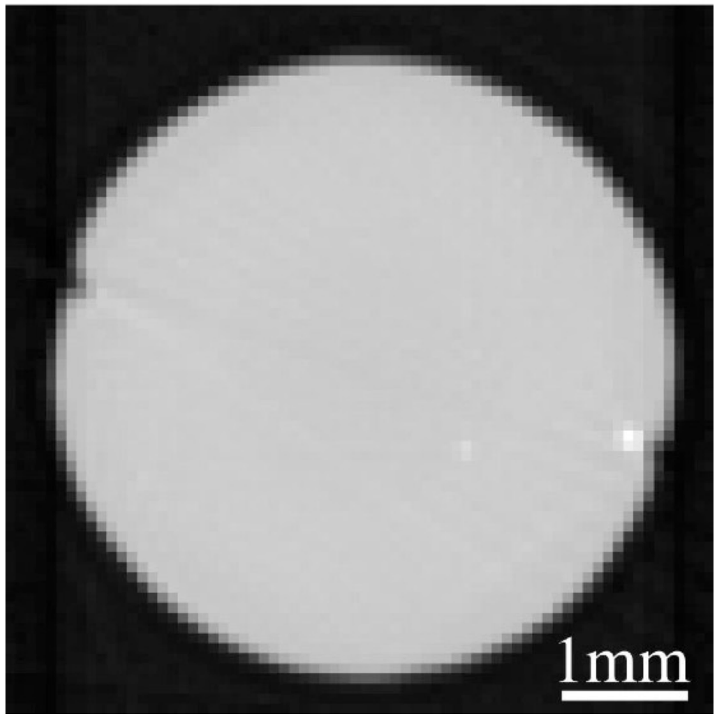

C. Schroer, et al., Appl. Phys. Lett. **88**, 164102 (2006)

SAXS Tomography

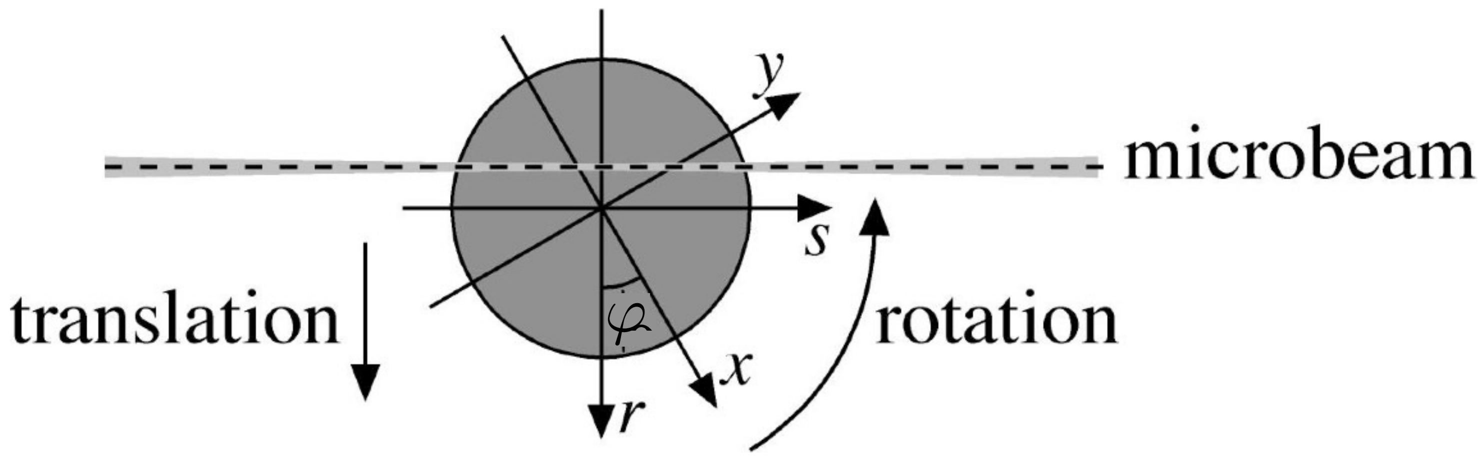

scattered signal:

$$I_{\vec{q}}(r,\varphi) = I_0 \int ds\ f(\varphi,s,r) p_{\vec{q},\varphi}(x,y) g(\varphi,s,r)$$

attenuation of primary beam:

$$f(\varphi,s,r) = \exp\left\{-\int_{-\infty}^{s} ds'\ \mu(x,y)\right\}$$

attenuation of scattered beam

$$g(\varphi,s,r) = \exp\left\{-\int_{s}^{\infty} ds'\ \mu(x,y)\right\}$$

Diffraction signal in forward direction:

$$I_1(r,\varphi) = I_0(r,\varphi) \cdot f(\varphi,s,r) \cdot g(\varphi,s,r)$$ independent of *s*

C. Schroer, et al., Appl. Phys. Lett. **88**, 164102 (2006)

SAXS Tomography

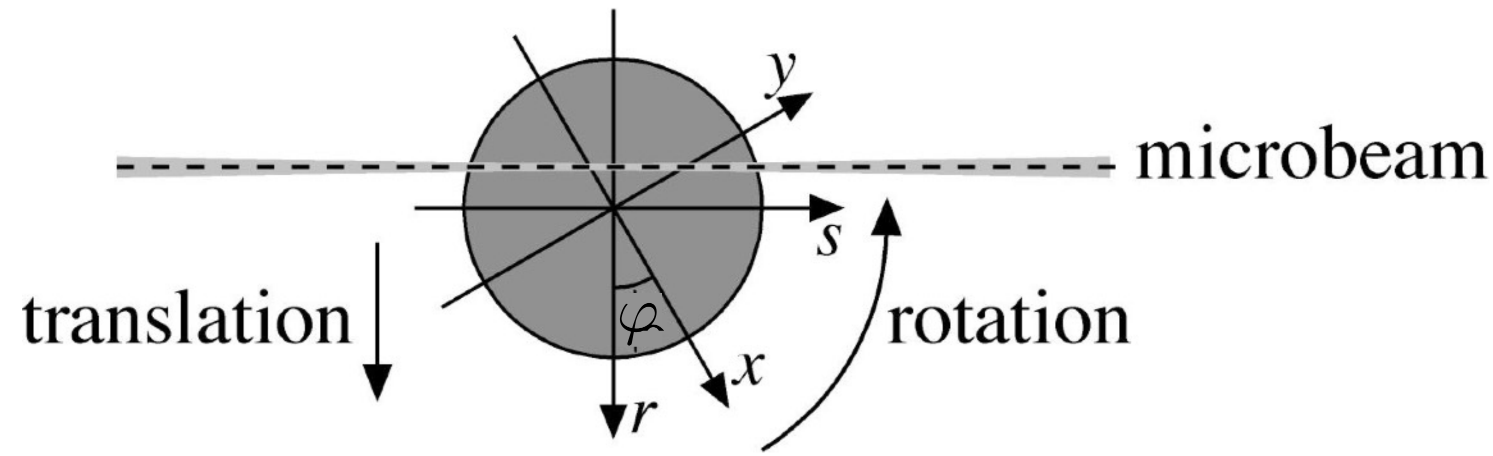

scattered signal:

$$I_{\vec{q}}(r,\varphi) = I_1 \int ds\; p_{\vec{q},\varphi}(x,y)$$

tomography works only if $p_{\vec{q},\varphi}(x,y)$ is independent φ

general case: $p_{\vec{q},\varphi}(x,y)$ complicated function

reconstruction only for $q_r = 0$
(q along rotation axis)

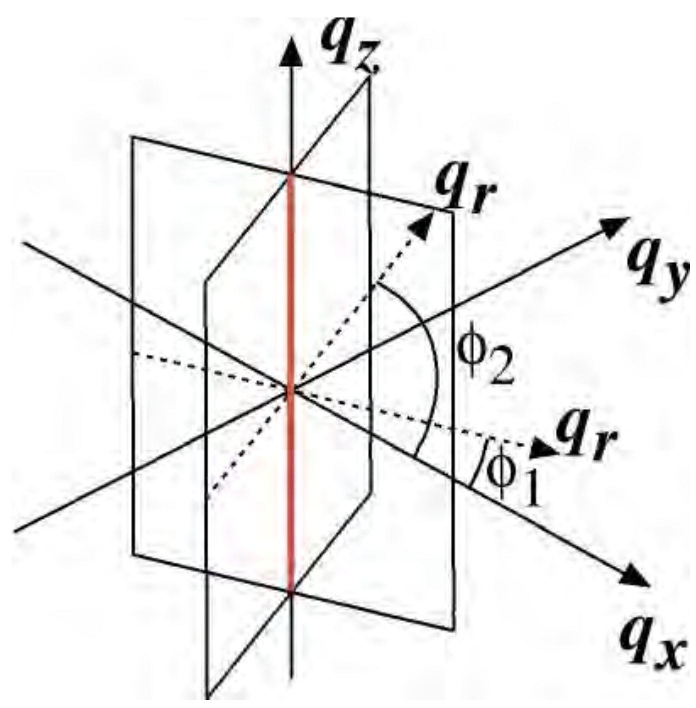

C. Schroer, et al., Appl. Phys. Lett. **88**, 164102 (2006)

SAXS Tomography

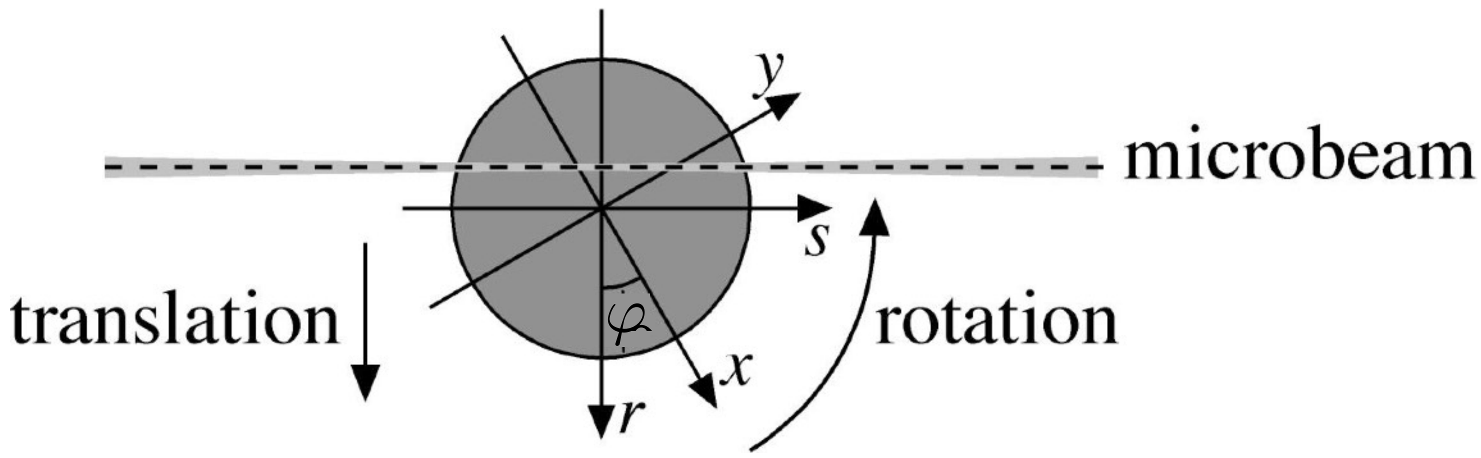

scattered signal:

$$I_{\vec{q}}(r,\varphi) = I_1 \int ds\; p_{\vec{q},\varphi}(x,y)$$

tomography works only if $p_{\vec{q},\varphi}(x,y)$ is independent φ

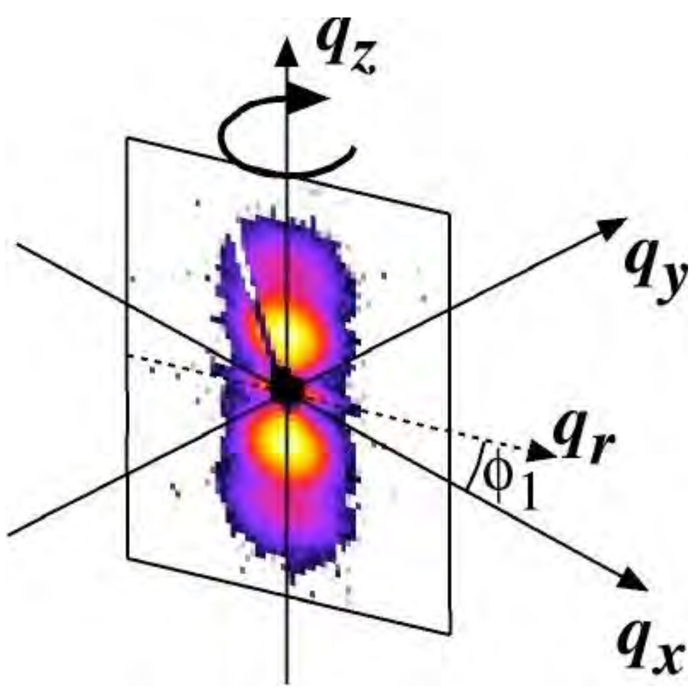

Special case: $p_{\vec{q},\varphi}(x,y)$ has rotation symmetry

around rotation axis

reconstruction of full SAXS cross section
in the vicinity of q = 0

C. Schroer, et al., Appl. Phys. Lett. **88**, 164102 (2006)

SAXS Tomography

reconstruction:

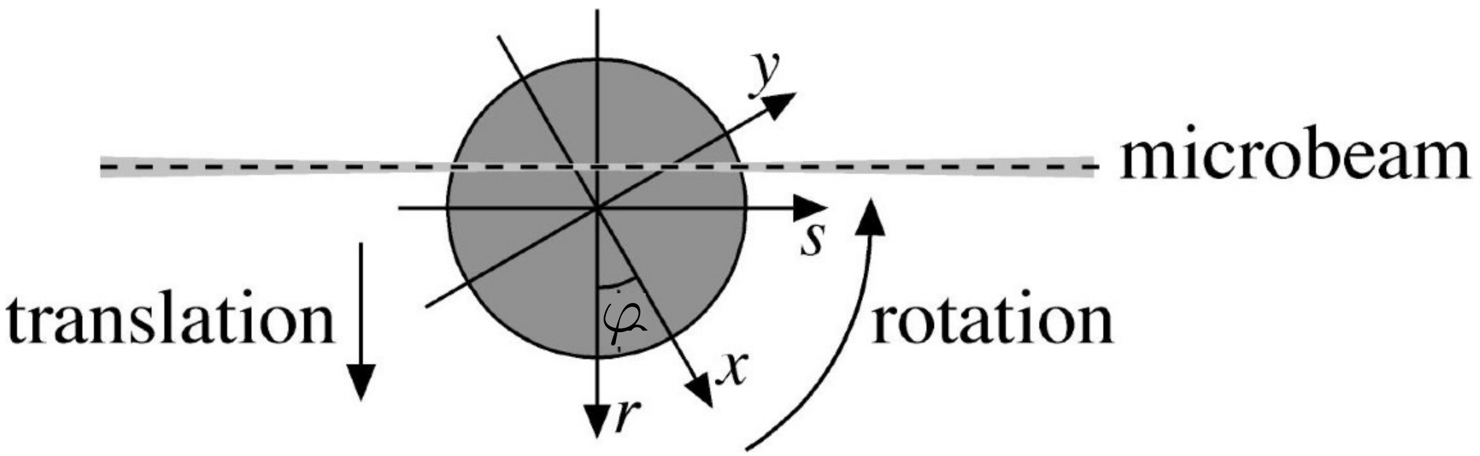

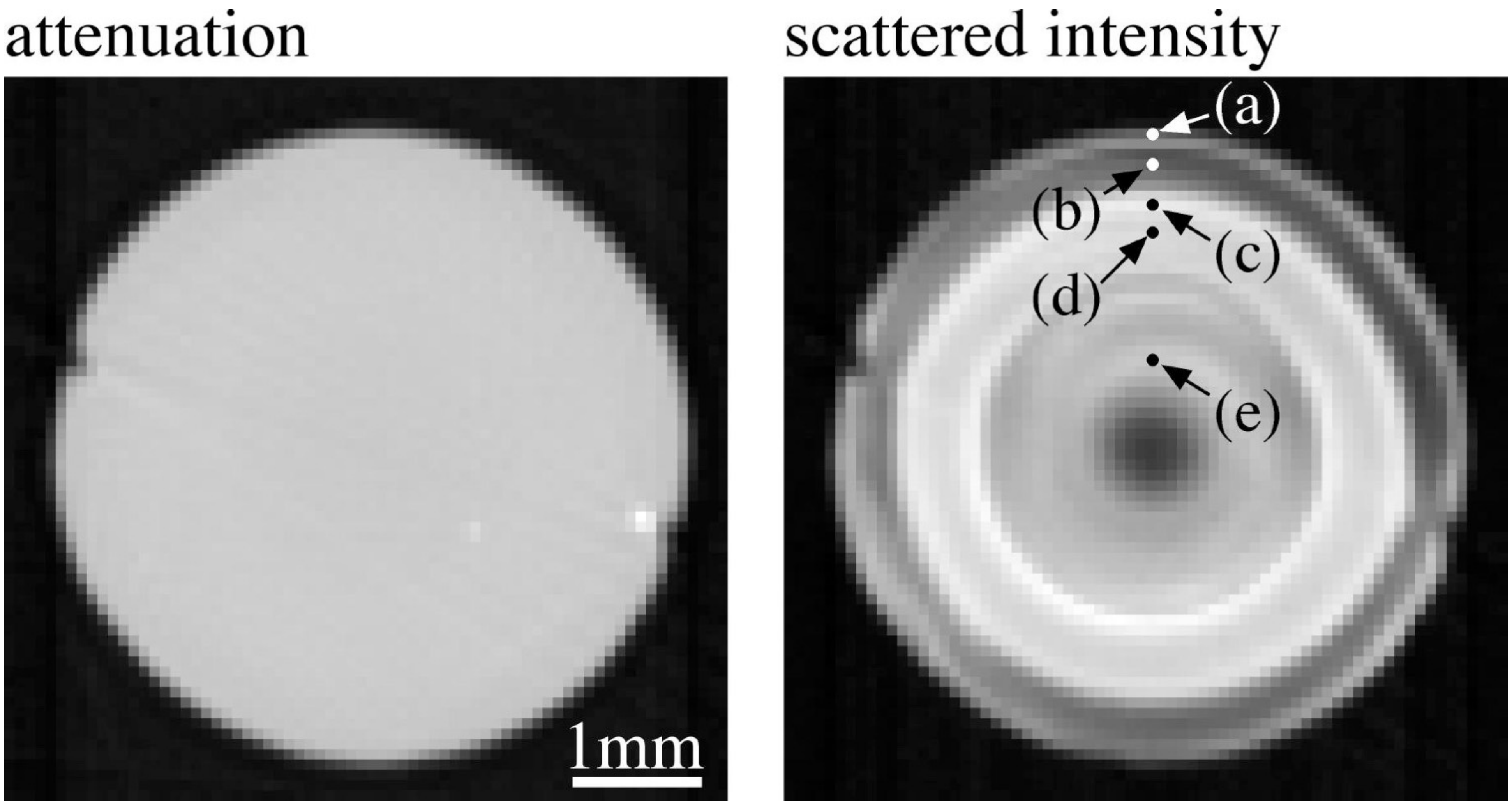

integral scattering cross section along rotation axis

SAXS Tomography

Sample with fibre texture:

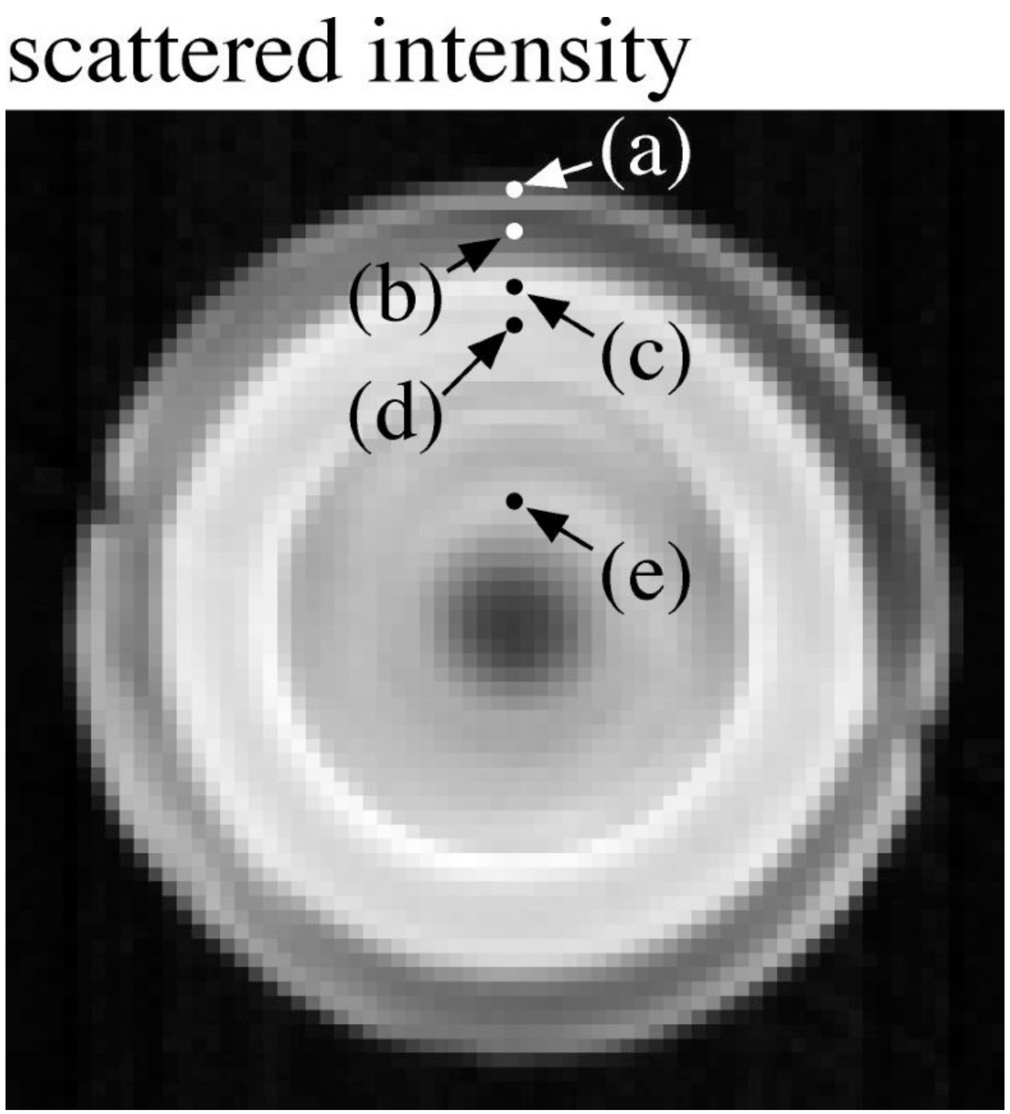

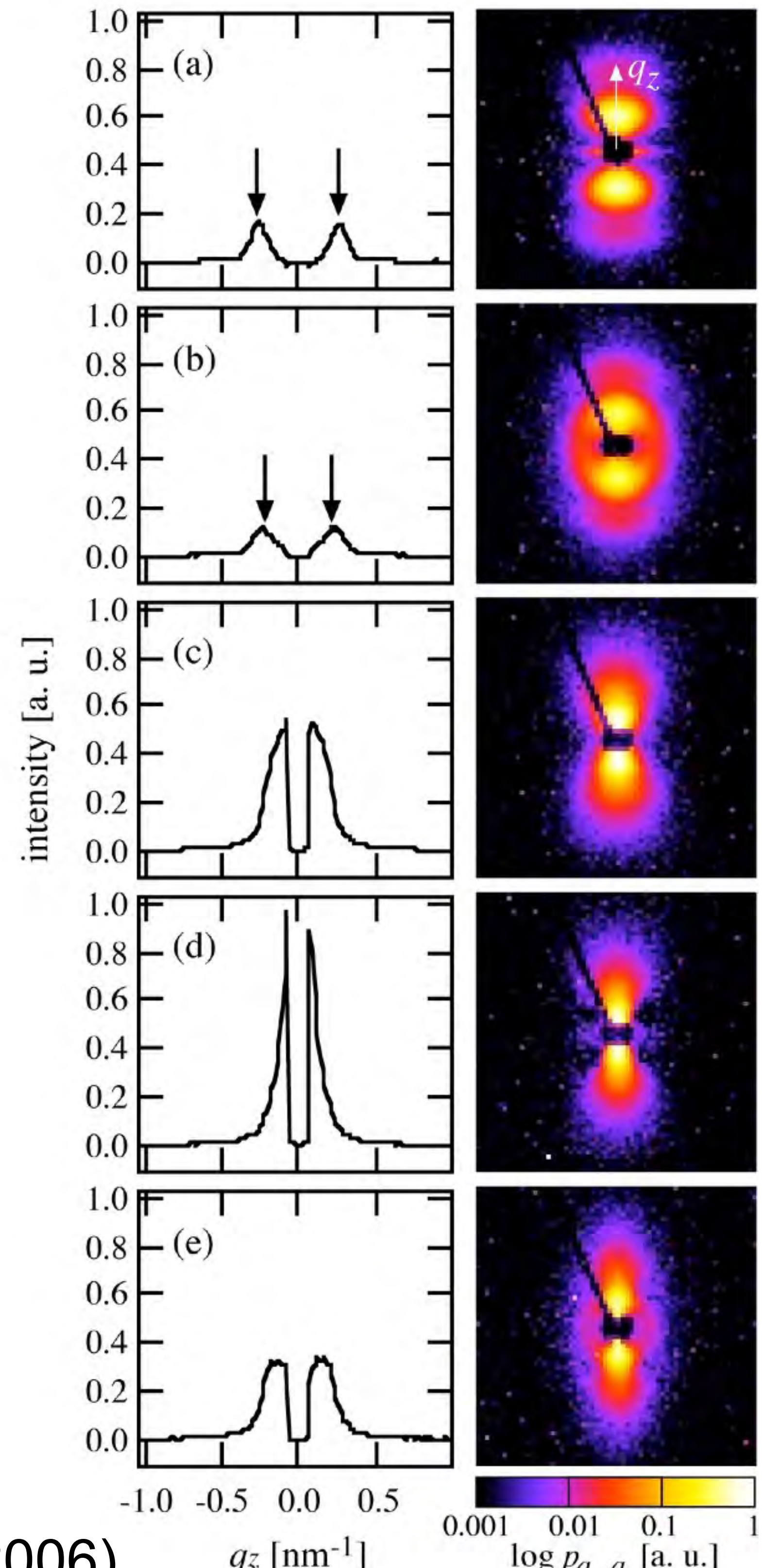

inhomogeneous nanostructure

scattering cross section in each pixel (rotation symmetry)!

C. Schroer, et al., Appl. Phys. Lett. **88**, 164102 (2006)

SAXS Tomography in 3D

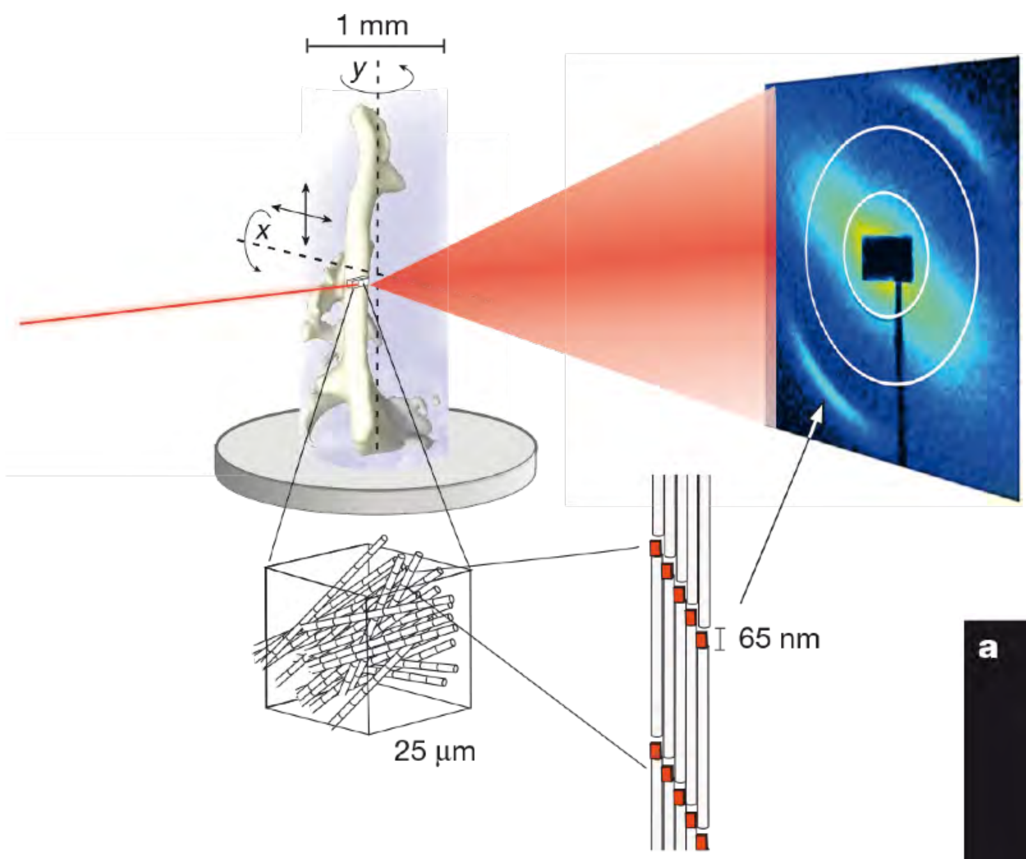

general SAXS-tomographic oroblem

in general: measure 6 dimensional information!

Scan in 4 dimensions and record 2D patterns (coarse mesh due to time limitations)

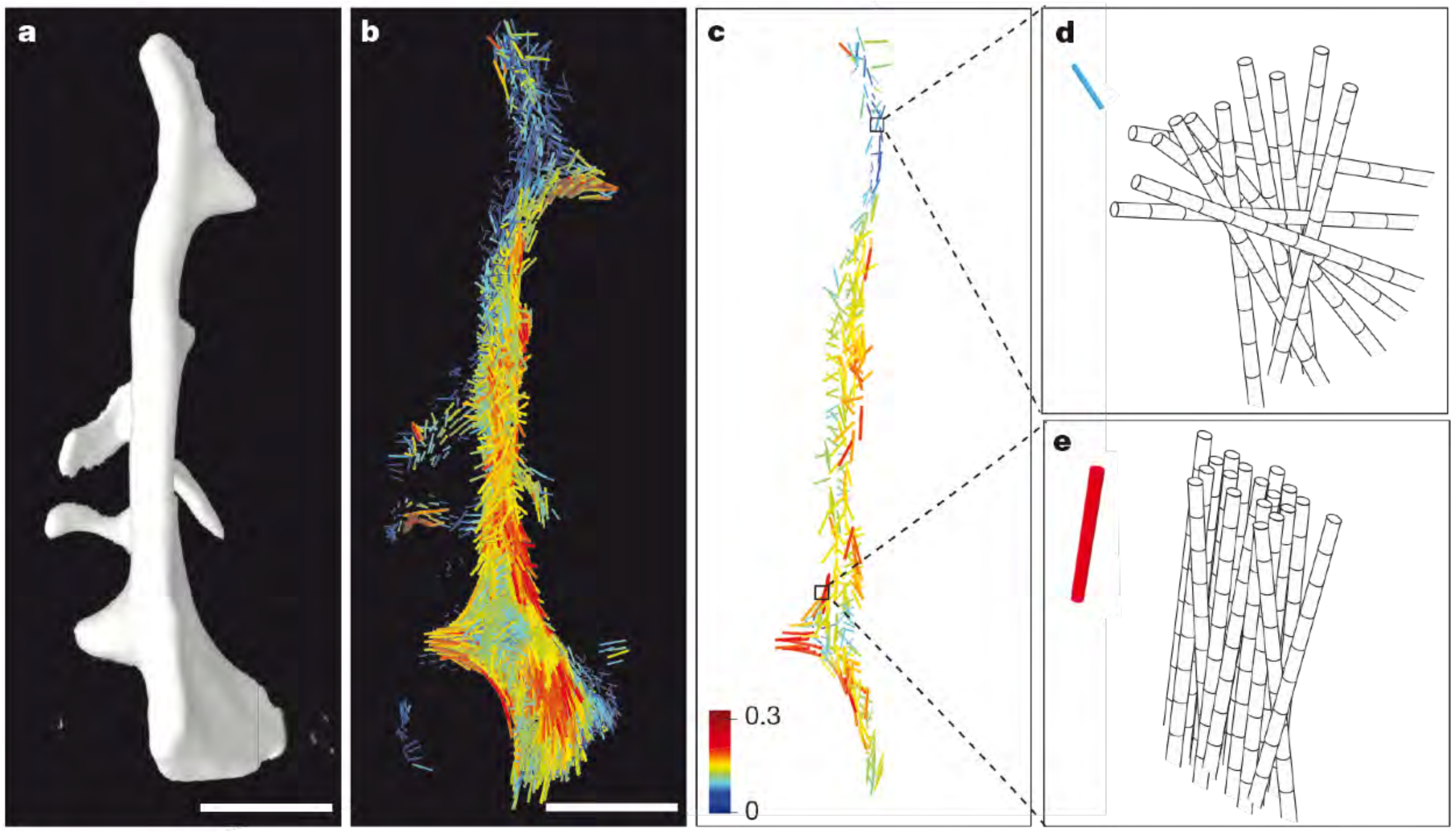

Liebi, M., et al., Nature, **527**(7578), 349–352. (2015).

Conventional X-Ray Microscopy

X-ray microscopy as a quantitative local measurement:

- Full-field microscopy: attenuation and phase contrast

→ measure complex refractive index of sample

- scanning microscopy:

→ all x-ray analytical techniques can be used as contrast:

  - x-ray fluorescence (XRF): chemical composition (quantitative analysis)
  - x-ray absorption spectroscopy (XAS): chemical state of given element (e. g. oxidation)
  - x-ray diffraction and scattering (SAXS & WAXS): local nanostructure
  - …

Full-field and scanning microscopy require x-ray optics

→ resolution limited by numerical aperture of optics

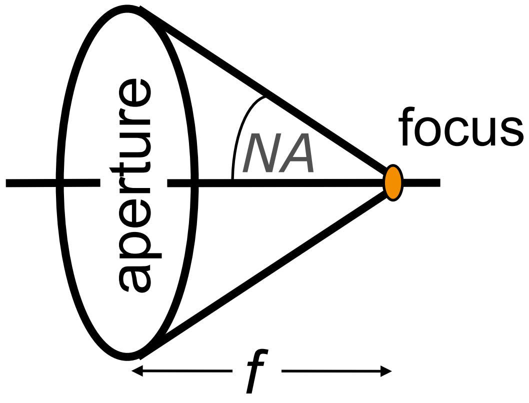

Next time: what are the limits and how can we overcome them?